EVALUATION OF LATERITIC SOIL AND (FUNGAL) *Agaricus Impudicus* BIOMASS FOR ADSORPTION–DESORPTION OF NITROGEN AND PHOSPHORUS FROM HUMAN URINE

FAITH CHEPKWONY

MASTER OF SCIENCE IN SOIL AND WATER ENGINEERING

JOMO KENYATTA UNIVERSITY

OF

AGRICULTURE AND TECHNOLOGY

2026

Evaluation of Lateritic Soil and (Fungal) *Agaricus Impudicus* Biomass for Adsorption–Desorption of Nitrogen and Phosphorus from Human Urine

Faith Chepkwony

A Thesis Submitted in Partial Fulfilment of the Requirements for the Degree of Master of Science in Soil and Water Engineering of the Jomo Kenyatta University of Agriculture and Technology

2026

DECLARATION

This thesis is my original work and has not been presented for a degree in any other University

Signature: …… Date: ……

Faith Chepkwony

This thesis has been submitted for examination with our approval as the University Supervisors.

Signature: ……... Date: ……

Prof. James Messo Raude, PhD

JKUAT, Kenya

Signature: ……... Date: ……

Prof. Patrick Gathongo Home, PhD

JKUAT, Kenya

Signature: ……... Date: ……

Dr. Austine Owuor Otieno, PhD

TUK, Kenya

DEDICATION

I dedicate this work to my parents (Mr and Mrs Chepkwony) and siblings for their endless prayers, love and support. I dedicate this also to my friends who encouraged me and graced all the difficult moments in this journey with laughter and love.

ACKNOWLEDGEMENT

First and foremost, I thank God for His mercies, courage, strength and the gift of life that He has bestowed upon me throughout my studies. I am also grateful to my supervisors Prof. Eng. James Raude, Prof. Patrick G. Home and Dr. Austine O. Otieno for their steadfast support and guidance in my studies. Thank you for always taking your time to review my work. May God bless you all abundantly. I would also like to appreciate the technicians at the Department of Civil engineering, Environmental laboratory for their guidance and support in setting up and conducting the experiments. I also appreciate the technical team of Department of Biological and Chemical Engineering, Aarhus University, Denmark for their assistance in elemental analysis of lateritic soil and fungi adsorbents. I express my sincere gratitude to DAAD, German Academic Exchange Service for sponsoring my Master's Degree education. I am grateful to my parents and siblings for their unwavering love and support throughout this phase of life. I appreciate my friends for their encouragements. Finally, to my classmates, thank you for making this journey more bearable and exciting through your amazing company and support.

TABLE OF CONTENTS

LIST OF TABLES

LIST OF FIGURES

LIST OF APPENDICES

ABBREVIATIONS AND ACRONYMS

AAS	Atomic Absorption Spectrometer
ANOVA	Analysis of Variance
ASTM	American Standard for Testing and Materials
BBD	Box-Behnken Designs
BDL	Below Detection Limit
BOD	Biochemical Oxygen Demand
CCD	Central Composite and Doehelrt
CE	Circular Economy
COD	Central Composite and Doehelrt
D-R	Dubinin-Radushkevich
EC	Electrical Conductivity
FTIR	Fourier Transfer Infrared
IEA	International Energy Agency
LS	Lateritic Soil
Lip	Lignin Peroxidase
Mnp	Manganese Dependent Peroxidase
NH_4^+-N	Ammonium Nitrogen
NPK	Nitrogen Phosphorus and Potassium
OFAT	One-Factor-at-a-Time
PFO	Pseudo First Order
PPB	Pineapple Peels Biochar
PSO	Pseudo Second Order
RMSE	Root Mean Square Error
SEM	Scanning Electron Microscope
SSE	Sum of Square Error
UDDTS	Urine Diversion and Dehydrating Toilets
UN	United Nations
WHO	World Health Organization
XRF	X-ray Fluorescence

ABSTRACT

Human urine contains high concentrations of nitrogen and phosphorus, whose uncontrolled discharge contributes to eutrophication and nutrient losses in agricultural systems. Recovering these nutrients using low-cost natural materials offers a sustainable alternative to synthetic fertilizers. This study evaluated the performance of lateritic soil (LS) and fungal biomass (*Agaricus impudicus*) as potential adsorbents and desorbents for the recovery of ammonium nitrogen (NH_4^+–N) and phosphorus (P) from human urine. The physicochemical properties of the adsorbents were characterized using Fourier Transform Infrared Spectroscopy, scanning electron microscope, X-ray Fluorescence (XRF), and elemental analysis. Batch adsorption experiments were conducted under varying operational conditions to evaluate nutrient recovery performance. Physicochemical properties of human urine were evaluated using atomic absorption spectrometry (AAS), nesslerization method, Molybdenum antimony colorimetric, pH meter and electrical conductivity meter. Time-dependent data were fitted using Pseudo first order (PFO), Pseudo second order (PSO), Elovich and Intra-Particle diffusion kinetic models. Equilibrium data were analyzed using Langmuir, Freundlich, and Dubinin–Radushkevich (D–R) isotherm models to elucidate adsorption mechanisms and capacities. Batch and column desorption experiments were conducted to evaluate the desorption behavior of lateritic soils and fungal adsorbent. Elemental and XRF analysis revealed that lateritic soils possess aluminium and iron oxides that facilitate ligand exchange and inner sphere complexation during adsorption. Fungal biomass on the other hand, contains carboxyl and hydroxyl that enable adsorption of $NH_4^+ - N$ and P via electrostatic bonding. PFO best described the time-dependent data for $NH_4^+ - N$ and P adsorption for the two adsorbents indicating physisorption was the dominating adsorption mechanism. For $NH_4^+ - N$ adsorption, the D–R model best described lateritic soil (R^2 = 0.968), indicating physical adsorption, whereas the Freundlich model best fitted *A. impudicus* biomass (R^2 = 0.813). Lateritic soil exhibited higher adsorption capacity (16.3 mg/g) than fungal biomass (12.0 mg/g). For phosphorus, the Langmuir model provided the best fit for both materials (R^2 = 0.939–0.946), with lateritic soil demonstrating a substantially higher capacity (24.6 mg/g) than fungi (6.2 mg/g), likely due to iron and aluminum oxides. Desorption tests showed that fungal biomass achieved the highest nutrient release (43.93% $NH_4^+ - N$ and 44.83% P). Overall, lateritic soil and *A. impudicus* biomass exhibited promising adsorption–desorption performance, demonstrating their potential as low-cost, environmentally sustainable materials for nutrient recovery and circular fertilizer production. Thus, these results provide comparative evaluation of lateritic soil and fungal biomass for simultaneous nitrogen and phosphorus recovery from human urine. These findings also demonstrate the potential integration of locally available natural materials into decentralized sanitation and nutrient recycling systems for sustainable agriculture.

CHAPTER ONE

INTRODUCTION

1.1 Background Information

With the world population projected to rise to 9.7 billion by 2050(United Nations, 2019), the demand of food is expected to increase drastically, subsequently amplifying the need for synthetic Nitrogen (N) and Phosphorus (P) fertilizers to enhance food production. Most of the synthetic N fertilizers are manufactured using the Haber Bosch processes which consumes approximately 2 % of the world's energy and directly emits about 450 Mt CO_2 per year (International Energy Agency, 2021; Zou et al., 2022). Synthetic P fertilizers on the other hand are derived from phosphates rock mines which are, non-renewable, limited and only available in few countries. Approximately 85 % of these mines are located in Algeria, China, Egypt, Morocco and Syria (U.S. Geological Survey, 2022). Reliance on phosphate rock mines as a source of synthetic fertilizer also has negative impacts such as disruption of natural phosphorus cycle, economic burdens in low- income countries and environmental degradation as a result of mining activities (Rakshit et al., 2017; Sarvajayakesavalu et al., 2018). Conversely, continuous use of synthetic fertilizers has led to increased phosphorus pollution in fresh water bodies caused by farm fertilizer losses due to leaching, erosion, surface runoff and draining (Grenon et al., 2021; Osmond et al., 2019). In an effort to alleviate these negative effects, alternative sources of organic N and P such as animal manure, sewage sludge, organic wastes and human urine have been identified (Karunanithi et al., 2016; Mihelcic et al., 2011).

Human urine, a readily available and nutrient-rich fluid, contributes approximately 80-90 % nitrates, 50-65 % phosphorus, and 50-80% potassium, but accounts for approximately 1% of the total volume of wastewater (Kujawa-Roeleveld & Zeeman, 2006; Wilsenach et al., 2007). The amount of nitrates and phosphorus that ends up in municipal wastewater is projected to increase with increase in human population. Thus, if not properly managed, high nutrient levels in human urine can exacerbate pollution in freshwater bodies increasing harmful algal blooms and proliferation of cyanobacteria (McDowell & Haygarth, 2024). In an effort to minimize the amount of nutrients that ends up in municipal wastewater, on-site sanitation facilities such as

urine diversion and dehydration toilets (UDDTs) have been developed. UDDTs help to physically separate urine and faeces into different collection chambers at the toilet interface enabling urine to be collected for other uses and faeces are dehydrated for ease in handling and disposal. UDDTs hence play a crucial role in large scale production of urine for diverse uses such as making organic fertilizers (Larsen et al., 2021; Sohn et al., 2023).

Human urine has been reported as a potential source of crucial nutrients such as nitrogen, phosphorus and potassium that are crucial for agricultural production (Viskari et al., 2018; H. Yu et al., 2026). Currently, several technologies have been established to help extract nutrients from the human urine. Some of the notable techniques include adsorption, biological methods (aerobic and anaerobic), membrane filtration, chemical precipitation, and electro-modification. Chemical precipitation produces large amounts of sludge, which may result in secondary pollution if not properly managed (Kabdaşlı & Tünay, 2018). Conversely, electrodialysis consumes a lot of energy especially when used for large-scale applications. Limitations of membrane filtration include high cost of operation and membrane fouling (An et al., 2017). Previous studies have suggested adsorption as a sustainable method for this process, citing advantages like environment-friendliness and sustainability as it utilizes agricultural wastes, forestry residues such as wood chips, sewage sludge, geological materials, algae, and fly ash (Konneh et al., 2021; Xiang et al., 2020).

The effectiveness of the adsorption process depends on the properties of the adsorbents like the porosity, surface area, and elemental composition (Otieno et al., 2021). The potential of different organic wastes and geological materials as adsorbents in extracting nutrients from wastewater has been widely explored, with different materials exhibiting varying adsorption capacities and behaviours (Usman et al., 2022). Certain approaches can be utilized to adjust the properties of these materials to enhance their adsorption capacities. For organic wastes, pyrolysis, which involves controlled heating of materials in low oxygen to yield biochar with enhanced porosity and larger surface area for adsorption, has been reported (Bischak et al., 2024; Konneh et al., 2021). Geological materials such as zeolites, clays and pumice are often modified through physical and chemical treatment methods to increase surface areas,

pore structure and functional groups for adsorption (Aziz et al., 2020; Indah et al., 2019). Fungal material such as non-edible and edible mushrooms are also modified through heat treatments to increase their porosity and surface areas for adsorption processes (Frutos et al., 2016; Toptas et al., 2014). Minimal studies have reported on their use for nutrients recovery with most researchers focusing on their use in removing heavy metals and dyes from municipal wastewater (Pecková et al., 2020; Sharma et al., 2020). Moreover, the desorption properties of the fungi are scarcely researched. Desorption studies are important to ascertain the potential of the adsorbents to release nutrients for crop use. On the other hand, although (Otieno et al., 2021) and (Otieno et al., 2023a) researched the potential of lateritic soil in the adsorption of phosphorus (P) and ammonium nitrogen (NH_4^+-N) in human urine but did not cover the desorption properties of lateritic soil.

Despite extensive research on adsorption-based nutrient recovery, limited attention has been given to fungal biomass and lateritic soils for ammonium and phosphorus recovery from human urine, particularly regarding desorption behavior and nutrient reuse potential. A comparative evaluation on the performance of the selected geological adsorbent with that of biological organic adsorbent provides a sustainable solution for nutrient recovery in decentralized systems. Hence, this study focused on evaluating the efficiency of the lateritic soils and fungi (*Agarius impudicus*) in recovering ammonium nitrogen and phosphorus from human urine and releasing adsorbed nutrients for agricultural production.

1.2 Statement of the Problem

Overdependence on synthetic fertilizers has negative impacts on environment. For instance, The Haber Bosch process used to produce inorganic nitrogen fertilizers emits approximately 450 Mt CO_2 yr^{-1} (equivalent to 123 Mt C yr^{-1}), contributing significantly to anthropogenic climate change (International Energy Agency, 2021). Additionally, continuous use of synthetic fertilizers causes eutrophication in freshwater water bodies and contamination of groundwater as a result of nutrient losses due to leaching, erosion, and surface runoff (Singh & Craswell, 2021). Although human urine has been identified as an alternative source of nitrogen and phosphorus,

most of it still end up in wastewater treatment systems or directly in the environment (Sengupta et al., 2015a). This practice further contributes to eutrophication and nutrient pollution in water bodies. Currently, a number of technologies have been developed to recover nitrogen and phosphorus from human urine. Some of these techniques have negative impacts on the environment. For instance, chemical precipitation produces large amounts of sludge, which may result in secondary pollution if not properly managed (Kabdaşlı & Tünay, 2018). Conversely, electrodialysis consumes a lot of energy especially when used for large-scale applications. Membrane filtration includes high cost of operation and membrane fouling. In the recent years, many researchers have explored the use of various low-cost adsorbents such as agricultural wastes, geological materials, forestry waste and sewage sludge in recovering nutrients (Ogunlalu et al., 2021; Semerci et al., 2021; Sen, 2023). However, limited knowledge exists on the suitability and reusability of fungal biomass and lateritic soils in nutrient recovery. Consequently, their use in development of low-cost and scalable nutrient recovery technologies is still uncertain.

Although, *Agaricus impudicus* possess functional groups such as carboxyl, hydroxyl that could bind ammonium and phosphate ions, limited studies have been reported on their performance in nutrient recovery from human urine. Most of the researches that have been done focused on their use in removing dyes and heavy metals from wastewater (Pecková et al., 2020), thus its potential in nutrient recovery remains unknown. Similarly, lateritic soils have been widely evaluated for its potential in adsorption of nutrients from wastewater, owing to its iron and aluminium oxides and clay minerals which provide abundant cation-exchange and electrostatic binding sites. However, its desorption properties remain scarcely studied. Without understanding the adsorption and desorption performance of fungal biomass and lateritic soils, the development of low-cost, reusable, and scalable nutrient recovery systems from human urine remains constrained.

1.3 Objectives

1.3.1 Main Objective

The main objective of this study was to evaluate the performance of fungi and lateritic soils as adsorbents and desorbents in nutrient recovery from human urine

1.3.2 Specific Objectives

The specific objectives of this study were to:

i. Characterize the physicochemical properties of lateritic soil, *Agaricus impudicus* and human urine relevant to ammonium nitrogen and phosphorus adsorption
ii. Determine the adsorption behavior and capacity of *Agaricus impudicus* and lateritic soil in adsorbing ammonium nitrogen and phosphorus from human urine
iii. Determine the desorption behavior of *Agaricus impudicus* and lateritic soil in releasing adsorbed ammonium nitrogen and phosphorus

1.4 Research Questions

i. How do the physicochemical properties of lateritic soil and *Agaricus impudicus* influence the adsorption of ammonium nitrogen and phosphorus?
ii. How do adsorption capacities and mechanisms differ between *Agaricus impudicus* and lateritic soils?
iii. How do desorption capacities and behavior of *Agaricus impudicus* and lateritic soils differ?

1.5 Justification of the Study

The extraction of nutrients from human urine is increasingly becoming popular as a way of reducing overuse of on synthetic fertilizers. The adoption of ecological systems such as urine-diverting dry toilets (UDDTs) has further enabled the separation of human urine at source for diverse uses such as application as a fertilizer. Over the past years, the direct utilization of human urine for farming (as fertilizer) has been practiced

in different regions, with studies showing higher crop yields as compared with synthetic fertilizers (Akpan-Idiok et al., 2012; Pradhan et al., 2007). Direct use of urine, however, has negative impacts. For instance, direct use of urine can cause pathogen contamination (Karak & Bhattacharyya, 2011). Additionally, it can affect the soil salinity, thus impairing the growth of crops (Sene et al., 2018). In an effort to eliminate these negative impacts, the World Health Organization recommends that human urine should be stored for at least six months before usage (WHO, 2006). This may not be suitable as it requires large space for storage and can cause environmental issues.

Nutrient recovery using low-cost adsorbents and subsequent reuse in crop production eliminates the need to store human urine for six months before usage, as recommended by WHO. However, use of fungal biomass (*Agaricus Impudicus*) in adsorption and desorption of ammonium nitrogen and phosphorus from human urine has been scarcely researched. Although a number of studies have been reported on the adsorption of nutrients using adsorbents derived from lateritic soils, limited studies have been done on their desorption properties. This study thus sought to evaluate the performance of *Agaricus Impudicus* and lateritic soils as adsorbents in nutrient recovery from human urine. It analyzed the potential of these adsorbents to release the trapped nutrients for crop use. The findings of this study are useful to organizations who provide sanitation services for management of human urine as a "valuable" resource that can be used in making fertilizers thus promoting circular economy. Additionally, this study provides comparative insights into the adsorption–desorption efficiency of natural, low-cost materials (*Agaricus Impudicus* and lateritic soils) applicable in decentralized sanitation systems.

1.6 Scope of the Study

The main focus of this study was to evaluate the efficiency of *Agaricus impudicus* and lateritic soils adsorbents in adsorbing ammonium nitrogen and phosphorus from human urine. Characterization of fungal and lateritic soil adsorbents were done to determine the physicochemical properties of these adsorbents that are crucial in adsorption of ammonium nitrogen and phosphorus. Batch adsorption experiments

were conducted to evaluate the adsorption behavior of the selected adsorbents under varying adsorbent loading, agitation speed, contact time and initial concentration. Lastly, desorption experiments were done to evaluate the desorption properties of the used adsorbents.

1.7 Limitations of the Study

Due to time constrains and high costs of performing batch adsorption experiments, only four factors that affect adsorption were analyzed in this study. Batch mode systems were used to conduct the adsorption experiments which may not fully represent complex real-world systems. The desorption experiments were conducted using laboratory conditions only thus may not fully describe the desorption behaviors of the adsorbents under field conditions.

CHAPTER TWO

LITERATURE REVIEW

2.1 General Overview

Human urine traditionally considered as waste has emerged as a highly valuable and underutilized resource especially within circular economy frameworks. Human urine contains valuable elements such as nitrogen, phosphorus and potassium that are crucial for crop production. Approximately 85% of the nitrogen is excreted in the form of urea, 10 % as organic N and 5% as ammoniacal nitrogen. Organic N majorly constitute of creatinine, uric acid and creatine (Martin et al., 2020; Rose et al., 2015; Udert et al., 2006). Phosphorus exists in a dissolved form as phosphate in urine (Udert et al., 2006). In order to recover these nutrients from human urine, UDDTs has been introduced in wastewater systems to help separate urine from other wastes and collect it at source for nutrient recovery. This facilitates post-treatment of diverted urine using different technologies such as ammonia stripping, struvite precipitation and adsorption. Additionally, they enable development of value chains for transforming human urine to fertilizers thus impacting the circular economy (Atanasova et al., 2021).

Nitrogen, an essential macronutrient, is predominantly present in fresh urine in the form of free ammonia (NH_3) and ammonium ($NH_4^+ - N$). However, NH_3 form easily lost from urine solutions through volatilization. $NH_4^+ - N$ on the other hand, increases with time as a result of hydrolysis caused by urease enzyme. This enzymatic reaction contributes to an increase in the concentration of NH_4^+ ions and a shift in the pH of urine from 6.0 – 6.5 to 9.0 -9.3 (Alemayehu et al., 2020; Wei et al., 2018). This alkalization process creates favorable physiochemical conditions in human urine such as increase ionic strength that significantly impact the adsorption of ions such as NH_4^+ and PO_4^{3-}.

2.2 Nutrient Recovery from Human Urine

Nutrient recovery from human urine has evolved from traditional practices such as direct use of human urine and storing it for six months before use into modern, tech-

enabled closed loop systems implemented at different scales (Simha et al., 2018). Globally, human urine has been reported as a critical resource for a bio-based economy as it consists of roughly 80-90 % of nitrates, 50-65 % phosphorus, and 50 -80 % potassium found in typical household wastewater (Baykal, 2019; Freguia et al., 2019; J. Liu et al., 2020a). Recovering and reusing all present in human urine could help to offset 16-21 % of global synthetic nitrogen fertilizers and 9-12 % of global synthetic phosphorus fertilizers demand in agricultural sector (Martin et al., 2023). Consumer acceptance plays an important role in this transition. A multinational survey that was conducted across 16 countries revealed that 59 % of the respondents were willing to replace inorganic fertilizers with urine-based fertilizers. However, the acceptance rate varied across countries with Jordan showing the lowest acceptance rate (14 %) and China recording the highest acceptance rate (80 %) (Simha et al., 2021).

At regional level, recovery of nutrients from wastewater such as human urine is often motivated by implementation of strategic environmental policies such as European Union's Circular Economy Action Plan (Avena Maia et al., 2023; Caspersen & Ganrot, 2018). Within Paris metropolis, the amount of nutrients excreted by approximately 12 million inhabitants of this city are estimated to be enough to replace all synthetic nitrogen and phosphorus fertilizers used in the region's intensive cropping systems (Martin et al., 2023). Within Sub-Saharan Africa region, the International Federation of Red Cross and Red Crescent Societies (IFRC) programs have succeeded in setting up roughly 1,000 urine diversion toilets Kenya, Burkina Faso, and Uganda to enable on-site nutrient recovery (Avena Maia et al., 2023; Freguia et al., 2019).

At local level, different cities and research institutions have set up pilot projects to evaluate the possibility of recovery nutrients from human urine and reusing it for agricultural production. For instance, in Tampere a city in Finland, research showed that the growth of barley fertilized with source-separated urine was the same as the growth of barley fertilized with mineral fertilizers (Martin et al., 2022). In Vellore, India, more than 80% of urea has been recovered from urine through coconut shell-activated carbon (Baykal, 2019; Ganesapillai et al., 2016). In Gothenburg, Sweden, the nutrient-enriched zeolite (NEZ) has been prepared and successfully used to nourish

plants such as sunflower (Caspersen & Ganrot, 2018). Hence, different technologies have been implemented to recover nutrient levels in human urine.

Some of the notable techniques include biological methods, membrane filtration, chemical modification, electro-dialysis, ion exchange, air stripping, construction of wetlands, struvite crystallization, membrane processes and adsorption mechanisms (Perera et al., 2019; Sengupta et al., 2015a). While these technologies have provided promising solutions in nutrient recovery, their applicability differ significantly depending on their cost, energy input, operational scale and environmental robustness. For instance, the use of air stripping to recover nutrients from human urine is ineffective because it's susceptible to pollution and limited to the removal of ammonia only (Wei et al., 2018). Although chemical modification is easy to operate and can be used to remove a wide range of pollutants, this technique involves the use of chemicals hence costly and may result in secondary pollution (Mehta et al., 2015; Najibul et al., 2021). Electrodialysis offer high recovery efficiencies but consumes a lot of energy making it less suitable for large scale applications (Mehta et al., 2015). Although, wetlands are easy to construct and operate it require larger spaces which may be challenging since land is a limited resource (Thorslund et al., 2017).

Adsorption mechanisms have been identified as the most suitable technology particularly for nutrient recovery. These systems are easy to construct and operate, requires low energy input, and can effectively target specific ionic species such as NH_4^+ and PO_4^{3-} that are dominant in human urine (Lepohi et al., 2022; Rathi et al., 2025). Additionally, they utilize local natural materials such as agricultural wastes, industrial wastes, soils and fungal materials (Saliu & Oladoja, 2021; S. Yadav et al., 2025), enhancing both economic viability and sustainability. Compared to other technologies, adsorption systems can be easily regenerated, scaled and integrated into on-site sanitation systems such as UDDTs. Consequently, when evaluated against criteria of operational cost, simplicity, energy demand, environmental impact, and suitability for decentralized implementation, adsorption emerges as practical and sustainable approach for nutrient recovery from human urine. Table 2.1 summarizes the merits and demerits of some of these technologies.

Table 2.1: Summary of Merits and Demerits of Nutrient Recovery Technologies

Technology	Merits	Demerits	References
Ion exchange	No formation of sludge Simple to operate Fast and efficient process	Requires large amounts of chemical agents to generate the resins. Risk of system logging. The regeneration of resins generates multiple secondary pollution problems.	(Wei et al., 2018)
Chemical Precipitation	Easy to manage Can operate within a high range of temperatures. Relatively fast	Production of large quantity of sludge Difficulty in the disposal of sludge	(Sengupta et al., 2015b; Ye et al., 2017)
Ammonia stripping	Effective for large scale applications Cost-effective and environmentally friendly	Not suitable for removal of phosphorus. limited to the removal of ammonia only	(Wei et al., 2018; D. Yang et al., 2022)
Electrodialysis	Favorable for use in solutions with low nutrient concentrations.	High operation cost as a result of high energy requirement and membrane fouling.	(Mehta et al., 2015)

Technology	Merits	Demerits	References
Construction of Wetlands	Require less energy for operation. Simple to construct Suitable for large scale application	Requires large space	(Ilyas & Masih, 2017; R. Liu et al., 2015)
Bioremediation	Relatively cheap. Treatment is onsite. Highly effective	Time consuming Not suitable for heavy metals. Sites used must have soils with high penetrability	(Pathy et al., 2021; Saravanan et al., 2021)
Urea hydrolysis	Fast precipitation High reduction of sludge Consumes less oxygen	Changes in efficiency with change in time. Formation of different compounds precipitates.	(Chen et al., 2017)
Microalgal accumulation	Production of a large amount of biomass.	Work under limited conditions Difficulties in biomass harvesting	(Behera et al., 2020; Santos & Pires, 2018)
Distillation and Nitrification	High efficieny Works well with other recovery methods	Substantial volatilization High energy use	(Udert & Wächter, 2012)

2.3 Low-Cost Adsorbents for Nutrient Recovery

The use of low-cost adsorbents for nutrient recovery is gaining popularity with many researchers focusing on their use in sustainable nutrient recovery. Excess nutrients, particularly nitrogen and phosphorus, are major contributors to water pollution and eutrophication in natural water bodies (Nie et al., 2018; Wurtsbaugh et al., 2019). This may cause harmful algal blooms, oxygen depletion, and destruction of aquatic habitats in water bodies (Devlin & Brodie, 2023; Dodds & Smith, 2016). Recovery of these nutrients not only minimize nutrient pollution but also allows for their reuse in agriculture, reducing overdependence on synthetic fertilizers. Natural adsorbents have emerged as an eco-friendly, cost-effective, and sustainable solution for nutrient removal and recovery because they are abundant in nature, biodegradable, and often derived from renewable resources (Laskar & Kumar, 2022; Thorat et al., 2025).

Natural adsorbents are derived from different materials each with unique properties that make them effective in adsorption of nutrients. Zeolites, for example, are naturally occurring aluminosilicate minerals with high cation exchange capacity, making them efficient in removing ammonium ions from wastewater (Guida et al., 2020). Biochar, a carbon-rich material produced through the pyrolysis of biomass, has a large surface area, porous structure, and functional groups such as carbonyl and hydroxyl that enables it to adsorb nutrients (Chakraborty et al., 2022). Clay minerals such as bentonite and kaolinites can remove nutrients such as phosphates through ion exchange and surface complexation (Biliani et al., 2024; Unuabonah et al., 2010). Additionally, agricultural wastes like rice husk, coffee husk, peanut shells, corncob, and pomegranate peels have shown a high potential as low-cost adsorbents of nutrients. Table 2.2 summarizes some of the low-cost adsorbents that have been used for adsorption of nutrients from wastewater.

Table 2.2: Summary of the Low-Cost Adsorbents

Adsorbent	Target Nutrient	Adsorption Capacity (mg/g)	Type of Experiment	Reference
Natural clay minerals	Ammonium nitrogen	9.97-50.06	Batch	(Alshameri et al., 2018)
Bentonites	Ammonium nitrogen	131.8-168.5	Batch	(Zamparas et al., 2021)
Rice husk biochar	Ammonium nitrogen	39.8	Batch	(Kizito et al., 2015)
Greensand (glauconite)	Ammonium nitrogen	19.24	Batch	(Naghipour et al., 2020)
Pineapple peel biochar	Ammonium nitrogen	13.40	Batch	(Otieno et al., 2021)
Pomegranate peels powder	Ammonium nitrogen	6.18	Batch	(Bellahsen et al., 2021)
Chitosan-Calcite	Phosphates	21.36	Batch and fixed bed	(Pap et al., 2020)
Natural clinoptitolite	Phosphates	7.57	Batch	(Mitrogiannis et al., 2017)
Fly ash	Phosphates	1.575	Batch	(Q. Liu et al., 2025)
Mussel	Phosphates	12.44	Batch	(Pap et al., 2022)
Oyster-shell	Phosphates	8.25	Batch	(Pap et al., 2022)
Seagrass residues of Posidonia Oceanica	Phosphates	8.3	Batch	(Photiou et al., 2021)

Overall, the use of low-cost adsorbents for nutrient recovery provides a sustainable solution for nutrient pollution and resource management. By focusing on renewable, low-cost materials and improving their adsorption capacities through using various modification techniques such as heat or chemical activation, natural and waste-derived adsorbents can play a key role in promoting nutrient recovery and environmental sustainability. This approach not only promotes cleaner water systems but also provides a pathway for reusing valuable nutrients, contributing to a more balanced and circular ecosystem.

2.3.1 Lateritic Soils and *Agaricus impudicus* Biomass as Adsorbents

Lateritic soils formed mostly in tropical and subtropical areas due to rapid weathering are known to possess low nutrient content thus not suitable for agricultural use. Owing to their limited nutrient content, lateritic soils have been predominantly utilized in the construction industry (Ng et al., 2019; Stoops & Marcelino, 2018). In recent years, however, their potential application as adsorbents has gained popularity, with most researchers focusing on their use in removal of heavy metals from wastewater (Chotpantarat et al., 2011; Iriel et al., 2018). Lateritic soils are rich in iron and aluminium oxides and clay minerals which provide abundant cation-exchange and electrostatic binding sites. These oxides provide surface hydroxyl groups that readily undergo either ligand exchange with P ions, forming strong, inner-sphere complexes that significantly enhance phosphorus removal (Mansing R & Rout, 2013). In contrast, NH_4^+ ions adsorption in lateritic soils occurs mainly through cation exchange and electrostatic interactions (R. Wang et al., 2025). The negatively charged surfaces of clay minerals and organic matter present within the soil matrix can exchange cations such as Na^+, K^+, or Ca^{2+} with ammonium ions in solution. This ion exchange process enables the soil to retain NH_4^+ in its exchangeable sites. The porous structure of the soil further facilitates physical adsorption and diffusion of ammonium ions, leading to

enhanced retention (S. Wang et al., 2023). These complementary mechanisms highlight the potential of using lateritic soils for simultaneous NH_4^+–N and P recovery. Hence, evaluating its adsorption capacity under varying adsorption factors such as agitation speed and adsorbent loading could provide useful insights on its suitability as a low-cost adsorbent in recovery of NH_4^+-N and P from human urine. Additionally, understanding its desorption efficiency could help in understanding its reusability in the agricultural sector.

Fungal biomass such as non-edible and edible mushrooms has also been identified as potential adsorbents with many studies focusing on their use in removal of heavy metals and dyes (Ayele et al., 2021; A. N. Yadav et al., 2019). Fungi belonging to Agaricus family possess cell walls rich in chitin, chitosan other polysaccharides with numerous functional groups such as carboxyl, hydroxyl and amino that are useful in binding NH_4^+-N and P ions (Sathya et al., 2021). Apart from surface chemistry, Agaricus biomass represents a renewable and potentially low-cost adsorbent as it grows naturally in forest ecosystems especially during the rainy seasons (Balan et al., 2022). Additionally, it can be cultivated on readily available and low-cost lignocellulosic agricultural residues under controlled conditions thus ensuring there are available in all seasons (Geng et al., 2024; Kosre et al., 2021). Despite all these advantages, there is limited information on the use *Agaricus impudicus* adsorbents in recovery of NH_4^+-N and P from human urine. Additionally, limited studies have been done to evaluate their ability to desorb the trapped nutrients.

Overall, although lateritic soils and fungal adsorbents possess favorable surface properties for nutrient adsorption, their comparative performance for both adsorption and desorption of NH_4^+–N and P from human urine remains largely unexplored. This study seeks to address this gap by evaluating the adsorption and desorption behavior of lateritic soils and fungal biomass. Thus, highlighting their novelty and potential as low-cost adsorbents for sustainable nutrient recovery from human urine.

2.4 Adsorption Process

Adsorption is a surface phenomenon involving the transfer of molecules (adsorbates) from a liquid or gas phase onto the surface of a solid (adsorbent). The physiochemical properties of adsorbates and adsorbent materials vary and are largely dependent on their structural composition and this influences adsorption. The process can be either physical or chemical in nature, depending on the interaction between the adsorbate molecules and the adsorbent solid surfaces (Lala et al., 2023). Adsorption process that is physical in nature is termed as physisorption. In this process, the interactions between adsorbents and adsorbate are driven by van der waals forces hence it is reversible (Barquilha & Braga, 2021). On the other hand, a process that involves chemical bonding is termed as chemisorption. Unlike physisorption, chemisorption processes occur only as monolayer and, thus, adsorbates transferred to adsorbents' surfaces cannot be removed easily as a result of strong chemical bonds involved (Pourhakkak et al., 2021).

2.4.1 Factors Influencing Adsorption Processes in Adsorbents

Adsorption kinetics and capacity of adsorbents depend on various factors such as the nature of the adsorbent, PH, adsorbent loadings, contact time, method of preparation of adsorbent, and stirring rate.

2.4.1.1 Physical and Chemical Properties of Adsorbents

The adsorbents' physical and chemical properties such as porosity, surface area, particle size, surface morphology and presence of functional groups have a major impact on their adsorption behavior. Adsorbents with higher surface area and porosity generally exhibit greater adsorption efficiency because they provide more active sites and allow faster intraparticle diffusion of molecules. For example, (Otieno et al., 2021) reported that pineapple peel biochar adsorbed higher amount of ammonium from human urine compared to lateritic soil, primarily due to its greater porosity, larger surface area, and high number of carbonates. Similar trends were observed by (Konneh et al., 2021), who found that coconut husk biochar outperformed rice and coffee husk biochar in nitrate from slaughterhouse wastewater due to porosity differences.

Adsorption of nutrients from aqueous solutions is highly influenced by the presence of functional groups such as carbonyl, hydroxyl, amine, alkine, carboxyl among others in the adsorbent materials used (Gunarathne et al., 2019; Leng et al., 2020). According to (J. Liu et al., 2020b), the surface functional groups have a major impact on N or P adsorption and may be basic or acidic. Basic surface functional groups are positively charged, containing OH ions, and they exchange phosphate ions in the solution, whereas negatively charged acidic functional groups (ionization of H+ ions) attract cationic ammonium species and exchange H+ on the surface of adsorbent material (Fan et al., 2019; Huong & Phuoc, 2024). Thus, adsorbent materials containing high number of functional groups are suitable for adsorption of nutrients.

2.4.1.2 Effect of Adsorbent Loadings on Adsorption

The amount of adsorbent utilized can influence adsorption capability. An increase in dosage can initially enhance adsorption capacity, but at a certain point, particle agglomeration may occur, lowering the number of available adsorption sites. (Konneh et al., 2021) conducted an experimental investigation to determine the influence of dose on adsorption kinetics. The authors used varying adsorbent loads of 0.5g, 1.0g, 1.5g and 2.0g in 50 mL. In this experiment, a gradual increase in adsorption capacity was witnessed up to 1.5g. Reduction of adsorption capacity in 2.0g adsorbent was observed and this can explain the particle agglomeration. Similar studies performed by (Maged et al., 2020) and (Divband et al., 2016) on the effects of adsorbent loadings on the removal of anions from an aqueous solution revealed the same trend.

2.4.1.3 Effect of pH on Nutrient Adsorption

The pH of the solution is a crucial operational parameter that directly impacts the adsorption behavior of nutrients such as ammonium and phosphate from aqueous solutions. Change in pH of an adsorbate can alter both the chemical speciation of the nutrients and the surface charge of the adsorbent (Kushwaha et al., 2013). For instance, fresh human urine typically has a pH near 6, but it undergoes significant chemical transformations such as urea hydrolysis during storage (Chipako & Randall, 2020). The enzymatic hydrolysis of urea causes the pH to rise to a strongly alkaline

range of 8.5–9.5. This alkalization is crucial as it increases the concentration of the target cation, NH_4^+ ions.

The impact of pH on adsorption behaviour is also dependent on the adsorbent type. For example, lateritic soils, which are rich in Fe and Al oxides, typically exhibit maximum phosphate adsorption at slightly acidic to neutral pH (Z. Tang et al., 2025). At these pH value, the surface hydroxyl groups are protonated and able to form strong ligand-exchange complexes with phosphate ions. At higher pH, these surfaces become deprotonated hence reduction in phosphate affinity (M. Li et al., 2025). Fungal biomass on the other hand consists of chitin and other protein-based functional groups such as hydroxyl and amine whose protonation varies with the pH. For instance, at lower pH amine group become protonated thus favouring anion binding whereas at neutral to slightly alkaline pH the carboxyl groups become deprotonated thus favouring the binding of cationic species such as NH_4^+ (Ertul et al., 2010; R. Tang et al., 2025).Thus, although low-pH model solutions are often used to establish the mechanisms, adsorption behaviour in raw human urine is majorly governed by its naturally alkaline pH and chemical changes such as alkalization. Urine alkalization during storage not only improves NH_4^+ availability but also alters surface interactions, making pH control a key factor in designing effective adsorption–desorption systems.

2.4.1.4 Effect of Agitation Rate of Adsorbate-Adsorbent Solution on Adsorption

Agitating or shaking of a solution loaded with adsorbent samples is essential as this creates a physical driving force of the processes. The rate at which agitation is done affects the adsorption mechanisms of adsorbent materials. (Bellahsen et al., 2021) explored the effects of agitation speed on the adsorption mechanisms of pomegranate peels in removal of ammonium from aqueous solutions. In this experiment, the agitation speed was varied from 100 to 400 rpm. The results revealed that maximum adsorption capacity (47.67%) occurred at 100 rpm. As agitation rate increased, there was a slight decrease in adsorption capacity. This can be attributed to formation of turbulence as a result of high rotation speeds thus causing detachment of adsorbed ammonium ions from the surface of adsorbent materials. Additionally, the interaction time between adsorbate and adsorbent molecules maybe limited at higher rotation

speeds thus affecting the adsorption mechanisms. Studies also conducted by (Genetie Abetu & Befekadu Kebede, 2021) and (Fetene & Addis, 2020) analyzed the impact of agitation speed on adsorption mechanisms. In their studies, (Fetene & Addis, 2020) varied the agitation speed from 100 to 250 rpm in 60 minutes. Results indicated maximum adsorption capacity at 200 rpm and beyond this point the authors witnessed a decrease in nutrients removed. (Genetie Abetu & Befekadu Kebede, 2021), on the other hand, varied the stirring speed from 50 to 300rpm in 120 minutes. Maximum adsorption capacity was recorded at 300rpm. All these studies demonstrate the significance of agitation rate on adsorption mechanisms.

2.4.1.5 Effect of Contact Time of the Adsorbent-Adsorbate Solution on Adsorption

Contact time refers to the duration of contact between the adsorbate and the adsorbent. It influences the amount of adsorbate that can be removed or retained by the adsorbent. (Konneh et al., 2021) in their experiment evaluated the effect of contact time on adsorption capacity of rice husk, coffee husk and coconut husk. Another experiment conducted by (Otieno et al., 2021) on the influence of contact time on adsorption capacity also showed the same trend. Gradual increase was exhibited between 0 to 60 minutes, slow decrease between 60 to 90 minutes beyond 90 minutes. Initially, when the adsorbate and adsorbent come into contact, rapid adsorption occur due to the availability of numerous adsorption sites on the surface of the adsorbent (Khan et al., 2015). This stage is often governed by film diffusion where target ions move from the bulk solution to the adsorbent surface. As contact time increases, the rate of adsorption gradually reduces as available adsorption sites are occupied. The process then transitions to a slower phase controlled by intraparticle diffusion, during which target ions move into the pores and internal structure of the adsorbent (Akafu et al., 2019). Once most active sites are occupied, the diffusion processes slow and an equilibrium state is attained, where no further significant change occurs.

2.4.2 Adsorption Kinetic Studies

Adsorption kinetic evaluations analyze the efficiency and rate-limiting steps of adsorbate removal and investigate adsorption mechanisms (Mohamed Nasser et al.,

2024; Serban et al., 2023). Various researchers have utilized different kinetic models in their adsorption studies. For example, (Alam & Anwar, 2020) and (X. Zhang et al., 2018) utilized pseudo-first-order kinetics, pseudo-second-order kinetics, Elovich and intraparticle diffusion models to generate kinetic curves in their studies. These models provide crucial information that can help in the development of low-cost and eco-friendly adsorbent materials.

The application of these kinetic models is particularly suitable for fungal and lateritic soils adsorbents due to their varying surface properties and different active functional groups. These adsorbents exhibit different adsorption mechanisms in nutrient recovery in human urine. Thus, PFO, PSO, and Elovich model help establish the dominating adsorption mechanisms for the two adsorbents (Guo & Wang, 2019). Additionally, the intraparticle diffusion model is essential in evaluating the contribution of pore diffusion and internal mass transfer in adsorption of ammonium nitrogen and phosphorus (Bian et al., 2024). Evaluating adsorption kinetics using these models therefore enables a better understanding of the dominant adsorption mechanisms governing the adsorption of nutrients from human urine.

2.4.2.1 Pseudo-First-Order Kinetic Model

This model is based on the assumption that rate of adsorption is proportional to the number of unoccupied active sites on the surface matrix of adsorbents (Chowdhury & Saha, 2011). In this model, the rate of adsorption is rapid at first when the active sites are still available on the adsorbent's surface. As these sites become progressively occupied, the adsorption rate declines until equilibrium is attained. The Pseudo First Order (PFO) kinetic model typically fits well for early-stage, surface-controlled adsorption, particularly when physisorption is the predominant mechanism. Equation 2.1 (X. Zhang et al., 2018) shows the non-linearized form of this model.

$$\mathbf{q_t = q_e(1 - e^{-K_1 t})} \tag{2.1}$$

Where:

Q_e = Equilibrium sorption capacity (mg/g)

Q_t = Sorption capacity at a specific time 't' (mg/g)

K_1 = rate constant (min^{-1})

2.4.2.2 Pseudo-Second Order Model

The Pseudo-Second Order (PSO) model is based on the assumption that the rate-limiting step in the adsorption process is chemisorption, involving valence forces through the sharing or exchange of electrons between the adsorbent and adsorbate (Chowdhury & Saha, 2011). In contrast to the PFO model, the PSO model fits better when adsorption process is governed by strong chemical interactions. The non-linear form of the pseudo-second-order kinetic model is expressed in Equation 2.2 (X. Zhang et al., 2018).

$$q_t = \frac{q_e^2 k_2 t}{1+q_e k_2 t} \tag{2.2}$$

Where:

q_e = Equilibrium sorption capacity (mg/g)

q_t = Sorption capacity at a specific time 't' (mg/g)

k_2 = Rate constant ($g(mg)^{-1}min^{-1}$)

2.4.2.3 Elovich Model

The Elovich model is commonly used to describe the kinetics of chemisorption on highly heterogeneous surfaces and is particularly useful when the adsorption process involves a new adsorbent with an unknown surface structure. The non-linearized form of this model is represented in Equation 2.3 (Khan et al., 2015).

$$q_t = \frac{1}{\beta} ln(1 + \alpha\beta t) \tag{2.3}$$

Where:

α = Initial rate of sorption (mg/g.min)

β = associated with the degree of surface coverage and the acti-

vation energy involved in the chemisorption process (g/mg)

2.4.2.4 Intra-particle Diffusion Model

This type of model is based on the assumption that adsorbates diffuse into the pores of adsorbents during the adsorption. It is used to identify whether the adsorption is controlled by intra-particle diffusion. Equation 2.4 shows the non-linearized form of this model (Alam & Anwar, 2020; Bellahsen et al., 2021).

$$q_t = k_i t^{\frac{1}{2}} + C_i \tag{2.4}$$

Where:

K_{di} = Intra-particle diffusion rate constant (mg/g$min^{o.5}$)

C = Intercept, which gives an idea about the boundary layer thickness (mg/g)

When $C_i = 0$, then rate-controlling step of the adsorption process is intra-particle diffusion and when $C_i \neq 0$ then the rate-controlling steps are film diffusion and intraparticle diffusion.

2.4.3 Adsorption Isotherm Studies

Adsorption isotherm models have been identified as significant tools in evaluating the efficiency and adsorption capacity of different adsorbents. These models provide useful information such as the adsorption mechanisms, equilibrium adsorption capacities and adsorbent-adsorbate affinities which are crucial in optimizing the adsorption systems. By fitting experimental data to isotherm models such as Langmuir, Freundlich and Dubinin–Radushkevich (D–R) model, one can be able to determine the nature of adsorption, whether it is monolayer or multilayer adsorption. Additionally, these models provide useful insights on the underlying adsorption mechanisms. They

help in distinguishing whether the adsorption process is governed by physiosorption (weak electrostatic interactions) or chemisorption (strong chemical bonding).

Isotherm models play a crucial role in designing and optimization adsorption systems for nutrient recovery. For instance, studies on recovery of ammonium nitrogen and phosphates from aqueous solutions rely heavily on isotherm models to obtain the equilibrium adsorption capacities and understand the adsorbent-adsorbate affinities (Bellahsen et al., 2021; Otieno et al., 2023a). These models also describe these how nutrients bind to the surface of the adsorbents thus providing insights on how easily they can be released and reused for crop production.

Lastly, the nature of the fitted isotherm behavior provides insights on the potential of adsorbents to release trapped nutrients (Rout et al., 2016). For instance, adsorbents that follow Freundlich or D–R isotherm behavior, are typically associated with heterogeneous surfaces and varying adsorption energies (Musah et al., 2022), which may facilitate easier nutrient desorption and controlled release. However, those best fitted with Langmuir model, may imply strong monolayer binding which may result in higher adsorption capacities but reduced desorption efficiency (Halajnia et al., 2013). Understanding these relationships is crucial in designing nutrient recovery systems.

2.4.3.1 Langmuir Model

The Langmuir model, as expressed by Equation 2.5, assumes that monolayer adsorption on a surface with a finite number of identical sites and no interaction between adsorbed molecules. When all the adsorption sites are occupied, there occurs no further adsorption, thus an equilibrium state is attained (Ayawei et al., 2017).

$$\frac{1}{q_e} = \frac{1}{q_m} + \frac{1}{K_L q_m C_e} \tag{2.5}$$

Where:

q_e =quantity of ions adsorbed at equilibrium state (mg/g)

q_m = maximum monolayer adsorption capacity of the adsorbent (mg/g)

C_e = concentration of the ions in the solution at equilibrium (mg/L)

K_L = Langmuir constant (L/mg)

2.4.3.2 Freundlich Model

This isotherm model is applied to heterogeneous systems, where it is assumed that different adsorption sites with varying adsorption free energies are present simultaneously, and it allows formation of multiple layers (H. Li et al., 2021). The linearized form of this model is shown in Equation 2.6 (X. Zhang et al., 2018).

$$Log\ q_e = Log\ K_f + \frac{1}{n} Log\ C_e \quad (2.6)$$

Where:

Ce = concentration of the ions in the solution at equilibrium state (mg/L).

K_f = Freundlich constant

$\frac{1}{n}$ = it indicates the adsorption intensity and the extent of heterogeneity of adsorbent's surface

The values of 1/n between 0 and 1 indicates the heterogeneity of adsorbent's surface with values closer to 0 indicating highly heterogeneous surfaces (Tan et al., 2008). When 1/n is less than 1, the adsorption process is considered favourable whereas, 1/n > 1, the adsorption process is considered as unfavourable and 1/n = 1 is considered irreversible (Kalam et al., 2021).

2.4.3.3 Dubinin–Radushkevich (D-R) Model

This isotherm model provides information on the mean free energy of adsorption, which can reflect the nature of the adsorption process; whether it is physical or

chemical. Equation 2.7 shows the linearized form of this model (Alrefaee et al., 2023; Musah et al., 2022).

$$lnq_e = lnQ_o - K_{DR}\,[RT(\ln\left(1+\frac{1}{C_e}\right)]^2 \quad (2.7)$$

Where:

Q_o = Maximum adsorption capacity (mg/g)

K_{DR} =D-R constant which gives the adsorption energy (E) (m)

R = Universal gas constant (8.314 J/mol·K),

T = Temperature (Kelvin)

Ce = Equilibrium concentration (mg/L).

Adsorption energy (E) can be calculated using Equation 2.8.

$$E = \frac{1}{\sqrt{2K_{DR}}} \quad (2.8)$$

The E value is used to establish the nature of adsorption process. If E < 8 kJ/mol nature of adsorption is considered to be physical and the adsorbates are held by weak electrostatic forces. When E values are between 8 and 16 kJ/mol then adsorption process is dominated by ion exchange mechanism and if E > 16 kJ/mol then the adsorption process is chemisorption in nature.

2.4.3.4 Temkin Model

The Temkin isotherm is used to describe adsorption systems in which the heat of adsorption of molecules in the layer decreases linearly with increasing surface coverage. It takes into consideration the indirect adsorbate/adsorbate interactions that influence the adsorption process (Foo & Hameed, 2010). The linear form of this model is shown in Equation 2.8 (Aslani & Amik, 2021).

$$q_e = \frac{R_T}{b} lnk_t + \frac{R_T}{b} \ln C_e \quad (2.8)$$

Where:

K_t= Equilibrium binding energy which corresponds to the optimum binding energy

(dm^3 /g)

B = Constant which is related to the heat of adsorption (J/mol)

R = Ideal gas constant (8.314 J/mol·K)

T = Absolute temperature (Kelvin)

2.5 Desorption Studies

Desorption has been identified as an effective way of recycling nutrients recovered from human urine and contributes to sustainable management of our resources in fields like agricultural production. Through desorption, nutrients trapped on the surface matrix of the adsorbents can be released in a controlled manner (Luo et al., 2021), enabling the reuse of the adsorbents and the recovery of nutrients in forms suitable for plant uptake. (Nguyen et al., 2021) evaluated the possibility of desorbing the nutrients adsorbed by biochar derived from rice husk and using it for production of hydroponic solution. (Ajmal et al., 2020) evaluated the efficiency of magnetically modified biomass-derived biochar in releasing trapped phosphates. Similarly, (Konneh et al., 2021) analysed the efficiency of biochar (rice husk, coffee husk, and coconut husk) in releasing the trapped nutrients for crop growth.

The desorption of nutrients can occur either through physical or chemical mechanisms (W. Zhang et al., 2022). Physical desorption is generally related to weak electrostatic and van der Waals forces and can be enhanced by changing the ionic strength through

dilution. On the other hand, chemical desorption is associated with disruption of ligand exchange reaction, strong ionic bonds, and surface complexations. This type of desorption often involves use of specific eluents or pH adjustments (Loganathan et al., 2014). The choice of desorbing agent and solution pH is crucial in desorption of nutrients. For instance, alkaline eluents are commonly used for phosphate desorption due to competitive hydroxyl ion exchange (Wu et al., 2019), whereas acidic eluents are used for ammonium desorption by since they alter the surface charge of adsorbents thus weakening the adsorbent-adsorbate interactions (Alcalde-Garcia et al., 2023). The use of distilled water as an eluent is common in desorption experiments there is need to minimize foreign ions or impurities that could interfere with the desorption process (Carleton & Cutright, 2020).

Understanding the desorption processes play a crucial in the design of adsorption-desorption systems that can be used in nutrient recovery for agricultural use. Desorption not only enhances the reusability and economic feasibility of adsorbents but also enables the recovered nutrients to be processed into alternative fertilizers or soil conditioners. Therefore, the recycling of nutrients via adsorption-desorption processes has the potential to mitigate the reliance on synthetic fertilizers, which are currently linked to environmental issues such as eutrophication, greenhouse gas emissions, and soil degradation.

2.6 Experimental Designs Commonly Used in Adsorption Studies

Experimental design plays a crucial role in adsorption studies, as it helps to establish the efficiency, robustness, and interpretability of the results. Several experimental designs have been reported in the literature, with the most commonly applied being the response surface methodology (RSM), factorial experimental designs and One-Factor-at-a-Time (OFAT) approach.

2.6.1 Response Surface Methodology (RSM)

Response Surface Methodology comprises of a number of statistical and mathematical techniques that are utilized in modelling and optimizing the adsorption systems. This is done by analyzing the effects of different process variables and their interactive

effects that impact the overall performance of the system. RSM is also used to build mathematical models that explain the overall process. Some of the commonly used designs in RSM include; central composite and Doehelrt designs (CCD) and Box–Behnken Designs (BBD). This method has been successfully used in optimizing the operating conditions of adsorption experiments while minimizing the number of experimental run (Bahrami et al., 2019; Benredouane et al., 2016).

The general equation for RSM is expressed in Equation 2.9.

$$y = \beta_{\circ} + \sum_{i=1}^{k} \beta_i X_i + \sum_{i=1}^{k} \beta_i X_i^2 + \sum_{i \neq j=1}^{k} \beta_i X_i X_{ij} + \in \quad (2.9)$$

Where:

y = predicted response (output variable)

X_{ij} = independent variables (factors)

k = number of factors

β_0 = intercept term

β_i = linear coefficients

β_{ii} = quadratic coefficients

β_{ij} = interaction coefficients

ε = ran dom error

However, RSM typically requires well-defined variable ranges and prior knowledge of system behavior, limiting its use in adsorption studies where effects of operating factors and adsorption behavior is not yet fully understood.

2.6.2 Factorial Experimental Designs

Factorial experimental designs are a form of multivariate approach, whereby two or more factors are varied simultaneously, enabling the evaluation of both main effects as well as interaction effects of variables (Montgomery, 2017). Full and fractional factorial designs have also been found to offer deeper insights into adsorption systems compared to the OFAT approach, especially when interaction effects of variables have a significant impact on adsorption systems (Panić et al., 2015). However, factorial experimental designs involve a significantly larger number of experimental runs as the number of factors is increased, which may not be feasible (Imessaoudene et al., 2023), especially when dealing with adsorption systems involving many operational parameters as well as costly analytical techniques.

2.6.3 One Factor at A time Approach

In this method, one variable is changed at a time while keeping other variables fixed to observe the effect of that variable on the response variable. The OFAT method is very common in adsorption studies because it is simple and easy to understand and is very useful as a preliminary tool (Husien et al., 2019). This method helps to identify the most important parameters that affect adsorption, e.g., contact time, adsorbent dose, pH, and concentration (Tibebu et al., 2025). Although it has faced criticism due to its failure to account for interaction effects (Montgomery, 2017), OFAT is considered as the most suitable experimental design method when parameter screening and understanding the adsorption mechanism are important, especially when working with new adsorbents or systems where limited information is known (Tibebu et al., 2025).

In the study, the OFAT method was used due to its suitability for evaluating the influence of different parameters on adsorption behavior of lateritic soils and fungal adsorbents. Additionally, scarce information is available on adsorption mechanisms of fungal adsorbents.

2.7 Summary of Literature Reviewed and Research Gap

With increasing global population, the food demand is also expected to rapidly rise. In an effort to promote food security, there is need to come up with sustainable alternative

fertilizer sources. Over the past years, Haber-Bosch processes and mine reserves for production of synthetic fertilizers have been relied on. However, Haber-Bosch process is energy-intensive whereas, mine reserves for phosphates are non-renewable (Geissler et al., 2015; International Energy Agency, 2021). Additionally, continuous use of synthetic fertilizers has negative impacts on the environment. In an effort to eradicate these demerits, the extraction of nutrients from human urine has been identified as a sustainable source of these crucial nutrients.

Techniques have been instigated to facilitate nutrient recovery from human urine which include ammonia stripping, chemical modification, construction of wetlands and adsorption mechanisms (Pathy et al., 2021; Saravanan et al., 2021). Among these techniques, adsorption mechanisms have been identified as an effective method as it involves the use of readily available materials as adsorbents. Additionally, adsorbents materials can be reused thus reducing secondary pollution. Although several studies have been done on nutrient recovery from human urine using different adsorbents. The use of fungi adsorbent and lateritic soils has not been adequately explored. Additionally, limited studies have been done exploring the influence of physicochemical properties of fungal adsorbent on its adsorption mechanisms and capacity. This analysis is aimed at evaluating the potential of using fungi (*Agaricus impudicus*) and lateritic soil as adsorbents for nutrient recovery in human urine and the possibility of reusing the recovered nutrients in agricultural production. Thus, reducing overdependence on synthetic fertilizers.

2.8 Conceptual Framework

A conceptual framework that shows the interconnection between independent and dependent variables in performance evaluation of the selected adsorbents in this study is shown in Figure 2.1

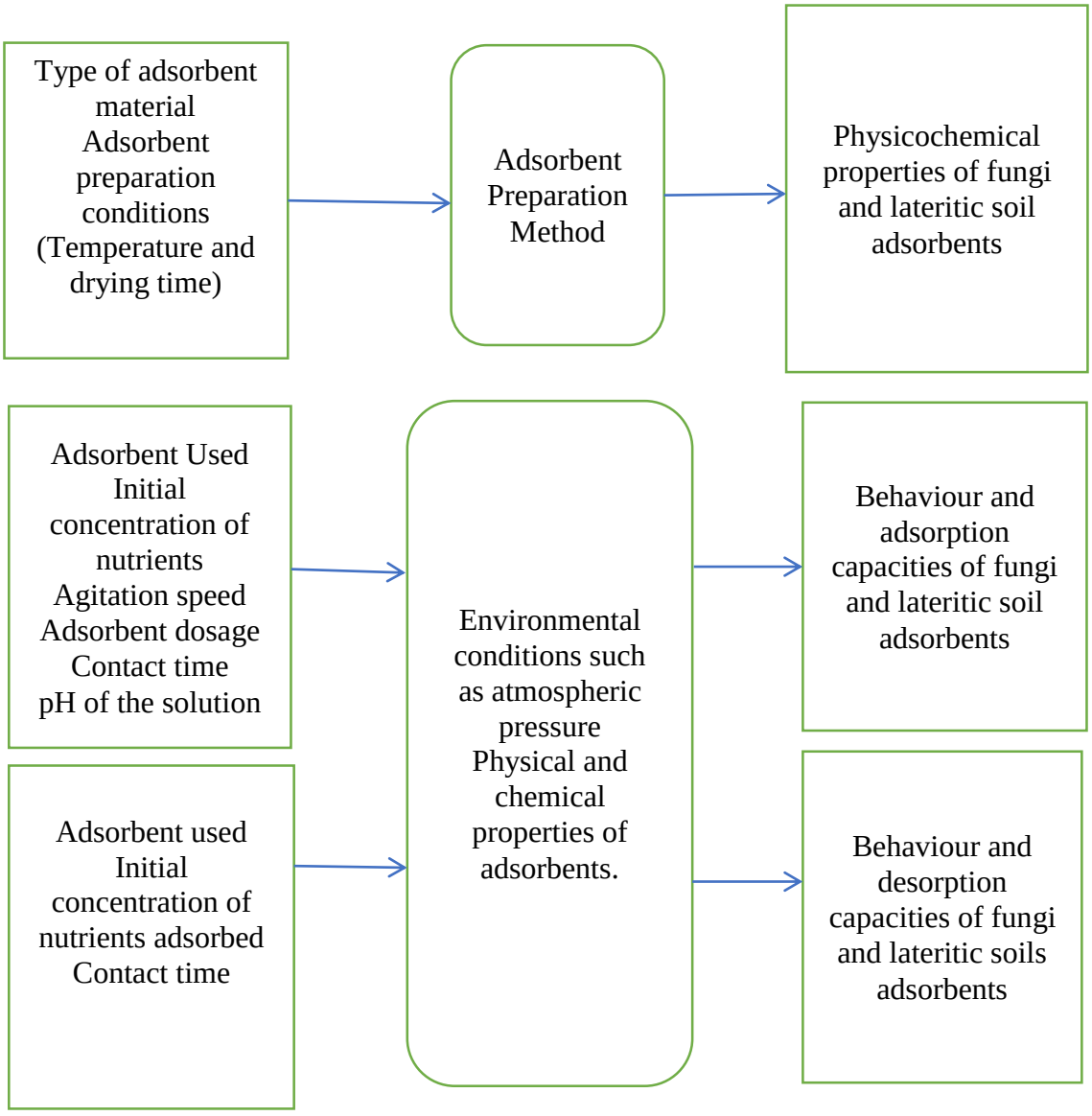

Figure 2.1: Conceptual Framework of the Study

CHAPTER THREE

MATERIALS AND METHODS

3.1 Description of the Experimental Location

The experiments for this study were carried out at Environmental Engineering Laboratory within the Department of Civil Engineering, Jomo Kenyatta University of Agriculture and Technology located in Juja, Kenya (1°05'44"S 37°00'44"E). Enviromental Engineering Laboratory was selected for experimental set up and data collection because it is well equipped with essential equipment for adsorption experiments. Figure 3.1 represent the experimental location.

Figure 3.1: A Map of the Experimental Location

3.2 Experimental Design

One Factor at a Time approach was used in designing the batch adsorption experiments for this study. Two different treatments (fungi and Lateritic Soils adsorbents) were used. Four factors (Initial concentrations, contact time, stirring rate

and dosage) were evaluated. One factor was varied while maintaining the other factors constant to determine its impact on adsorption capacity.

In evaluating the effect of initial concentrations, six varying concentrations of urine (Otieno et al., 2021) were prepared by diluting 100 mL collected urine sample with different amounts of distilled water (0, 20, 40, 60, 80 and 100 ml). The obtained concentrations were treated with 0.5 g of fungi adsorbent, and the concentration of ammonium nitrogen and phosphorus adsorbed determined. The same procedure was repeated for the lateritic soil adsorbents. In analyzing the effect of contact time, time duration of 100 minutes was considered while maintaining the other factors constant. The concentration of ammonium nitrogen and phosphorus adsorbed at each time duration were determined. Agitation speed was varied from 100 rpm to 190 rpm (Beig et al., 2023; Wystalska & Kwarciak-kozłowska, 2021) while holding the other factors at constants. The amount of ammonium nitrogen and phosphorus adsorbed by the selected adsorbent were determined for each stirring rate. Lastly, adsorbent dosage was varied from 0.125 g to 0.5 g (Wu et al., 2019; S. Yang et al., 2013) and the concentration of ammonium nitrogen and phosphorus adsorbed by each dosage determined.

Experimental runs were conducted in four replications for accuracy, reliability and validity of the experimental results. Treatments were assigned in a random order to reduce systematic errors (Gilman et al., 2021; Mtaallah et al., 2018). The data obtained from these experiments were plotted graphically to observe the trends. Analysis of Variance (ANOVA) were used to analyze the significance of each factor. Time-dependent batch adsorption data were analyzed using pseudo-first-order (Eqn. 2.1), pseudo-second-order (Eqn. 2.2), and Elovich (Eqn. 2.3) and intra-particle diffusion (2.4) Equations for kinetic modelling. Equilibrium data obtained were fitted using adsorption isotherm models (Langmuir (2.5), Freundlich (2.6) and Dubinin-Radushkevich (D-R) (2.7) models.

3.3 Physicochemical Properties of Fungi and Lateritic Soil Adsorbents

Figure 3.2 shows the overall methodological framework adopted in this study. It outlines the sequence of all the activities that were carried out to achieve specific objective one.

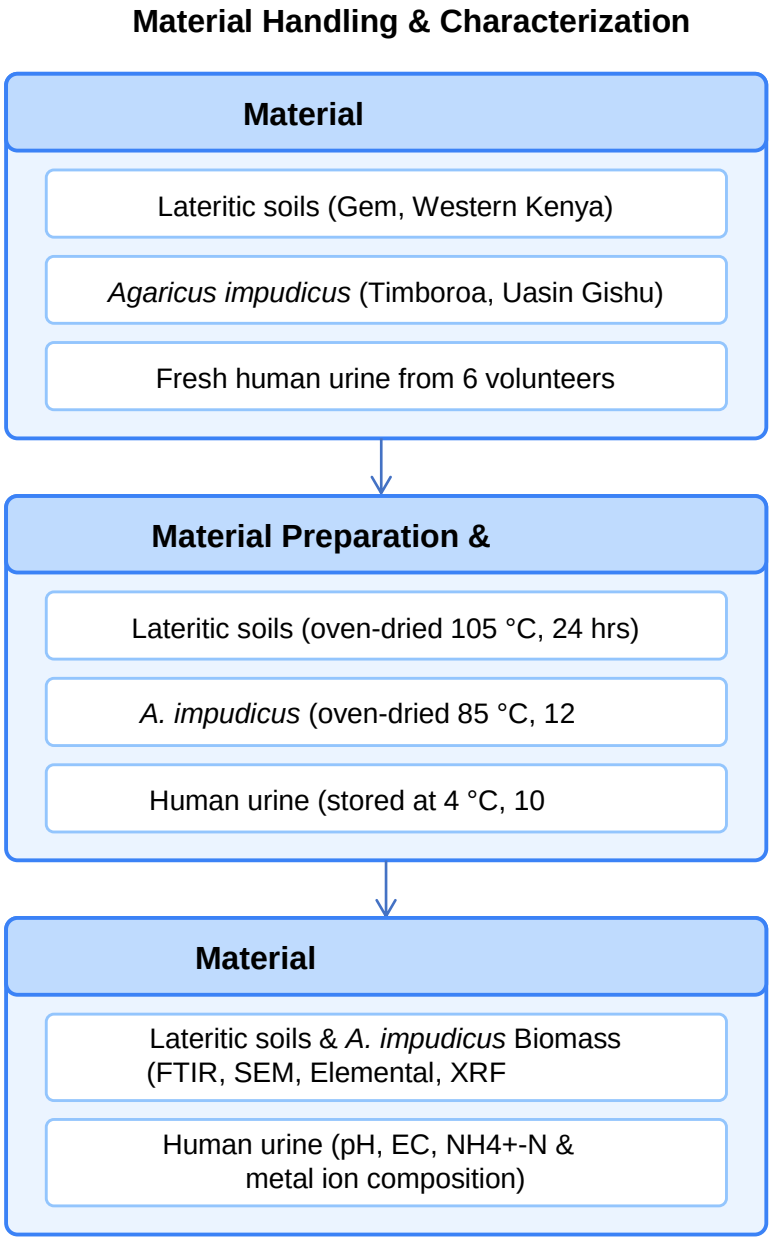

Figure 3:2: A Flowchart Showing all the activities for Determination of Physicochemical Properties of the Materials

3.3.1 Materials Preparation

A total of 24 Litres of fresh human urine samples were collected from six volunteers using clean plastic containers. The individual samples were combined to form a composite sample, minimizing variability and ensuring adequate volume for experimental use. The collection and use of human urine were reviewed and approved by the Scientific and Ethics Review Committee of Jomo Kenyatta University of Agriculture and Technology under reference number JKU/2/4/898B. All participants provided informed consent after being briefed on the study objectives, and no personal identifiers were recorded to maintain confidentiality. Immediately after collection, the composite urine sample was refrigerated at 4 ℃ for one week to minimize changes in physicochemical properties and suppress enzymatic activity prior to the analysis. No chemical preservatives were applied in order to preserve the natural composition and pH of the urine.

Fresh *Agaricus impudicus* (Rea) Pilát belonging to the mushroom family *Agaricaceae* were collected from Timboroa forest in Uasin Gishu County in Kenya. The specimens were identified and authenticated by a Taxonomist from the Department of Botany, Jomo Kenyatta University of Agriculture and Technology (JKUAT). The voucher specimens were deposited in the JKUAT Botany Herbarium (JKUATBH) with the accession numbers; FC-JKUATBH/001F/2025. Lateritic soil was collected from Gem, Siaya County, Western Kenya where it was dominant. Samples were collected by excavating 20 cm from the ground surface to ensure there are no surface organic contamination, minimize contamination and to obtain a more homogeneous mineral composition (J. Gao et al., 2023; Pepper & Gerba, 2015). Fungi were oven-dried at 85℃ for 12 hours to remove excess moisture while maintaining the contents of the cell wall such as chitin crucial for adsorption (Low et al., 2022). The dried samples were grounded and sieved to particle sizes ≤ 600 which was adopted from previous studies (Kalaruban et al., 2016; Krishna et al., 2016). Particle size reduction through grinding was done to increase the specific surface area and enhance accessibility of active adsorption sites, thereby improving mass-transfer kinetics and adsorption performance (Maleki & Karimi-jashni, 2017; H. Zhang et al., 2016). The grounded samples were kept in air-tight plastic containers for further analysis and use in batch

adsorption experiments. Similarly, lateritic soils were oven-dried at 105℃ for 24 hours, crushed, sieved to ≤600 μm and kept in air tight containers for experimental analysis.

3.3.2 Determination of Physicochemical Properties of Fungi and Lateritic Soil Adsorbents

Scanning electron microscope (JCM-7000-JEOL, Japan) was used to analyze the morphological appearance of the adsorbents. The dried samples were mounted on aluminium stubs using conductive carbon tape and sputter-coated with a thin layer of gold to minimize charging effects. SEM imaging was conducted under high-vacuum conditions at an accelerating voltage of 10.0 kV, with a working distance of approximately 18.2 mm. Micrographs were acquired at a magnification of ×1,500, corresponding to a scale bar of 10 μm. The SEM images obtained provided insights on the surface morphology and porosity of the adsorbents which influence adsorption kinetics.

Different functional groups that are crucial for adsorption in the adsorbents were examined using the Fourier Transform Infrared (FTIR) spectroscopy technique (ALPHA, Bruker Optics GmbH & Co. KG, Germany). Average IR spectra for each run were obtained from 32 scans at $4cm^{-1}$ resolution within a frequency range of within 4000-400 cm^{-1} Presence of Carbon, Hydrogen, Nitrogen, Sulphur in the adsorbents were evaluated using a CHNS elemental analyzer (Vario MACRO cube, Elementar Analysensysteme GmbH, Langenselbold, Germany). The ash content was determined the American Society for Testing (ASTM) (ASTM, 2003; (K. Liu, 2019) whereas the oxygen content was calculated using Equation 3.1(Demirbas, 2004).

$$O\ (\%) = 100 - (C + H + N + S + Ash) \quad (3.1)$$

Where:

C = Percentage of carbon content

H = Percentage of hydrogen content

N = Percentage of nitrogen content

S = Percentage of sulphur content

Ash = Percentage of Ash content

Chemical composition of the adsorbents was analyzed using X-ray Fluorescence (XRF) (Bruker SI TITAN 800, USA)

3.3.3 Determination of the Physicochemical Characteristics of Human Urine

Physicochemical attributes of human urine like pH, electrical conductivity and metal ion composition, ammonium nitrogen concentration, and phosphorus concentration were analyzed. Metal ion analysis of human urine samples was performed using the Atomic Absorption Spectrometer (AAS) technique. This was done to determine whether the metal concentrations in the human urine were within acceptable WHO regulatory limits. Metals analyzed include nickel (Ni), cadmium (Cd), chromium (Cr) and lead (Pb) calcium (Ca), copper (Cu), iron (Fe), and zinc (Zn). Before the analysis, 50 mL of urine was filtered using Whatman filter paper No. 1. and poured into 100 mL volumetric flask. 10 mL of concentrated nitric acid was then added to filtered urine samples and heated for 15 minutes at 120 ℃ to ensure complete digestion (Afridi et al., 2010; Camacho-delaCruz et al., 2025). After heating, the mixture was allowed to cool to room temperature. Quality assurance and quality control procedures including use of analytical grade chemicals in the sample preparation and digestion were adhered to in metal analysis. Sample replicates (n=3) and blanks were incorporated in the analytical procedure for accuracy and reproducibility. Instrument calibration was performed using standard solutions with metal elements to ensure analytical accuracy and instrument stability throughout the analysis. pH of Urine samples was measured using the HANNA 211 Microprocessor pH meter, while the electrical conductivity was measured using a conductivity meter.

3.4 Determination of Behaviour and Adsorption Capacity of Fungi and Lateritic Soils in Adsorbing Ammonium Nitrogen from Human Urine

In establishing the behaviour and adsorption capacities of Agaricus Impudicus Biomass and lateritic soils, a series of experimental activities were done. A summary of all the activities carried out have been presented in Figure 3.3.

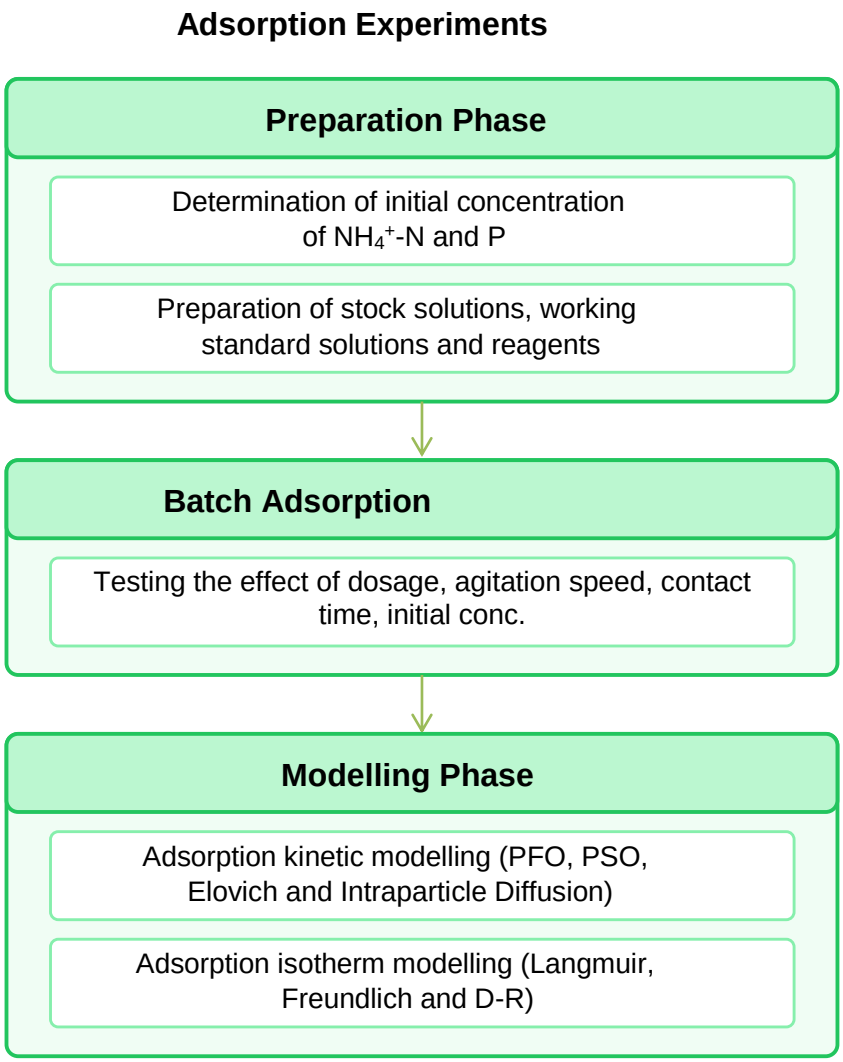

Figure 3.3: Summary of all the Activities for Adsorption Studies

3.4.1 Determination of Ammonium Nitrogen Concentration in Human Urine

Nesslerization method an analytical technique commonly used to determine the concentration of ammonia nitrogen in water samples were used to determine the concentration of $NH_4^+ - N$ in human urine (Zhou & Boyd, 2016).

3.4.1.1 Preparation of Reagent

Rochelle salt used in this experiment were prepared by dissolving 50g of potassium sodium tartrate tetrahydrate in 100 mL of distilled water. Nessler reagent was prepared by dissolving 100g of mercuric iodide (HgI_2) and 70 g of potassium iodide (KI) in a small quantity of water. The obtained mixture was slowly added, with stirring, to a cool solution of 160 g of sodium hydroxide (NaOH) dissolved in 500 mL distilled water (H_2O). This mixture was then diluted to 1 L and stored in rubber-stoppered borosilicate glassware.

3.4.1.2 Preparation of Ammonium Chloride Stock and Working Standard Solutions

NH_4Cl Stock solutions were prepared by dissolving 3.819 g anhydrousNH_4Cl, dried at 105℃, in distilled water and diluting it to 1000 mL. NH_4Cl Working standards were prepared by diluting 10 mL of stock solution to 1000 mL.

3.4.1.3 Determination of Calibration Line and Concentration Levels of Ammonium Nitrogen in Human Urine

In determining the calibration line, a series of working standards was made first by pipetting 1.0, 2.0, 4.0, 10.0, 20.0, 30.0 and 40.0 mL of standard solutions to different 50 mL volumetric flasks. Distilled water was then added to each volumetric flask up to 50 mL mark and the following concentrations were obtained; 0.2, 0.4, 0.8, 2, 4, 6 and 8 ppm. 0.5 mL of Rochelle solution were added to the diluted solutions and stirred. 0.5 mL of Nessler Reagent were added also and stirred as well. The absorbance of the obtained solutions was measured after 15 minutes at 425 nm wavelength using UV-VIS-1800 spectrophotometer (Shimadzu UV-1800, Japan). A mathematical expression for the calibration line was determined using excel. The resulting calibration curve exhibited a linear correlation ($R2 \geq 0.990$).

In determining the concentration of $NH_4^+ - N$, 0.1 mL of urine was pipetted into 100 mL volumetric flasks and diluted to volume with distilled water to minimize color interferences and the dilution factor used to calculate the final concentration. Additionally, to minimize color and turbidity interferences from calcium and magnesium precipitation, 0.5 mL of Rochelle salt solution was added to each diluted

sample. Subsequently, 0.5 mL of Nessler's reagent was introduced and the mixture was allowed to react for 15 minutes at room temperature to develop the characteristic yellow-brown coloration. The absorbance of the resulting solutions was measured at 425 nm using UV-VIS-1800 spectrophotometer.

Since Nessler's reagent contains mercury, all mercury-bearing wastes generated during the analysis were collected separately in clearly labelled, sealed containers, and stored for disposal through an JKUAT waste management facility in compliance with institutional policies and environmental safety regulations.

3.4.2 Phosphorus Quantification by Colorimetry

The concentration of phosphorus was determined using Molybdenum antimony colorimetric method (Sereenonchai et al., 2022).

3.4.2.1 Preparation of Reagents

Table 3.1 summarizes the chemicals and methods used to prepare the combined reagent (ascorbic acid-molybdate reagent) used in determining concentration of P in human urine.

Table 3.1: Chemicals and Methods of Preparation

Chemicals	**Formula**	**Preparation/Concentration**	**Storage conditions**
Ammonium heptamolybdate	$NH_4)6Mo_7O_{24}.4H_2O$	Ammonium heptamolybdate solution was prepared by dissolving 6g of $(NH_4)6Mo_7O_{24}.4H_2O$ salt in 200 mL of distilled water in 250 mL beaker.	Used immediately
Potassium antimonyl tartrate	$K(SbO)C_4H_4O_6.\frac{1}{2}H_2O$	Potassium antimonyl tartrate was prepared by dissolving 0.24 g	Used immediately

		$K(SbO)C_4H_4O_6.\frac{1}{2}H_2O$) of salt in 100ml distilled water 250 mL beaker.	
Sulphuric acid	H_2SO_4	H_2SO_4 solution was prepared by pouring 40 ml of distilled water in a beaker and adding 80 mL of concentrated H_2SO_4 in 250 mL volumetric flask.	Used immediately
Ammonium sulphamate	$NH_4SO_3NH_2$	Ammonium sulphamate solution was prepared by diluting 5 g of $NH_4SO_3NH_2$ salt in 80 mL of distilled water in 250 mL beaker.	Used immediately
Molybdate Reagent		Molybdate reagent was made by mixing the reagents prepared in the following order: 200 mL of $(NH_4)6Mo_7O_{24}.4H_2O$, 100 mL of $K(SbO)C_4H_4O_6.\frac{1}{2}H_2O$), 120 mL of H_2SO_4, and 80 mL of $NH_4SO_3NH_2$ in a 500 mL volumetric flask.	Stored using a glass stoppered bottle at room temperature.
Ascorbic acid solution		Ascorbic acid solution was prepared by dissolving 7.2 g of ascorbic acid in 100 mL of distilled water in 250 mL beaker.	Stored using a glass stoppered bottle at room

		temperature.
Combined reagent (Ascorbic acid+molybdate reagent)	Combined reagent was made by mixing molybdate reagent and ascorbic acid solution in the ratio of 5:1 in a 250 mL beaker.	Stored using a glass stoppered bottle at room temperature.

3.4.2.2 Preparation of Phosphorus (P) Stock and Standard Solutions

P stock solution of 1000 ppm was prepared by dissolving 4.39 g of Potassium dihydrogen phosphate (KH_2PO_4) (dried at 105℃) in 1000 mL of distilled water in 1000 mL volumetric flask. 2.5 mL of the obtained 1000 ppm P stock solution was measured and poured in 250 mL volumetric flask and diluted to 250 mL mark using distilled water to obtain P working standards of 10 ppm.

3.4.2.3 Determination of Calibration Line and Concentration of Phosphorus in Human Urine

In determining the calibration line, the following amounts of P working standard solution (1, 1.5, 2, 2.5, 3, 3.5 and 4 mL) were pipetted into different 50 mL volumetric flasks and diluted to 50 mL mark using distilled water. From the dilutions, 0.1, 0.2, 0.3, 0.4, 0.5, 0.6, 0.7 and 0.8 ppm standard solutions were obtained. 0.5 mL of combined reagent (ascorbic acid-molybdate reagent) was added to the obtained standard solutions. The absorbance of the obtained solutions was measured after 15 minutes at 880 nm wavelength using UV-Vis-1800 spectrophotometer (Shimadzu UV-1800, Japan). A graph of absorbance against concentration of P in the obtained solutions was plotted and the calibration curve obtained was used to determine the unknown concentrations of P in filtered human urine samples.

Concentration of P in urine samples were determined by pipetting 0.1 mL of filtered urine samples into a 100 mL volumetric flask and adding 0.5 mL of Molybdate reagent. The absorbance of the solution was measured using UV-VIS spectrophotometer at 880 nm after 15 minutes with a 1 cm cell against distilled water. The absorbance readings obtained were used to calculate the concentration of P in human urine samples.

3.4.3 Batch Adsorption Experiments

Batch adsorption experiments were carried out in this study to evaluate the effect of adsorbent dosage, effect of agitation speed, contact time and initial concentration on adsorption of phosphorus from human urine using lateritic soil and fungi adsorbents. The experiments were done in four replicates each at room temperature of 23 ± 1 ℃ and the mean values and standard deviations were calculated. Volume of human urine used was 25 mL. pH of the urine samples was adjusted to 7.16 ± 0.12 and 7.08 ± 0.35 before the $NH_4^+ - N$ and P experiments respectively using sodium hydroxide (NaOH) and hydrochloric acid (HCl). Untreated human urine was used as control samples in these experiments.

3.4.3.1 Effect of Adsorbent Loading

The effect of adsorbent loadings during adsorption studies were investigated by varying the adsorbent loadings. Loadings of 0.125 g, 0.25 g, 0.375 g, and 0.5 g of each adsorbent were added separately to each batch of beakers containing 25 mL of urine samples. The obtained mixture was agitated at 130 rpm and centrifuged at 2500 rpm for 10 minutes and filtered using Whatmann filter paper No. 42. The concentration of the NH_4^+-N and P in residual solutions were determined using a Spectrophotometer (Shimadzu UV-1800, Japan). The quantity of nutrients adsorbed and removal efficiency were calculated using Equation 3.2 and 3.3 respectively.

$$Q_t = \frac{(C_0 - C_t)V}{m} \tag{3.2}$$

$$Removal\ efficiency\ (\%) = \frac{C_0 - C_t}{C_0} \times 100 \tag{3.3}$$

Where:

Q_t = quantity of $NH_4^+ - N$ and P adsorbed by the adsorbents,

C_0 = initial concentration of $NH_4^+ - N$ and P in mg/L

C_t = the concentration of $NH_4^+ - N$ and P at time, t, in mg/L,

V = the volume of urine (L)

m = the mass of adsorbent (g).

Furthermore, one-way analysis of variance (ANOVA) was conducted to evaluate statistically significant differences in the adsorption data using Microsoft Excel, OriginPro, and the R statistical software (Version 4.4.2). Differences were considered statistically significant at $p < 0.05$. The use of multiple analytical platforms ensured consistency and robustness in the statistical evaluation of the experimental results.

3.4.3.2 Effect of Agitation Speed

Effect of agitation speed on adsorption was investigated by varying the agitation speed. 0.5 g of each adsorbent was added separately to each batch of beakers containing 25 mL of urine samples and agitated at 100 rpm, 130 rpm, 160 rpm and 190 rpm. After agitation, the samples were centrifuged at 2500 rpm for 10 minutes and filtered. The concentration of the NH_4^+-N in residual solution was determined using a Spectrophotometer (Shimadzu UV-1800, Japan). The quantity of nutrients adsorbed were calculated using Equation 3.2.

3.4.3.3 Effect of Contact time and Initial Concentration

Six samples of urine with different NH_4^+-N and P concentrations were used in these experiments. For NH_4^+-N adsorption the following concentrations were used; 556.78, 371.82, 351.54, 295.46, 280.44, and 208.65 mg/L. Table 3.2 summarizes the dilution scheme that was used to prepare these solutions.

Table 3.2: Dilution Scheme for Preparing Urine Samples with Varying NH4+-N Concentrations

Dilution	Urine Volume (mL)	Distilled water added (mL)	Total Volume Obtained (mL)	Final NH_4^+-N Concentration Obtained (mg/L)
1	100	20	120	556.78
2	100	80	180	371.82
3	100	160	260	351.54
4	100	240	340	295.46
5	100	320	420	280.44
6	100	400	500	208.65

For P adsorption experiments the following concentrations were used; 594.56, 505.74, 444.39, 408.60, 377.28, and 223.74 mg/L. These different concentrations were prepared by diluting original urine samples with 20, 80, 160, 240, 320 and 400 mL of distilled water. Table 3.3 summarizes the dilution scheme that was used to obtain the six different concentrations of P used in these experiments.

Table 3.3: Dilution Scheme for Preparing Urine Samples with Varying P Concentrations

Dilution	Urine Volume (mL)	Distilled water added (mL)	Total Volume Obtained (mL)	Final P Concentration Obtained (mg/L)
1	100	20	120	594.56
2	100	80	180	505.74
3	100	160	260	444.39
4	100	240	340	408.60
5	100	320	420	377.28
6	100	400	500	223.74

The influence of initial concentration on adsorption was evaluated by separately adding an adsorbent loading of 0.5 g in each batch of urine samples with varying nutrient concentrations. The mixed solutions were agitated at a speed of 130 rpm. Samples were withdrawn using syringes after every 10 minutes for 100 minutes and analyzed for $NH_4^+ - N$ concentration. The withdrawn samples were centrifuged at 2500 rpm for 10 minutes and filtered. The concentration of the NH_4^+-N and P in residual solutions were determined using a Spectrophotometer (Shimadzu UV-1800, Japan). The quantity of nutrients adsorbed and removal efficiency were calculated using Equation 3.2 and 3.3 respectively.

3.5 Adsorption Kinetics

Adsorption kinetic models were used to analyze the rate at which nutrients are adsorbed on the surface of adsorbents. Adsorption process was analyzed over time (0-100 mins) using 0.5 g of adsorbents and 25 mL urine samples. Time-dependent batch adsorption data was analyzed using pseudo-first-order (2.1), pseudo-second-order (2.2), and Elovich (2.3) and intra-particle diffusion Equations for kinetic models. Validation of these kinetic models was done comparing the R^2 and chi-square (x^2) values obtained after fitting the experimental data.

3.6 Isotherm Studies

Batch isotherm experiments were conducted to establish equilibrium adsorption capacities of the adsorbents. Six different concentrations of urine samples ranging from 208.7 mg/L to 556.8mg/L were used in batch experiments for $NH_4^+ - N$. For P experiments, six samples of urine with different nutrient concentrations (594.59, 505.74, 444.39, 408.60, 377.28, and 223.74 mg/L) were used. 0.5 g each of lateritic soil and fungi adsorbents were added separately to the 25 mL urine samples with different $NH_4^+ - N$ and P concentrations and agitated at 130 rpm at temperature 24 ± 1 ℃ for 100 minutes. The amount of nutrients adsorbed at equilibrium state was calculated using Equation 3.2.

Equilibrium adsorption data obtained were fitted using three models (Langmuir, Freundlich, and Dubinin–Radushkevich (D–R)). In evaluating the reliability of each isotherm model in describing batch adsorption equilibrium data, different statistical indicators which include; coefficient of determination (R^2), root mean square error (RMSE) and Sum of squared errors (SSE) were calculated. R2 and SSE values were directly obtained from the OriginPro 2024 (OriginLab Corporation, Northampton, MA, USA) software which was employed in fitting the adsorption data. RMSE values were calculated using Equation 3.4 (Imessaoudene et al., 2023).

$$\text{RMSE} = \sqrt{\frac{SSE}{DF}} \tag{3.4}$$

$$\text{DF= n-p} \tag{3.5}$$

where DF is the degree of freedom, n is the number of observed data and p is the number of parameters of the model

3.7 Desorption Behaviour of Fungi and Lateritic Soils Adsorbents in Releasing Adsorbed Nutrients

In determining the rate of release of ammonium nitrogen and phosphorus trapped in *Agaricus impudicus* and lateritic soils, batch and column desorption experiments were conducted. Figure 3.4 summarizes all the activities that were done to achieve specific objective 3.

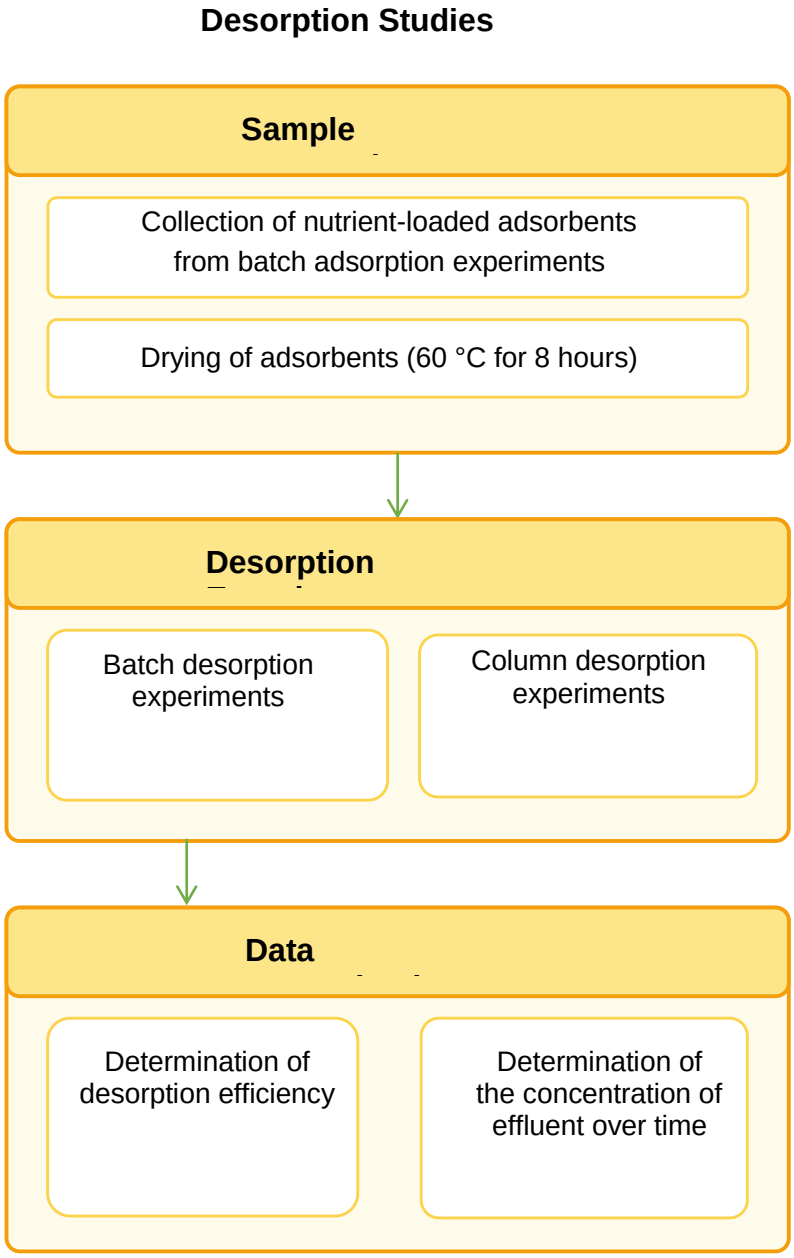

Figure 3.4: A Flowchart Summarizing the Desorption Studies

3.7.1 Desorption Studies

In desorption experiments, lateritic soils and fungi residues obtained from batch equilibrium adsorption experiments were used to analyse the release rate of adsorbed $NH_4^+ - N$ and P. These experiments were performed in four replicates and their mean values and standard deviations were calculated to reduce random experimental errors. Distilled water was used for the desorption experiment in order to minimize foreign

ions or impurities that could interfere with the desorption process (Carleton & Cutright, 2020). The control samples for these experiments were untreated distilled water. The residues were first oven-dried at 60 ℃ for 8 hours and their mass determined. 0.5 g of the dried samples were taken and added to separate beakers containing 25 ml of distilled water. The resultant mixtures were then transferred to a mechanical shaker and agitated at a speed of 130 rpm. Different samples were taken after 30, 60, 90, 120, 150, 180 and 210 minutes and centrifuged for 10 minutes to separate the solids from the liquids. The concentration of the nutrients in the desorption solution was then determined. The desorption efficiency was calculated using Equation 3.6 (Ajmal et al., 2020).

$$\text{Desorption Efficiency} = \frac{C \times V}{q \times m} \times 100\% \quad (3.6)$$

Where:

c = Amount of ions desorbed into the desorption solution (mg/L)

v = Desorption solution volume (L)

q = Equilibrium adsorbed amount of the ions before desorption (mg/g)

m = Mass of the adsorbent used in desorption experiment (g)

In order to mimic the field conditions, column experiments were performed to evaluate the desorption behaviour of fungi and lateritic soils. Column desorption experiments were carried out using plastic columns with 2.6 cm internal diameter and 20 cm length. Mass of the adsorbent packed on the column was 10 g and the bed height was 2 cm. A plastic sieve, followed by glass wool and acid-washed silicon beads was placed at the bottom of the plastic column to prevent the adsorbents from flowing out with the effluent. Distilled water was fed into the column using peristalic pump at a rate of 2.4 ml/min to flush the saturated columns for 390 minutes. The samples were collected over time and the concentration of ammonium nitrogen and phosphorus analyzed. Graph plots were drawn to show the rate of desorption of selected nutrients over time. Figure 3.5 Shows the experimental set up for column desorption experiments.

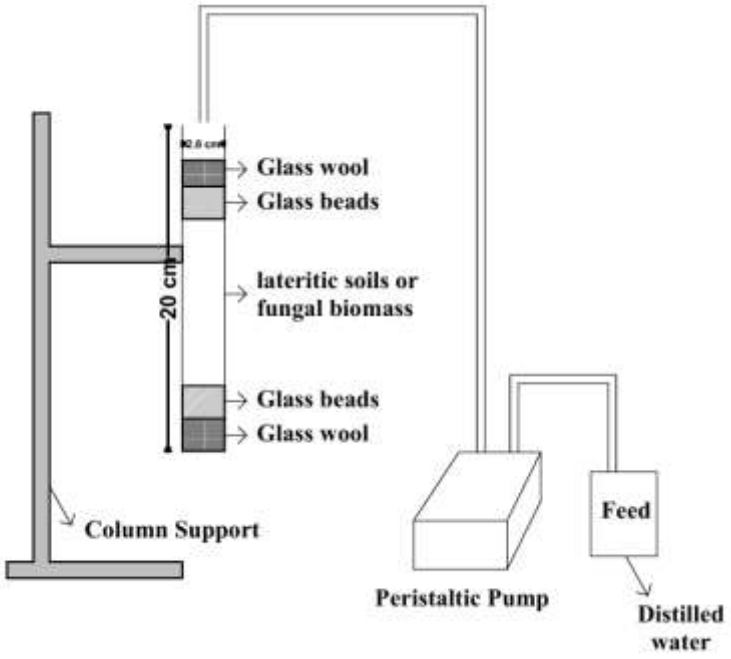

Figure 3.5: Experimental Set up for Column Desorption Experiments

CHAPTER FOUR

RESULTS AND DISCUSSION

4.1 Material Characterization

4.1.1 Physicochemical and Structural Properties of *Agaricus Impudicus* and Lateritic Soil Adsorbents

4.1.1.1 Fourier Transform Infrared (FTIR) Spectra of Lateritic Soils and *Agaricus Impudicus* before and after NH_4^+-N Adsorption Studies

The FTIR spectra of lateritic soils and *Agaricus impudicus* before adsorption studies were compared to the FTIR spectra after the adsorption. Figure 4.1a and b represent the FTIR spectra of lateritic soils and *Agaricus impudicus* respectively.

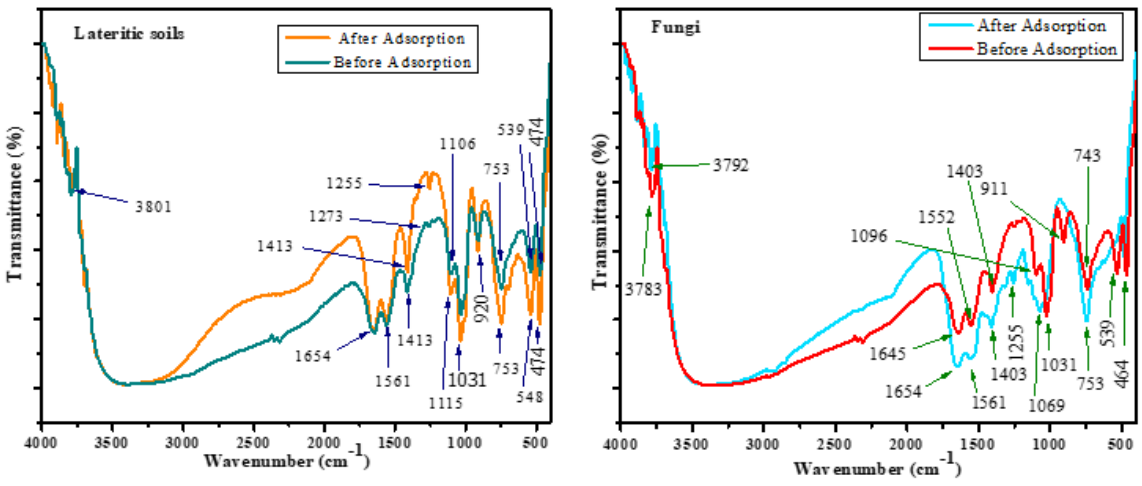

Figure 4.1: Fourier Transform Infrared Spectra Analysis of Lateritic Soils (a) and *Agaricus Impudicus* (b) before and after NH4+-N Adsorption

The FTIR spectrum of lateritic soils in Figure 4.1a before and after NH_4^+-N adsorption revealed noticeable shifts in wavenumbers and intensities of a number of functional groups, indicating their involvement in the adsorption process. For instance, before adsorption, –OH stretching vibrations appeared at 3798 cm^{-1} and a peak shift of -74 was noticed after adsorption. Additionally, the broad band at 3600-3000 cm^{-1} shifted to 3550-3100 cm-1 after adsorption. These changes could be as a result of hydrogen

bonding and electrostatic bonding of ammonium ions with -OH and C=O groups. Additionally, the peaks at 1660 cm^{-1} attributable to the C=O group stretch of the mica mineral and the peak at 1554 cm^{-1}, due to the OH group stretch of inner water molecules, and C–H, C-C, and C=C of typical alkyl and alkene stretching groups respectively, recorded a slight increase in intensities consistent with findings by (Otieno et al., 2023b). The changes are ascribed to occur due to hydrogen bonding of ammonium ions with -OH and C=O groups in the lateritic soils, as well as electrostatic and non-electrostatic interactions between ammonium nitrogen and the functional groups in the lateritic soil (Pham et al., 2017).

Related observations were recorded when fungal biomass were used as an adsorbent for removing ammonium nitrogen. As shown in Figure 4.1b, the FTIR spectrum of fungi before adsorption exhibited peaks at 3783, a broad band (3600-3200), 1645, 1552, 1403, 1038, 915, 752, and 545 cm^{-1}. After the adsorption of ammonium nitrogen, the peaks shifted to 3808, 1646, 1398, 1067, and 731 cm^{-1}, with the disappearance of the peak at 545 cm^{-1}, indicating both an increase and a decrease in peak intensities. It was observed that the peak at 3783 cm^{-1} shifted to a slightly narrower peak at 3792 cm^{-1}, while the peaks at 1645 and 1552 cm^{-1} shifted to higher wavenumbers and decreased in intensity, with new peaks emerging after adsorption at 1654 and 1561 cm^{-1} due to C=O and C=C functional groups in hemicellulose (Rudakiya & Gupte, 2019). A noticeable peak appeared after adsorption at 1255 cm^{-1}, which is attributed to the C-O functional groups that are regarded as adsorption sites within the fungal adsorbent (Alprol et al., 2025) . Moreover, a remarkable peak at 1069 cm^{-1} shifted to a narrow and more intense peak at 1067 cm^{-1}. This peak could be attributed to interactions between ammonium ions and C-H and C-O functional groups present in the adsorbent (Dong et al., 2013).

4.1.1.2 FTIR Spectra of Lateritic Soils and *Agaricus Impudicus* before and after P Adsorption Studies

Figure 4.2 a and b represent the FTIR spectra for lateritic soils and fungal biomass.

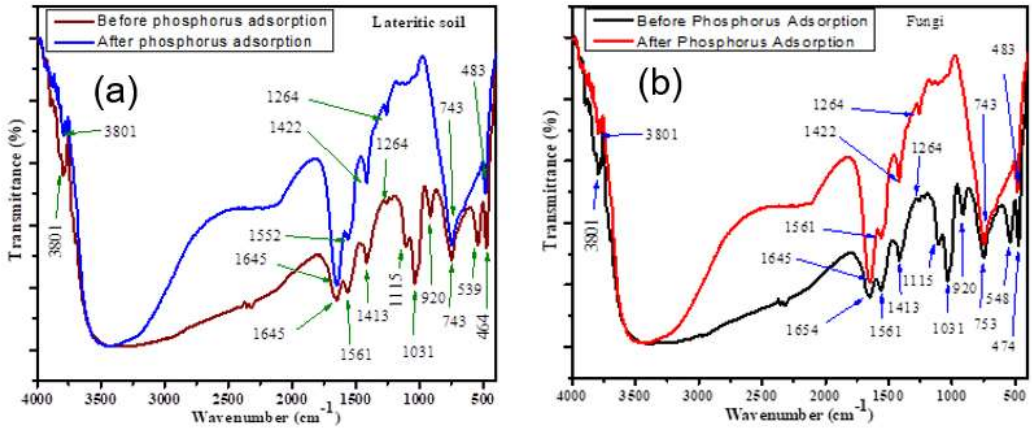

Figure 4.2: Fourier Transform Infrared Spectra Analysis of Lateritic Soils (a) and *Agaricus Impudicus* (b) before and after Phosphorus Adsorption

The FTIR spectra of lateritic soil and fungal biomass before and after adsorption exhibited significant changes in specific functional groups, indicating their involvement in the adsorption of phosphate ions in human urine. In lateritic soils IR spectrum, the surface hydroxyl groups (OH) at 3801 cm^{-1} showed a decrease in intensity after adsorption, suggesting that these sites acted as adsorptive sites of phosphate ions via hydrogen bonding or ligand exchange (L. Zhang et al., 2021). The carbonyl groups (C=O) at 1645 cm^{-1} increased in intensity post-adsorption, highlighting their role as polar binding sites that enhance phosphate retention. Notably, peaks corresponding to Al–OH (1115 cm^{-1}), Fe–OH (1031 cm^{-1}), and bridging groups such as Si–O–Fe (920 cm^{-1} and Al–O–Si (539 cm^{-1}) attributed to mineral components in the lateritic soil (Eisazadeh et al., 2012; Santha Kumar et al., 2022) changed significantly after adsorption. This suggests their involvement in phosphate ions binding. The surface functional groups Al–OH and Fe–OH act as active sites for phosphate adsorption through ligand exchange, while bridging groups such as Si–O–Fe and Al–O–Si enhance surface reactivity and charge distribution (M. Li et al., 2025; Suvokhiaw et al., 2025).

Remarkable changes in wavenumbers and peak intensities were noticed on fungal biomass IR spectra 4.2b after adsorption. A significant increase in peak intensity was recorded for the peak at 1654 cm^{-1} before adsorption as a new peak appeared at 1645 cm^{-1}, which is related to C=O stretching vibrations ascribed to hemicellulose in fungi

(Rudakiya & Gupte, 2019). This imply that C=O functional groups play a crucial role in adsorption of phosphate ions. C=O act as active sites for adsorption of phosphate ions as they facilitate complexation reactions (Xia et al., 2023). The peaks at 1115, 1031, 920, and 548 cm^{-1} shifted after the adsorption process and were related to C-H, C-O, and C-H out-of-plane functional groups (Rudakiya & Gupte, 2019). The shifting of these peaks could be attributed to hydrogen bonding whereby protonated phosphate ions form hydrogen bonds with C-O and C-H groups (Feng et al., 2022; Trinh et al., 2020). The peak intensity at 753 cm^{-1} increased after phosphate adsorption and shifted to 743 cm^{-1}. The peak at 474 cm^{-1} exhibited a slight decline in the intensity and changed to 483 cm^{-1}. The changes in wavenumbers and peak intensities indicates the contribution of functional groups as active adsorptive sites for sorption of phosphates.

4.1.2 Scanning Electron Microscopy (SEM) of Lateritic Soils and *Agaricus Impudicus*

Morphological structures of lateritic soils and fungal biomass were examined using scanning electron microscope. Figure 4:3 shows the images obtained from SEM.

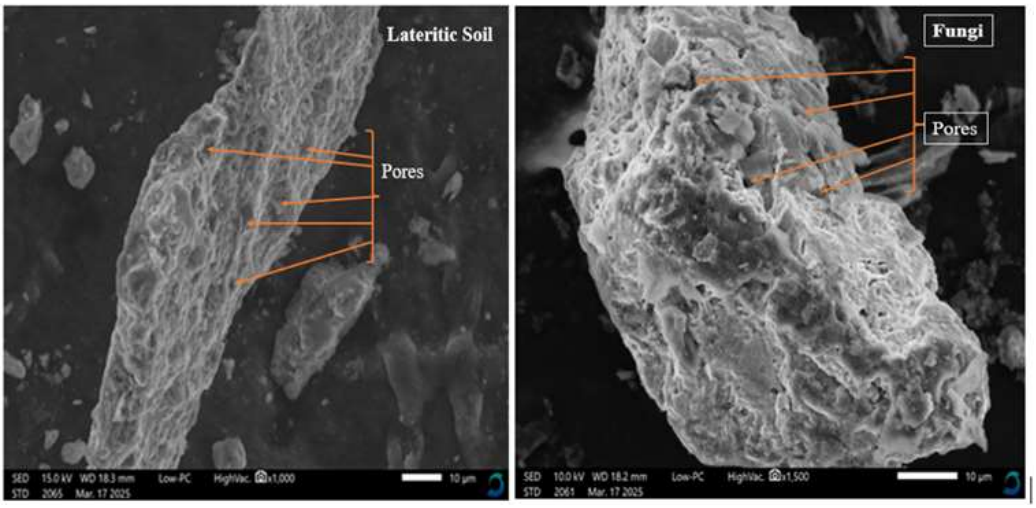

Figure 4.3: SEM Images of Lateritic Soils and *Agaricus Impudicus*

The SEM images for lateritic soils and fungal biomass were further visualized using ImageJ software to qualitatively assess the roughness nature of the adsorbents and pore distributions. The SEM micrograph of lateritic soils revealed elongated particles with highly irregular and rough surfaces. The overall structure appeared flake-like with

micropores. This aligns with the findings of (Y. Gao et al., 2021). Similarly, the surfaces of the fungal biomass were irregular and rough, likely due to the grinding process and the inherent nature of the material. This roughness is crucial for adsorption, as it enhances the contact rate between the adsorbent and the adsorbate, consistent with the conclusions of (Lu et al., 2020). Additionally, rough and irregular surfaces provide more active sites and enable faster mass transfer by minimizing diffusion limitations at the solid-liquid interface (Hellal et al., 2023). Thus, adsorbents with higher surface roughness generally exhibit faster adsorption rates and shorter times to reach equilibrium compared to smoother materials. Lastly, the surface exhibited microstructures, indicating a high surface area, which is beneficial for adsorption applications by increasing the material's capacity to trap and hold target molecules.

4.1.3 Elemental Analysis Results for Lateritic Soils and *Agaricus Impudicus*

Elemental analysis was done to identify the percentage of elements (carbon, nitrogen, hydrogen, sulphur, oxygen and ash content) present in lateritic soil and fungal biomass. Table 4.1 present the elemental results obtained.

Table 4.1: Elemental Results of Lateritic Soils and Fungal Biomass

Parameter	Lateritic Soils	Fungal Biomass
Carbon (%)	0.270 ± 0.06	39.810 ± 0.30
Nitrogen (%)	0.035 ± 0.02	7.455 ± 0.08
Hydrogen (%)	1.017 ± 0.06	6.078 ± 0.15
Sulphur (%)	0.020 ± 0.01	0.281 ± 0.01
Oxygen (%)	65.325 ± 0.51	28.430 ± 0.42
Ash content (%)	33.333 ± 0.58	17.946 ± 0.38

Lower carbon contents (0.270 ± 0.06 %) and high oxygen content (65.328 ± 0.51 %) were recorded in lateritic soils. This is reflective of the predominance of inorganic mineral oxides such as Fe- and Al-oxides in lateritic soils that are recognized to possess surface hydroxyl groups able to adsorb anions (Nandi et al., 2024). In contrast, fungi have higher carbon content (39.810 ± 0.30 %) and moderate oxygen (28.430 ± 0.42

%) content. This indicate the presence of organic functional groups (carboxyl, hydroxyl, amino) which are commonly found in cell wall components such as chitin and lignin-derived structures in white rot fungi (Akcay et al., 2023). The higher amount of nitrogen content (7.455 ± 0.08 %) in fungal biomass also indicates the presence of functional groups (**–**COOH**,** –OH, and –NH_2) which are crucial for binding cations via hydrogen bonding, ion exchange and electrostatic attractions (Das et al., 2008). Presence of high ash content (33.333 ± 0.58 %) in lateritic soils supports its mineralogical nature. Mineral components, especially iron and aluminum oxides are dominant in lateritic soils. These oxides help in adsorption of anionic pollutants. Elemental analysis of fungal biomass showed lower ash content (17.946 ± 0.38 %) as compared with lateritic soils (33.333 ± 0.58 %) due to predominant organic composition in the fungi cell wall. Fungi cell wall components contain a number of biosorption sites that are useful in elimination of a wide range of contaminants through adsorption mechanisms such as ion exchange, complexation, and surface precipitation (Latif et al., 2023).

4.1.4 Chemical Composition of Lateritic Soils and *Agaricus Impudicus* using X-ray Fluorescence (XRF) Analysis

The dominant components in lateritic soils which are significant for adsorption of nutrients from human urine as revealed by XRF analysis are SiO_2, Al_2O_3 and Fe which had 53.073 %, 22.466 % and 18.501 % respectively. High Al oxides and Fe are significant because they provide active adsorption sites for phosphate through ligand exchange and inner-sphere complexation (C. Liu et al., 2022; Z. Yang et al., 2024). Fungal biomass on the other hand, exhibited higher amount of MgO (18.985 %) and moderate amount of CaO (2.506 %). Presence of MgO content is crucial for removal of ammonium and phosphate ions in aqueous solutions. MgO readily hydrates in aqueous solutions to form magnesium hydroxide ($Mg(OH)_2$), generating surface –OH groups that contribute to a negatively charged surface at neutral to alkaline pH conditions (Amaral et al., 2010). These surface hydroxyls facilitate NH_4^+ ions adsorption primarily through electrostatic attraction between the positively charged NH_4^+ ions and negatively charged -OH sites. On the other hand, dissolved Mg^{2+} ions released from MgO hydration react with phosphate to form low-solubility magnesium

phosphate phases ($Mg_3(PO_4)_2$)), enhancing phosphate removal from solution (Kiani et al., 2018). The presence of CaO further supports phosphate precipitation via calcium phosphate phases ($Ca_3(PO_4)_2$, hydroxyapatite) (Ou et al., 2023; Y. hui Yu et al., 2023), enhancing phosphorus removal. The summary of XRF results is shown in Table 4.2.

Table 4.2: XRF Results for Lateritic Soils and *Agaricus Impudicus*

Element	**SiO_2**	**Al_2O_3**	**Fe**	**Cl**	**MgO**	**CaO**
% composition in lateritic soils	53. 073	22.466	18.501	0.127	_	0.245
% composition in *Agaricus impudicus*	_	2.912	0.865	3.279	18.985	2.506

4.1.5 Physicochemical Properties of Human Urine

pH of the human urine was found to be 7.40 ± 0.18. Electrical conductivity was 10,610 ± 0.35 µS/cm. The concentrations of calcium, copper, iron, and zinc were 19.78 ± 0.05 mg/L, 0.213 ± 0.15 mg/L, 1.97 ± 0.05 mg/L, and 0.14 ± 0.03 mg/L respectively. Cadmium, chromium, nickel and lead were below detection limit (BDL). The concentration of ammonium nitrogen and phosphorus were found to be 0.758 ± 0.15 g/L and 0.893 ± 0.21g/L respectively. The value of pH obtained in this study is within the recommended limits by FAO (FAO & others, 2017) which is 6.5-8.4. Electrical conductivity value obtained was above the recommended limits by FAO (2250 µScm-1). High EC values in human urine can be attributed to presence of dissolved salts and nutrients ions such as ammonium (NH_4^+), calcium (Ca^{2+}), potassium (K^+), phosphates (PO_4^{3-}) and Cl^- (Mitrogiannis et al., 2023). Adsorption mechanisms provide an effective way of reducing EC through selective removal of ionic species. Metal ion analysis of the human urine revealed the presence of plant-essential metals, including calcium, copper, iron, and zinc whose concentrations were within the recommended limits by WHO (WHO, 2006). These findings compare closely with those reported by (Patel et al., 2021). Plant non-essential metals (Cadmium, chromium, Nickel and Lead)

were below detection limit (BDL) in the sample which suggests the urine was free from heavy metal contamination thus safe for nutrient recovery and reuse in agriculture. The summary of the physico-chemical properties is presented in Table 4.3

Table 4.3: Physical and Chemical Properties of Human Urine

Parameter	Unit	Value	WHO Limit
Physiochemical properties			
Ammonium Nitrogen	g/L	0.758 ± 0.15	
Phosphorus	g/L	0.893 ± 0.21	
pH		7.40 ± 0.18	6.5-8.4
Electrical Conductivity	µS/cm	10,610 ± 0.35	≤ 2250
Metal ion composition			
Plant essential metals			
Calcium	mg/L	19.78 ± 0.05	100
Copper	mg/L	0.21 ± 0.15	1
Iron	mg/L	1.97 ± 0.05	10
Zinc	mg/L	0.14 ± 0.03	0.5
Plant non-essentials metals			
Cadmium	mg/L	BDL	0.1
Chromium	mg/L	BDL	0.05
Lead	mg/L	BDL	0.005
Nickel	mg/L	BDL	1

4.2 Determination of Behaviour and Adsorption Capacity of *Agaricus Impudicus* Biomass and Lateritic Soil in Adsorbing Ammonium Nitrogen from Human Urine

4.2.1 Effect of Adsorbent Loading on NH_4^+-N Adsorption

The effect of adsorbent loading on the percentage removal of $NH_4^+ - N$ by fungal biomass and lateritic soil was investigated by varying adsorbent quantity in the range of 0.125-0.5 g, and the results are presented in Figure 4.4.

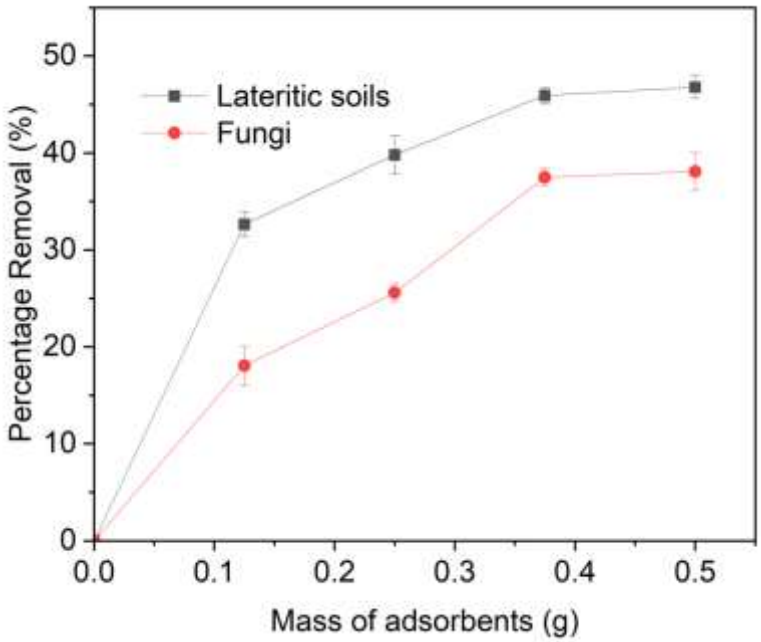

Figure 4.4: Effect of Adsorbent Loading on Ammonium Nitrogen Removal

It was noticeable that there was a gradual increase in percentage removal of NH_4^+-N with the increase in adsorbent loading from 0.125 to 0.5 g in both lateritic soils and fungal biomass. Both adsorbents exhibited a gradual increase in percentage removal between 0.125 g and 0.375g. However, beyond 0.375 g percentage removal gradually decreased. At 0.125 g, 32.63± 1.27 % and 18.08 ± 2.03 % percentage removal were obtained for lateritic soils and fungal biomass, respectively. At the highest adsorbent loading of 0.5 g, the percentage removal of 46.78 ± 1.16 % and 38.08 ± 1.94 % for lateritic soils and fungal biomass were obtained, respectively. The gradual increase in percentage removal of NH_4^+-N between 0.125g and 0.375 g in both adsorbents can be attributed to increased active adsorption sites as the amount of adsorbent increased. There was an insignificant increase ($p = 0.07$ for lateritic soils and $p = 0.10$ for fungal biomass) in percentage removal by both adsorbents when dosage was 0.375 g to 0.5 g. This may be associated with overlapping of adsorbent layers as the loadings increased thus obscuring the oxidizing active sites (Dey et al., 2021). This reduction could also

be linked with particle aggregation as a result of high adsorbent dosage which reduces the surface area available for adsorption.

Similar studies have been undertaken to investigate the effect of adsorbent loadings on adsorption of ammonium. In a study by (Alshameri et al., 2018), a similar trend was observed whereby the amount of $NH_4^+ - N$ adsorbed by natural clay minerals increased rapidly with an increase in adsorbent loading from 0.1 g to 0.3 g, beyond which no noticeable increase occurred. (Nguyen et al., 2021) observed a similar trend in their studies on removal of $NH_4^+ - N$. In these studies, adsorption efficiency increased gradually and stabilized with a further increase in adsorbent dosage. This phenomenon was attributed to increased active adsorption sites with the initial dosage increase. However, when the adsorbent loading was increased to a certain amount, the ions' adsorption did not increase significantly because of the overlap of the adsorbent layers, thus obscuring the oxidizing active sites (Gelaw et al., 2024).

4.2.2 Effect of Agitation Speed

Figure 4.5 shows the quantity of ammonium nitrogen removed by lateritic soils and fungal biomass at agitation speeds of 100, 130, 160 and 190 rpm.

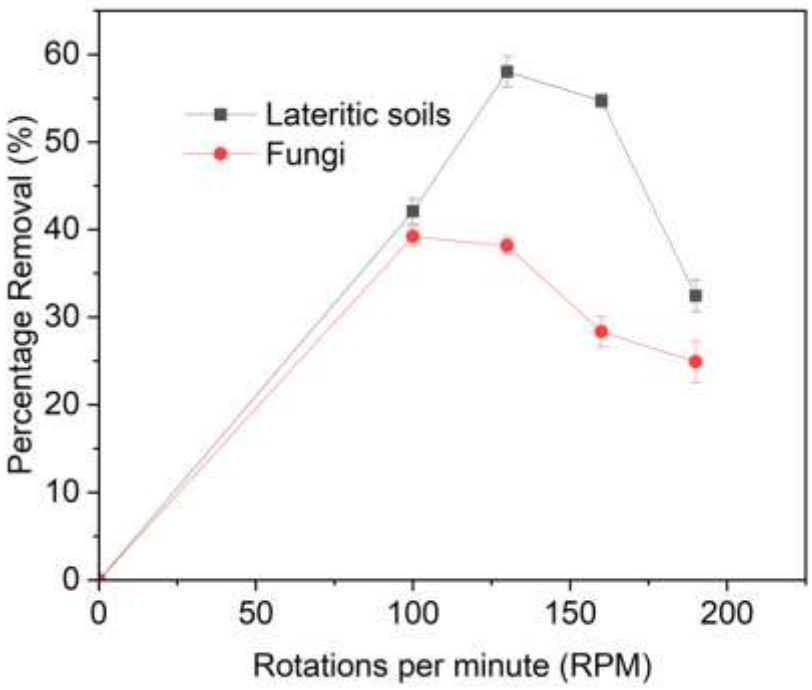

Figure 4.5: Effect of Agitation Speed on Ammonium Nitrogen Removal

An increase in the amount of $NH_4^+ - N$ removed was recorded with increase in agitation speed between 100 rpm and 130 rpm in lateritic soils. Beyond 130 rpm, the percentage removal decreased. In fungal biomass, between 100 rpm and 130 rpm a decrease on quantity of $NH_4^+ - N$ adsorbed was noticed. Beyond 130 rpm, a gradual decrease in quantity $NH_4^+ - N$ of adsorbed was observed. In lateritic soils, the highest removal percentage of 58.03 ± 1.77 % was recorded at 130 rpm while the highest removal of 39.21 ± 1.11 % for fungi was achieved at 100 rpm. The removal percentage gradually decreased as the agitation speed was increased from 130 rpm to 190 rpm for both adsorbents. The initial increase in the quantity of $NH_4^+ - N$ of adsorbed with an increase in agitation speed can be attributed to the even distribution of adsorbent in the adsorbate (Manikam et al., 2019). Gradual decrease exhibited beyond 130 rpm can be associated with the formation of turbulence due to high agitation speeds, thus causing detachment of adsorbed ions from the surface of adsorbent materials (Bellahsen et al., 2021). (de Luna et al., 2018) observed a similar trend in their study on $NH_4^+ - N$ removal from aqeous solution using chitosan-based bentonite. In their respective studies on chromium (Kumar & Chauhan, 2019) and fluoride (Tefera et al., 2020) adsorption, similar trends were observed. Both studies showed an initial increase in percentage removal with increased agitation speeds, attributed to the dispersion of adsorbent particles in the aqueous solution, which can reduce the boundary layer for mass transfer.

4.2.3 Effect of Initial Concentration and Contact Time

The quantity of ammonium nitrogen adsorbed onto lateritic soils and fungal biomass with varying initial concentrations and contact time is presented in Figure 4.6.

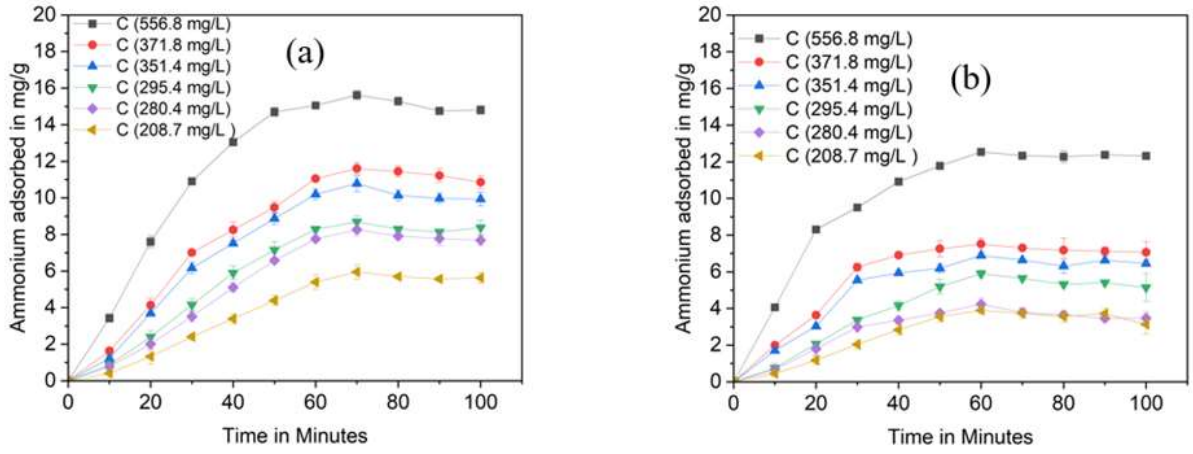

Figure 4.6: Effect of Contact Time and Initial Concentration on Ammonium Nitrogen Removal

The quantity of $NH_4^+ - N$ adsorbed increased gradually as contact time increased from 0 to 100 minutes for all the concentrations in both lateritic soils and fungal biomass. In lateritic soils, fast adsorption was observed between 0 and 40 minutes. Between 40 and 70 minutes the adsorption rate gradually decreased with equilibrium being attained at 70 minutes. Beyond 70 minutes, there was no significant change in $NH_4^+ - N$ adsorbed. In fungal biomass, the adsorption rate was high between 0 and 30 minutes. Between 30 and 60 minutes, the adsorption rate started to decrease gradually and equilibrium was achieved at 60 minutes. Beyond 60 minutes, there was no significant change in the amount of $NH_4^+ - N$ adsorbed. The fast initial adsorption rate observed can be attributed to unoccupied active adsorption sites at the start of the experiment, which allowed the adsorbates to diffuse and quickly attach to these sites. The gradual decrease in adsorption rate for both adsorbents could be as a result of most active sites being occupied. At equilibrium almost all sites have been occupied hence limiting adsorption. Similar trends were observed in studies that were conducted by other authors on the removal of ammonia using calcium alginate beads and removal of nitrates using activated charcoal (Isik et al., 2021; Mazarji et al., 2017). These authors attributed the increase in the removal rate at the start of the experiment to availability of many active sites for adsorption. These sites however become occupied as time increases causing the adsorption rate to drop and become insignificant. Another study

by (Konneh et al., 2021) reported similar trends on removal of nitrates and nitrites and explained this phenomenon to be as a result of availability of many adsorption sites for ions to occupy initially. As time progressed, these sites were occupied thus the adsorption rate slowed down and eventually an equilibrium state was attained.

On the effect of initial concentration, at the lowest concentration (208.7 mg/L), the quantity removed by lateritic soils and fungi were 5.95 ± 0.39 mg/g and 3.90 ± 0.19 mg/g respectively after equilibrium time (70 minutes). At the highest concentration (556.8 mg/L), the quantity removed by lateritic soils was 15.62 ± 0.25 mg/g and that of fungal biomass was 12.53 ± 0.19 mg/g after 70 minutes. The increase in quantity of $NH_4^+ - N$ adsorbed as the initial concentration of $NH_4^+ - N$ increased could be as a result of a concentration gradient that is formed between the adsorbate and adsorbent with increase in the number of ions which contribute to increase in diffusion rate. The results of this study compare closely with those reported in existing literature. For instance, (Wahab et al., 2010) noticed the same trend in their study on $NH_4^+ - N$ biosorption using sawdust and they attributed this to concentration gradient that existed between the sawdust biosorbent and aqueous solution. Similar studies conducted by (Kabuba & Lephallo, 2023) investigating the efficiency of activated carbon prepared using waste tyres in $NH_4^+ - N$ removal exhibited a similar trend when initial concentration was increased from 30 mg/L to 50 mg/L with percentage removal of $NH_4^+ - N$ increasing from 38% to 77%. The authors attributed this trend to increase in the mass driving force and diffusion rate of ammonium ions into the adsorbent as concentration of $NH_4^+ - N$ in aqueous solution is increased. Further, (Otieno et al., 2021) reported a similar trend on ammonium recovery using pineapple peel biochar and lateritic soils. The authors attributed this phenomenon to increase in the number of ions available for adsorption as initial concentration increases. Thus, it can be concluded that initial concentration influences the rate of the adsorption process.

4.2.4 Adsorption Kinetics for Equilibrium Adsorption Data for Ammonium Nitrogen

Four kinetics models (Pseudo first order, Pseudo second order, Elovich and Intra-particle diffusion) were utilized to analyze the nature and rate at which ammonium nitrogen is adsorbed by lateritic soils and fungi. These models were employed in fitting

the time-dependent adsorption data help to elucidate the rate-controlling steps and nature of adsorption, whether it is physisorption or chemisorption. Figure 4.7 represent the graphical plots obtained from time-dependent adsorption data of lateritic soils and fungal biomass.

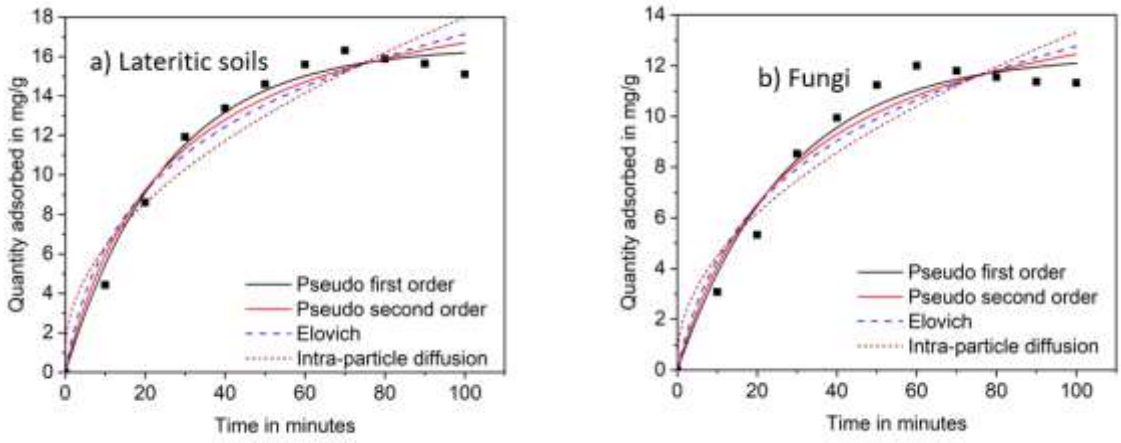

Figure 4.7: Non-linear Plots of Pseudo First Order, Pseudo Second Order, Elovich and Intraparticle Diffusion Models for Ammonium Nitrogen Removal

Each kinetic model estimates different kinetic parameters that are crucial in analyzing the dynamic interaction between ammonium ions and the surface of lateritic soils and fungal adsorbents. Different kinetic parameters obtained from the three models are presented in Table 4.3.

Table 4.3: Kinetic Model Parameters for Ammonium Nitrogen Adsorption

Kinetic Model	Parameter	Lateritic soil	Fungi
Pseudo First Order	K (min^{-1})	0.040	0.037
	$q_{e\ Cal}$ (mg/g)	16.500	12.403
	$q_{e\ exp}$ (mg/g)	16.314	12.004
	R^2	0.985	0.969
	x^2	0.439	0.529
Pseudo Second Order	K (min^{-1})	0.0018	0.0021
	q_e (mg/g)	20.957	16.120
	R^2	0.967	0.948
	x^2	0.943	0.872
Elovich Model	β	0.181	0.223
	α	1.174	0.730
	R^2	0.947	0.928
	x^2	1.550	1.233
Intra-particle diffusion	C_i	0.945	0.404
	K_i	1.705	1.290
	R^2	0.899	0.885
	x^2	2.946	1.945

The Pseudo-First-Order model exhibited a good fit for both adsorbents, with high correlation coefficients ($R^2 = 0.985$ for lateritic soils and $R^2 = 0.969$ for fungal biomass), suggesting ammonium ions uptake was predominantly governed by physical adsorption. The calculated equilibrium adsorption capacities ($q_{e,cal}$) were 16.500 mg/g and 12.403 mg/g for lateritic soil and fungal biomass, respectively, which compared closely with the experimental values ($q_{e,exp}$ = 16.314 mg/g and 12.004 mg/g). The close agreement between calculated and experimental q_e values, together with high R^2, indicates that the PFO model adequately described the adsorption process for both materials. However, the slightly higher rate constant ($k = 0.040$ min^{-1}) for lateritic soil compared to fungal biomass ($k = 0.037$ min^{-1}) suggests that ammonium ions

were adsorbed more rapidly onto the mineral surface of lateritic soil than onto fungal biomass.

For pseudo second order model, lateritic soils also exhibited a higher $q_{e,cal}$ value of 20.957 mg/g as compared to the value of fungi which was 16.120 mg/g. Lateritic soils had a higher R^2 value of 0.967 as compared to fungal adsorbent which had a R^2 of 0.948. This implies that both adsorbents have additional active sites involved in the binding of ammonium ions through stronger interactions such as ion exchange or surface complexation. The slightly higher rate constant ($k = 0.0021$ min^{-1}) for fungal biomass compared to lateritic soil ($k = 0.0018$ min^{-1}) suggests that the chemisorption step occurred more rapidly on fungal surfaces, possibly due to the presence of carboxyl and hydroxyl groups that favor ammonium binding.

For Elovich model, lateritic soils exhibited a higher initial adsorption rate (α) (1.174 mg/g·min) compared to fungal biomass (0.730 mg/g·min). This imply that lateritic soils initially adsorbed ammonium ions more rapidly due to its abundance of iron and aluminum oxide sites and high surface charge as depicted by XRF and Zeta potential results. The desorption constants (β) were 0.181 for lateritic soil and 0.223 for fungal biomass, suggesting a slightly higher surface heterogeneity on fungal biomass.

Time dependent data was further fitted using intra-particle diffusion model to determine the rate-limiting steps in adsorption of ammonium ions from human urine. From the results in Table 4.3, Ci value for lateritic soils was 0.945 and that of fungi was 0.404 for fungal biomass. This suggests that intra-particle diffusion was not the only rate controlling step since the $C_i \neq 0$ for both adsorbents. Film diffusion and surface reaction also played a role in adsorption of ammonium ions from human urine. The intra-particle diffusion rate constant (K_i) was higher for lateritic soil (1.705 mg/g·min$^{1/2}$) than for fungal biomass (1.290 mg/g·min$^{1/2}$), meaning ammonium ions diffused faster into the pores or surface sites of the mineral matrix than into the fungal biomass.

In general, for both adsorbents, PFO model best described the experimental data as they recorded higher R^2 values (lateritic soils = 0.985, fungal biomass = 0.969) and lower x^2 values (lateritic soils = 0.439, fungal biomass = 0.529). The results of this study compare closely with those reported in existing literature materials. For instance, (Muscarella et al., 2024) in their studies on recovery of ammonium from treated wastewater using zeolites reported pseudo first order model best described the adsorption mechanism and concluded that the number of ammonium ions adsorbed was solely dependent on the surface area of zeolite adsorbent. Similar, studies by (Halder et al., 2023) on recovery of ammonium nitrogen from synthetic wastewater using biochar derived from biosolids also reported that their experimental data was best fitted by pseudo first order model. The authors concluded that adsorption rate was rapid fast since ammonium ions occupied the external film layer first. When the external layer was filled up, the ions diffused to the internal pores. Thus, the adsorption rate was rapid at the beginning of the experiment and the rate slowed down as it approached equilibrium. In another study by (X. Li & Shi, 2022) on the adsorption of ammonium by iron and nitrogen modified biochar, the experimental was best fitted by pseudo first order and the authors concluded that the nature of adsorption mechanism was physical. Thus, the results of this study highlight the potential of recovering and reusing ammonium ions from human urine since physisorption processes are reversible and less energy-intensive.

4.2.5 Adsorption Isotherms for Equilibrium Adsorption of Ammonium Data for Lateritic Soils and *Agaricus Impudicus*

In analyzing the adsorption behaviour and capacity of lateritic soils and fungi adsorbents, three commonly used isotherm models namely; Langmuir, Freundlich, and Dubinin–Radushkevich (D–R) were employed to fit experimental data to describe the equilibrium adsorption behavior. Figure 4.8 a, b and c show the graphical plots for Langmuir, Freundlich and D-R models obtained from adsorption data of lateritic soil and fungal biomass.

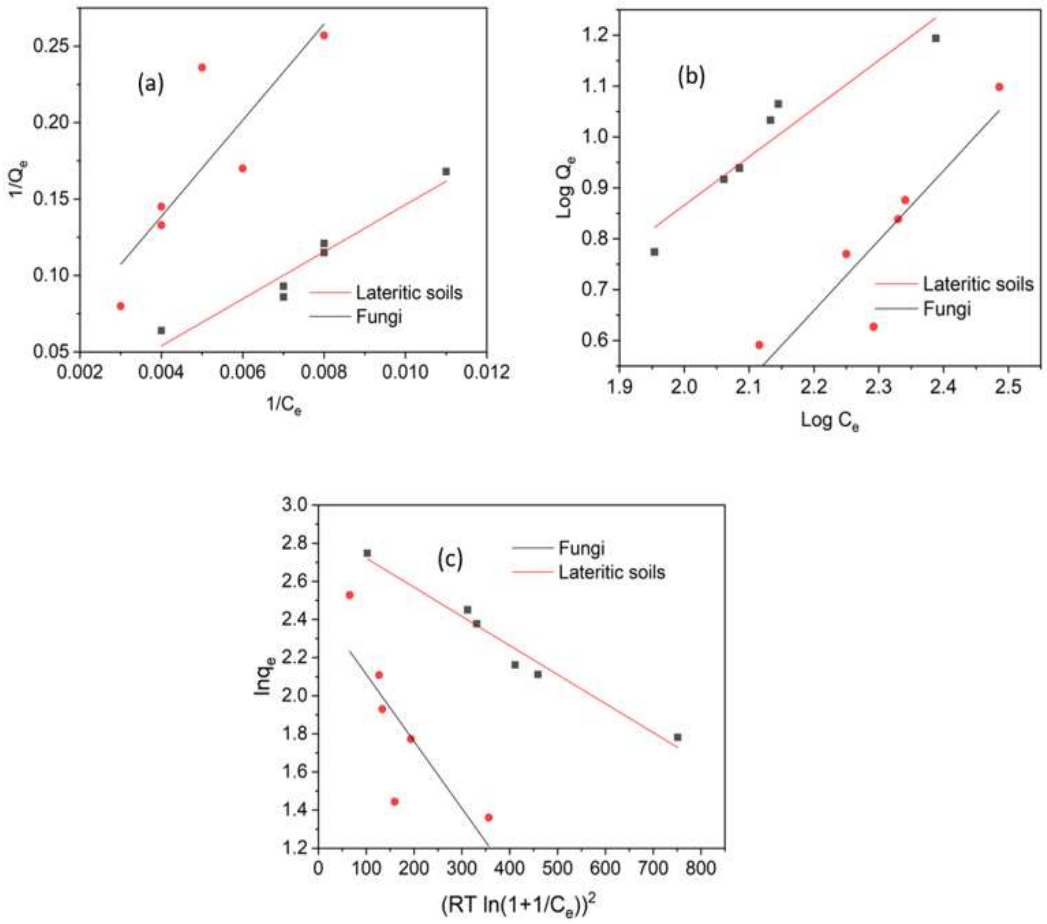

Figure 4.8: Graphical Plots for Langmuir(a), Freundlich (b) and Dubinin Radushkevich (c) Models for Ammonium Nitrogen Removal

Each model applies different assumptions and mathematical equations to explain the nature and mechanism of the adsorption process. Table 4.4 summarizes the values obtained for different parameters for the three models

Table 4.4: Isotherm Model Parameters for Ammonium Nitrogen Adsorption

Isotherm	Parameter	Lateritic Soils	Fungi
Langmuir	$q_{max,}$ (mg/g)	131.406	32.400
	K_L	0.065	0.032
	R^2	0.935	0.718
	SSE	4.214×10^{-4}	0.006
	RMSE	1.053×10^{-4}	1.5×10^{-3}

Freundlich	K_f	0.093	0.004
	R^2	0.908	0.813
	1/n	0.949	1.373
	SSE	0.009	0.032
	RMSE	2.25×10^{-3}	8×10^{-3}
Dubinin Radushkevich (D-R)	Q_0 (mg/g)	17.7	11.751
	K_{D-R}	0.0015	0.0035
	E (kJ/mol)	1.814×10^{-2}	1.192×10^{-2}
	R^2	0.968	0.649
	SSE	0.018	0.331
	RMSE	4.5×10^{-3}	0.083

Lateritic soils equilibrium adsorption data were best fitted by the D-R model which exhibited a higher R^2 value of 0.968 as compared to Langmuir (R^2 = 0.935) and Freundlich models (R^2 = 0.908). This suggest that the adsorption was physical in nature, which can be attributed to the porous nature of lateritic soils as revealed in SEM images. The calculated mean adsorption energies were 0.01814 kJ/mol as presented in Table 4.4 suggesting that attachment of ammonium ions onto the adsorbent's surface was governed by weak electrostatic interactions. This is ideal for regeneration and reuse of the adsorbent since most of the adsorbed ions can be easily desorbed using regenerating agents. Finally, the calculated adsorption capacity of lateritic soils by the D-R model (17.7 mg/g) closely compare with the experimental maximum adsorption capacity (16.314 mg/g).

Fungal biomass experimental data on the other hand was best fitted by Freundlich model which recorded the highest (R^2 = 0.813) which implied that adsorption occurred on a heterogeneous surface with varying affinities. The SEM image of the fungal adsorbent had an irregular shape with microstructures. These characteristics suggest a non-uniform and heterogeneous surface morphology, likely influenced by the raw material composition and the grinding process. However, Freundlich constant n, reflecting the measure of favorability of adsorption, was 0.728, indicating weaker and less favorable adsorption process which could be as a result of weaker interactions

between adsorbate and the adsorbent at higher concentrations. The results of this study compare closely with a number of studies that have been undertaken to investigate adsorption of ammonium nitrogen using different natural-based adsorbents. For instance, (Tosun, 2012) in their study on adsorption of ammonium from aqueous solutions using clinoptilolite reported that D-R model best fitted their experimental results with E<8 kJ/mol implying physisorption occurred. Similarly, studies conducted by (Zamparas et al., 2021) on recovery of ammonium from wastewater using bentonites reported higher adsorption capacity ranging from 131.8 mg/g to 159.6 mg/g. In this study, Langmuir model had the best fit for their experimental data. Another study by (Naghipour et al., 2020) using glauconite reported that Freundlich model best described the adsorption process and concluded that ammonium adsorption occurred on heterogenous surfaces.

4.3 Determination of Behaviour and Adsorption Capacity of *Agaricus Impudicus* and Lateritic Soil in Adsorbing Phosphorus from Human Urine

4.3.1 Effect of Adsorbent Loading on Phosphorus Adsorption

Figure 4.9 shows the removal percentage of P by *Agaricus impudicus* and lateritic soil under varying adsorbent amount in the range of 0-0.5 g.

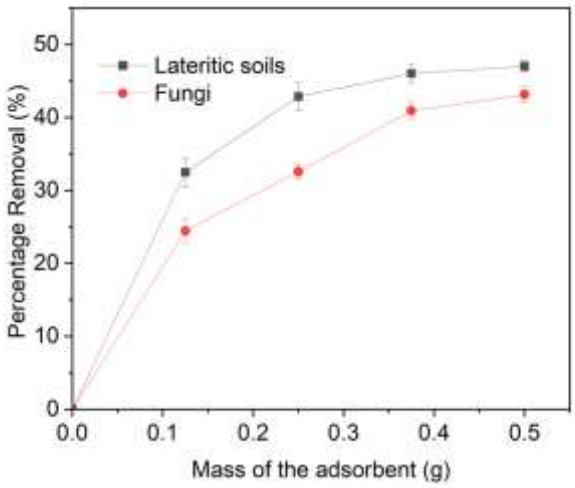

Figure 4.9: Effect of Adsorbent Loading on Phosphorus Removal

The removal percentage of P was observed to increase gradually with the increase in the adsorbent loading. At 0.125 g of fungal biomass and lateritic soil, the removal

percentage of 24.45 ± 1.57 % and 32.50 ± 1.96 % respectively was attained which increased to 43.14 ± 1.12 % and 47.72 ± 0.75 % respectively at 0.5 g of these adsorbents. The increase in removal percentage of P with the increase in fungal biomass and lateritic soil quantity can be attributed to increased surface areas of the adsorbents which provide adsorption sites for the sorption of the P from urine samples (Manawi et al., 2024). The results of this study closely compare with those recorded in existing literature materials. For instance, (islam et al., 2025a) observed a similar trend in their studies on removal of phosphate from water using Parthenium hysterophorus-derived iron-coated biochar. The authors observed an increase in phosphate removal from 58.03 % to 99.22 % with increase in biochar loading from 0.02 g to 0.06 g. This phenomenon was attributed to increase in the number of available active sites for phosphate ions adsorption with increase in adsorbent loadings. A study conducted by (Khalil et al., 2022) using activated carbon composites to remove phosphates in synthetic water also exhibited a similar trend. The authors attributed this behaviour to increase in contact surface area and the number of adsorption sites with increase in the adsorbent loadings. Another study by (Shumiye et al., 2024) reported a similar trend on their study on removal of phosphates from wastewater using activated adsorbent prepared using wastewater treatment plant sludge. The authors observed a rapid increase in phosphate removal from 60.0 % to 83.8 % when adsorbent loading was changed from 1 g/L to 3 g/L. However, small changes in phosphate removal were noticed when adsorbent loading was further increased from 3 g/L to 7 g/L with an interval of 1 g/L. Rapid increase in removal rate between 1 g/L and 3 g/L was attributed to increase in the number of adsorption sites whereas minimal changes experienced between 3 g/L and 7 g/L was attributed to attainment of equilibrium state thus removal rate tend to a constant value. From all these studies, it is evident that adsorbent loading influences the adsorption behaviour.

4.3.2 Effect of Agitation Speed on Phosphorus Adsorption

The effect of agitation speed on the removal percentage of P in human urine samples was investigated by varying the agitation speed in the range of 0- 190 rpm. The resulting removal percentages were plotted as shown in Figure 4.10.

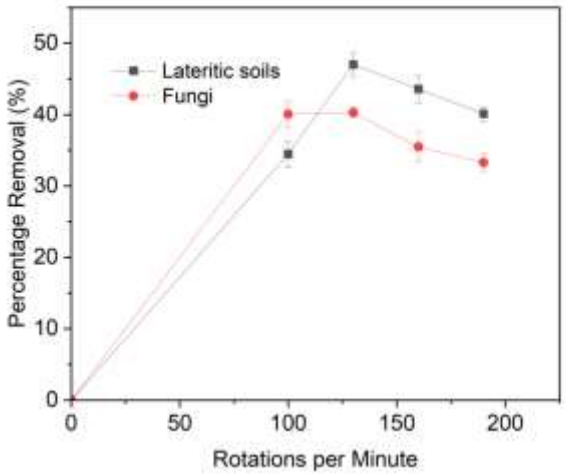

Figure 4.10: Effect of Agitation Speed on Phosphorus Removal

There was an increase in P adsorbed on the surface of lateritic soils when agitation speed was increased from 100 rpm to 130 rpm with the highest removal percentage of 47.02 ± 1.72 %. Beyond the agitation speed of 130 rpm, the removal percentage of P declined with increase in agitation speed. On the other hand, negligible changes were observed on percentage removal of P by fungal adsorbent when agitation speed was increased from 100 rpm (40.05 ± 1.85 %) to 130 rpm (40.28 ± 0.70 %). However, beyond 130 rpm, percentage removal declined with increase in agitation speed. Increase in percentage removal of P by lateritic soils with increase in agitation speed from 100 rpm to 130 rpm could be linked to proper distribution of adsorbent when agitation is increased thus improvement of adsorption rate. The decrease in the removal percentage of P at elevated agitation speed is ascribed to the desorption of P from lateritic soils and fungal biomass adsorptive sites. Compared to lateritic soils, the fungal biomass exhibited lower structural resilience under increased shear forces, likely due to its softer, organic matrix, which limits its adsorption efficiency with increasing agitation and promotes detachment of weakly bound P ions. One-way ANOVA was performed to statistically confirm these observations. The results showed a significant effect of agitation speed on phosphate ions removal for both lateritic soils ($p = 0.0319$) and fungal biomass ($p = 0.0014$).

The findings of this study compare closely with those reported in existing literature materials. For instance, (Djekoune et al., 2024) and (Fetene & Addis, 2020) observed similar trends on their studies on removal of phosphates from wastewater using dried alum sludge and Ethiopian rift pumice respectively. Another study by (Belaye et al., 2023) on phosphate removal from aqueous solutions using Ce(III)- BDC metal−organic framework reported a similar trend. The authors attributed the increase in percentage removal of phosphates when agitation speed was increased to proper distribution of adsorbent particles in the adsorbate hence reduction in boundary mass transfer resistance and formation of film boundary layer that slows down adsorption. The decrease in percentage removal of phosphates at higher agitation speeds was linked to vortex phenomenon and possible detachment of phosphate ions from adsorption sites (Olawale, 2020). Thus, it can be deduced that agitation speed significantly impacts the adsorption process.

4.3.3 Effect of Initial Concentration and Contact Time on Phosphorus Adsorption

Effect of contact time on P adsorption from human urine was evaluated by varying contact time up to 100 minutes for both lateritic soil and fungal biomass. Similarly, effect of initial concentration was evaluated using six different initial concentrations (223.74, 377.28, 408.60, 444.39, 505.74, and 594.56 mg/L). The results on effect of contact time and initial concentration on the quantity of P removed by lateritic soil and fungal biomass were graphically represented in Figure 4.11 a and b respectively.

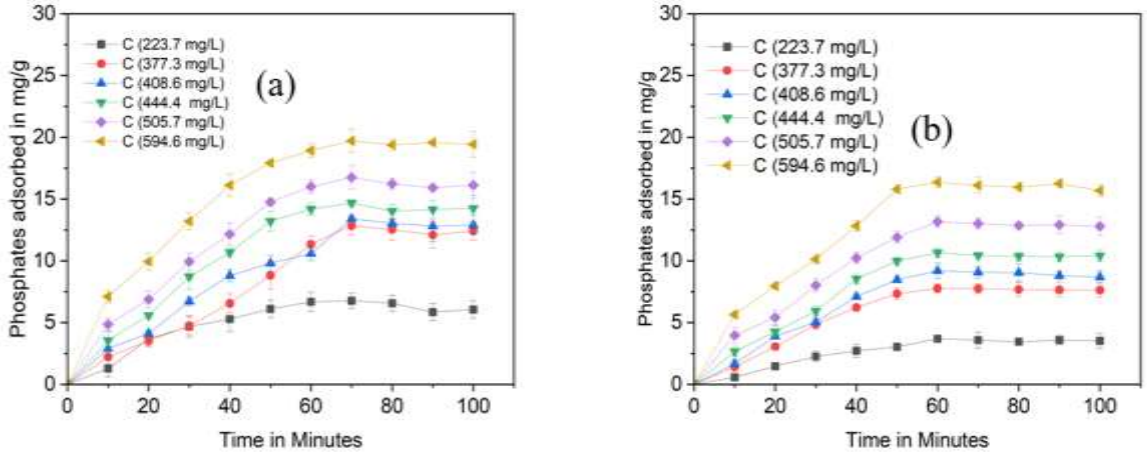

Figure 4.11: Effect of Contact Time and Initial Concentration on Phosphorus Removal

It was noticeable that the quantity of P adsorbed by lateritic soils increased with the increase in the initial concentration of P from 223.74 to 594.59 mg/L. At the initial concentration of 223.74 mg/L, the quantity adsorbed after 10 minutes was 1.28 ± 0.67 mg/g and that adsorbed at equilibrium time (70 minutes) was 6.76 ± 0.61 mg/g. The adsorption capacity of P by lateritic soils started declining gradually beyond 70 minutes, as illustrated in Figures 4.11a. Similar observations were noted in other initial concentrations where quantity of P adsorbed increased with time until equilibrium state was attained beyond which negligible changes were noticed. The highest adsorption capacities were determined to occur at the initial concentration of 594.59 mg/L, in which the quantity adsorbed increased from 7.11 ± 0.53 mg/g at 10 minutes to 19.71 ± 0.95 mg/g at equilibrium time (70 minutes).

Similarly, the quantity of P adsorbed increased with the increase in initial concentration when fungi were used as an adsorbent. However, the adsorption capacity for P in fungi was slightly lower than those obtained using lateritic soils as an adsorbent. At the lowest initial concentration of P at 223.74 mg/L, the quantity adsorbed increased from 0.57 ± 0.64 mg/g to 3.69 ± 0.59 mg/g between 10 and 60 minutes as shown in Figure 4.11b. In comparison, at the highest initial P concentration of 594.59 mg/L, the quantity of P adsorbed increased from 5.65 mg/g at 10 minutes to 16.35 mg/g at equilibrium time (60 minutes). Beyond equilibrium time for both adsorbents, the

change in quantity of P adsorbed was negligible for all the six different concentrations considered.

Generally, there was an increase in quantity of P adsorbed with the increase in the initial phosphate concentration by lateritic soils and fungi adsorbents. This could be explained by the rise in the strength of the adsorption driving force, which increases with the increase in the adsorbate concentration. One-way ANOVA was done to further explain the differences in adsorption capacities recorded between the six different concentrations used in this study. The ANOVA results exhibited significant effect of initial concentration of adsorbate on the adsorption capacity of lateritic soils ($p = 0.0001$) and fungal biomass ($p = 0.0005$). Similar results were reported by (Otieno et al., 2023b), in which they varied phosphate initial concentration from 164.12 mg/L to 680.21 mg/L, with the maximum adsorption capacity of 15.5 mg/g achieved on lateritic soils. Elsewhere, (Bhattacharjee et al., 2021) reported a similar trend of increasing adsorption capacity with an increase in the initial concentration of the phosphates by laterite soils. Phosphorus ions are slowly diffused through the lateritic soils or fungi adsorbents at low phosphate concentrations (Qian et al., 2023). However, at higher concentrations, phosphorus ions diffuse faster. This can be explained by the increase in concentration gradient between the adsorbate solution and the adsorbent which act as the driving force (Bhattacharjee et al., 2021).

On the effect of contact time, the quantity of P removed in the six different concentrations of human urine increased as contact time increases from 0 to 100 minutes for both adsorbents. In lateritic soils, P adsorption rate was noticed to be rapid between 0 and 30 minutes. Between 30 and 60 minutes, adsorption rate was moderate. After 60 minutes, it gradually declined and reached equilibrium at 70 minutes. After 70 minutes, the changes in quantity of P adsorbed by lateritic soils were negligible. For fungi adsorbent, rapid adsorption rate was observed between 0 and 40 minutes. After 40 minutes the adsorption rate gradually declined and equilibrium was attained at 60 minutes. Fast adsorption rate observed at the beginning of the experiments for both adsorbents could be explained by availability of many active unoccupied sites. As time progresses, most active sites become saturated with P ions hence decline in adsorption rate and eventually an equilibrium state is attained. The results of this study

compare closely with those reported in existing literature materials. For instance, (Paul et al., 2022) observed a similar trend on the effect of contact time on phosphates removal from aqeous solutions using snail shell dust. In this study, the authors observed a fast uptake of phosphate ions in the first 80 minutes. After 80 minutes, uptake of the ions decreased and equilibrium was attained at 160 minutes. The authors attributed the decrease in uptake after 80 minutes and equilibrium state to difficulty in occupying the remaining vacant sites due to repulsive forces between the adsorbed phosphate ions in the adsorbent and the aqueous solutions. Similarly, (Genetie Abetu & Befekadu Kebede, 2021) and (islam et al., 2025b) reported similar trends on their studies on removal of phosphates using crushed concrete and Parthenium hysterophorus-derived iron-coated biochar respectively. The authors attributed this behaviour to high number of vacant sites in the adsorbent materials and fast filling of adsorbent sites as a result of boundary layer diffusion.

4.3.4 Adsorption Kinetics for Equilibrium Adsorption Data for Phosphorus

Four kinetic models (pseudo first order, pseudo second order, Elovich and intra-particle diffusion) were used in fitting the experimental data to evaluate the adsorption mechanisms in removal of phosphorus from human urine. Figure 4.12 represent the graphical plots obtained from time-dependent adsorption data for lateritic soils and fungal biomass.

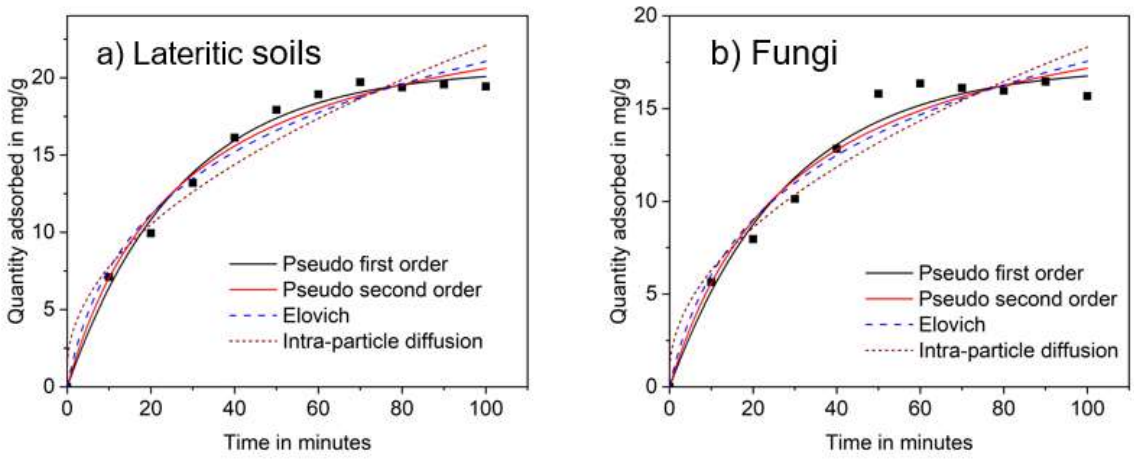

Figure 4.12: Non-linear Plots of Pseudo First Order, Pseudo Second Order, Elovich and Intraparticle Diffusion Models for Phosphorus Removal

These models are crucial in understanding the adsorption mechanisms which are significant in optimizing the adsorption processes. The kinetic parameters obtained from these models which include; rate constant (K), equilibrium adsorption capacities (q_e), coefficient of determination (R^2), chi-square (x^2), and Elovich constants (α and β) are summarized in Table 4.5.

Table 4.5: Kinetic Model Parameters for Phosphorus Adsorption

Kinetic Model	Parameter	Lateritic soil	Fungi
Pseudo First Order	K (min^{-1})	0.037	0.035
	$q_{e\ Cal}$ (mg/g)	20.566	17.260
	$q_{e\ exp}$ (mg/g)	19.715	16.354
	R^2	0.992	0.976
	x^2	0.360	0.797
Pseudo Second Order	K (min^{-1})	0.0014	0.0015
	q_e (mg/g)	26.210	22.299
	R^2	0.986	0.966
	x^2	0.670	1.136
Elovich Model	β	0.145	0.165
	α	1.391	1.038

	R^2	0.976	0.955
	x^2	1.116	1.516
Intra-particle diffusion	C_i	1.129	0.714
	K_i	2.096	1.761
	R^2	0.948	0.928
	x^2	2.462	2.437

For PFO, lateritic soils exhibited a higher rate constant (K_1 = 0.037 min^{-1}) as compared to fungal biomass (0.035 min^{-1}), indicating faster initial phosphorus uptake by the soil. The equilibrium adsorption capacities (q_e, cal) predicted by the PFO model were 20.566 mg/g and 17.260 mg/g for lateritic soil and fungal biomass, respectively. These values closely compared with the experimental values (q_e, exp = 19.714 mg/g for lateritic soils and q_e, exp = 16.354 mg/g for fungal biomass). Both adsorbents showed good correlation coefficients (R^2 = 0.992 for lateritic soil and 0.976 for fungal biomass), implying that the PFO model adequately described the adsorption behavior. Additionally, the chi-square (χ^2) values (0.360 and 0.797) suggest a better agreement between experimental and calculated values.

For PSO, the rate constants (K_2) were relatively low (0.0014–0.0015 min^{-1}), but the predicted q_e, cal values (26.210 and 22.299 mg/g for lateritic soil and fungal biomass, respectively) were higher than those obtained from the PFO model. Although the PSO model also showed good fits (R^2 = 0.986 and 0.966), the slightly higher χ^2 values (0.670 and 1.136 for lateritic soils and fungal biomass respectively) indicate a weaker correlation compared to PFO. This imply that phosphorus adsorption onto both materials is not purely chemisorption-controlled. Thus, the adsorption process likely involves a combination of ligand exchange, inner-sphere surface complexation and diffusion within pores or soil and fungal matrices.

The Elovich model parameters provide insight into the surface heterogeneity of the adsorbents. The α constant, which represents the initial adsorption rate, was higher for lateritic soil (1.391 mg/g·min) than for fungal biomass (1.038 mg/g·min), implying more active adsorption sites and faster uptake initially. Meanwhile, the β constant,

which relates to surface coverage and activation energy, was slightly lower for lateritic soil (0.145) than for fungal biomass (0.165). However, the χ^2 values (lateritic soils =1.116 and fungi = 1.516) were higher than for the PFO model, indicating a less accurate overall fit.

For intra-particle diffusion model, rate constants (K_i) were 2.096 mg/g·min$^{0.5}$ for lateritic soil and 1.761 mg/g·min$^{0.5}$ for fungal biomass, showing that diffusion contributes significantly to the adsorption process for both materials. The intercept (C_i) values (lateritic soils = 1.129 and fungal biomass = 0.714) suggest that boundary layer effects are present, indicating that intra-particle diffusion is not the sole rate-limiting step. Although R^2 values (0.948 and 0.928) confirm some linearity, the relatively high χ^2 values (2.462 and 2.434) indicate that this model alone cannot fully describe the kinetics of P adsorption. Thus, it can be deduced that the adsorption process involves both surface adsorption and intra-particle diffusion.

In general, the results from kinetic models indicate that the pseudo-first-order model best fits the experimental data for both lateritic soil and fungal biomass, as evidenced by the highest R^2 and lowest χ^2 values. This suggests that phosphorus adsorption is dominated by physical interactions, such as electrostatic attraction and ion exchange with surface hydroxyl groups. The findings of these studies compare closely with those reported by other authors. For instance, (Lee et al., 2022) in their study on removal of P from water using calcium-rich organic waste reported that PFO best explained their kinetic data. The authors concluded that the adsorption of P onto the surface of the adsorbent was mainly through physical interactions. (Lacerda et al., 2021) also reported that the adsorption of phosphate onto unmodified and chemically activated red ceramic waste was best described by the pseudo-first-order kinetic model, suggesting a dominant physisorption mechanism involving weak surface interactions. Similarly, (Hou & Wu, 2026) found that phosphate adsorption onto corn straw-derived biochar/sodium alginate composite also followed the pseudo-first-order model ($R^2 >$ 0.95), reflecting rapid surface adsorption controlled mainly by diffusion and physical binding processes.

4.3.5 Adsorption isotherms for equilibrium adsorption data for Phosphorus

Three isotherm models (Langmuir, Freundlich and Dubinin Radushkevich (D-R) models) were used in fitting the experimental data to evaluate the nature of adsorption mechanism, adsorption capacities and behaviours in removal of phosphorus from human urine. Figure 4.13 a,b and c represent the graphical plots for Langmuir, Freundlich and D-R models obtained from equilibrium adsorption data for lateritic soils and fungal biomass.

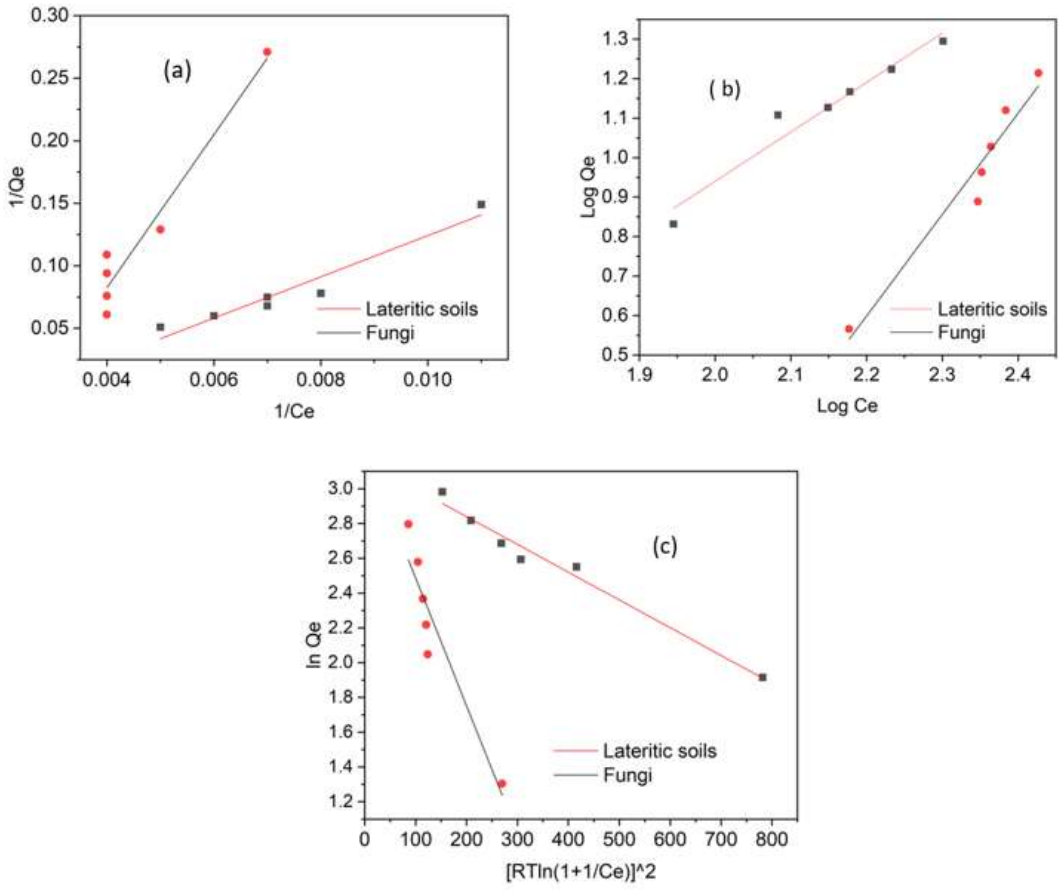

Figure 4.13: Graphical Plots for Langmuir (a), Freundlich (b) and Dubinin Radushkevich (c) Models for Phosphorus Removal

Isotherm models provide useful insights on adsorption mechanisms, adsorption capacities, surface properties of the adsorbents and their affinities to the targeted adsorbates. This information is essential in scaling and optimizing adsorption systems. The isotherm parameters obtained from these models are summarized in Table 4.6.

Table 4.6: Adsorption Isotherm Parameters for Equilibrium Adsorption Data of Phosphorus

Isotherm	Parameter	Lateritic Soils	Fungi
Langmuir	q_{max} (mg/g)	24.558	6.166
	K_L	0.061	0.016

	R^2	0.939	0.946
	SSE	3.778 ×10-4	0.0016
	RMSE	9.45×10^{-5}	3.95×10^{-4}
Freundlich	K_f	0.027	8.990×10^{-6}
	R^2	0.951	0.951
	1/n	0.800	0.390
	SSE	0.0061	0.012
	RMSE	0.0004	0.003
Dubinin	q_0 (mg/g)	25.074	23.524
Radushkevich (D-R)	K_{D-R}	0.0016	0.0074
	E (kJ/mol)	1.768×10^{-2}	8.248×10^{-3}
	R^2	0.977	0.893
	SSE	0.015	0.145
	RMSE	0.0038	0.036

The Langmuir model assumes monolayer adsorption on a homogenous surface with equal and finite adsorption sites. For both adsorbents, this model exhibited a good fit with correlation coefficient values of 0.939 and 0.946 for lateritic soils and fungal biomass respectively, implying that the adsorption mechanism governing adsorption of phosphorus from human urine may partially include monolayer adsorption. Fungal biomass exhibited a lower maximum adsorption capacity (6.166 mg/g) than lateritic soils (24.558 mg/g). This suggests that lateritic soil possess more active adsorption sites, likely due to presence of iron and aluminum oxides as depicted in XRF results, which have higher affinities for phosphate ions. Additionally, the higher K_L value recorded for lateritic soils (0.061) as compared to that of fungal biomass (0.016) further explains the high affinity of Al and Fe oxides for phosphate ions.

Although Freundlich model exhibited relatively high R^2 of 0.951 for both adsorbents, the model yielded lower values of 1/n (0.800 for lateritic soils and 0.390 for fungl

biomass) implying that adsorption was unfavourable. This could be attributed to weak binding of phosphate ions onto the surface of adsorbents (Xu et al., 2023), likely dominated by weak electrostatic interactions and surface hydrogen bonding as revealed in FTIR results. Freundlich constant (K_f), however, exhibited a higher value for lateritic soils (0.027) as compared to that of fungi (8.99×10^{-3}) implying the adsorption sites for lateritic soils had a higher affinity for phosphates ions compared to that of fungal biomass.

For the D-R model which is commonly used to establish whether physical or chemical adsorption is dominant by calculating the mean adsorption surface energy, lateritic soils recorded a higher R^2 value (0.977) as compared to fungal biomass which recorded a slightly lower value of R^2 (0.893). Lateritic soils exhibited a higher maximum adsorption capacity (25.074 mg/g) as compared to that of fungal biomass (23.524 mg/g) which suggest that lateritic soils had more active adsorption sites as compared to fungal biomass. Both adsorbents recorded E values that are less than 8 kJ/mol which imply that physical adsorption was predominant in the adsorption of phosphates ions from the urine.

For all the three models, Langmuir model best described the experimental data for both adsorbents with R^2 value of 0.939 for lateritic soils and 0.956 for fungal biomass implying monolayer adsorption was predominant in the removal of P from human urine. Additionally, the model exhibited lower SSE and RMSE values for both adsorbents which indicate minimal variations between the experimental data and model predicted data. Lateritic soils had SSE of 3.778×10^{-4} and RMSE of 9.45×10^{-5}. On the other hand, fungal biomass had SSE of 0.0016 and RMSE of 3.95×10^{-4}. The findings of this study can be compared closely with those reported in existing literature. For instance, (Sun et al., 2024) in their study on the use of eggshell-fly ash in removing phosphate ions from aqueous solutions reported that their experimental data was best fitted by Langmuir model implying that adsorption was controlled by monolayer adsorption. Similarly, (Sarker et al., 2023) reported that Langmuir provided favorable conditions for adsorption of phosphate ions using bamboo-eggshell as adsorbents. Lastly, studies conducted by (Huang et al., 2022) on phosphate removal using adsorbents derived from rice husk also recorded that phosphate adsorption was

governed by a single molecule on finite adsorption sites. Thus, it can be concluded that elemental composition of adsorbents influences their adsorption capacities and behaviors.

4.4 Desorption behaviour of Ammonium Nitrogen and Phosphorus from *Agaricus Impudicus* and Lateritic Soil Adsorbents

4.4.1 Desorption behaviour of Ammonium nitrogen from *Agaricus Impudicus* and Lateritic Soil Adsorbents

4.4.1.1 Batch Experiments for Ammonium Nitrogen Desorption from Lateritic Soils and *Agaricus Impudicus*

Batch desorption experiments were conducted using distilled water to evaluate the potential of lateritic soils and *Agaricus impudicus* to release the adsorbed $NH_4^+ - N$. Figure 4.14 shows the desorption rate of lateritic soils and fungal biomass respectively.

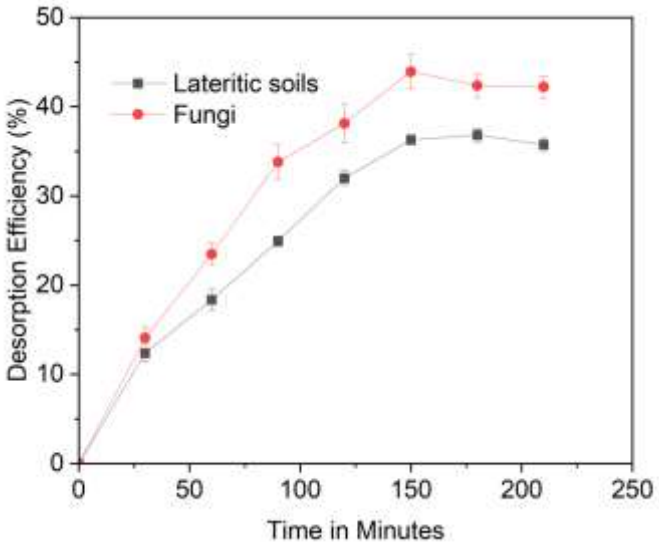

Figure 4.14: Desorption Efficiencies of Lateritic Soils (a) and Fungal Biomass (b) at an Agitation Speed of 130 rpm

In Figure 4.14, the desorption rate of $NH_4^+ - N$ from lateritic soils was rapid from 0 to 150 minutes, with desorption efficiency increasing from 0 to 36.29 ± 0.54 %. The rapid release rate recorded between 0 to 150 minutes could be explained by fast release

of $NH_4^+ - N$ ions that are loosely bounded to the outer surface of lateritic soils adsorbents by weak electrostatic bonds. The insignificant change between 150 and 210 minutes indicate that the loosely bound ammonium ions have already been released, and the remaining ions are either more strongly adsorbed or located deeper within the soil structure as depicted in SEM images of lateritic soils.

In Figure 4.14, the release rate of $NH_4^+ - N$ from fungal biomass was rapid between 0 and 90 minutes, with desorption efficiency increasing from 0 to 33.78 ± 1.92 %. Between 90 and 150 minutes, the release rate was moderate, with desorption efficiency increasing from 33.78 ± 1.92 % to 43.93 ± 1.25 %. Beyond 150 minutes, the graph began to flatten indicating equilibrium had been reached. The rapid release of ammonium ions from fungal adsorbent could be attributed to weak van-der walls forces. FTIR spectra and elemental results of fungal adsorbent exhibited presence of functional groups (-COOH, -OH and -NH2) indicating adsorption of ammonium ions onto the surface of fungal adsorbent is governed by physical interactions. The desorption trend obtained in this study compare closely with those reported by other authors. For instance, (L. Zhang et al., 2020) evaluated the desorption of $NH_4^+ - N$ ions from poly (acrylic acid)-Grafted Chitosan and biochar adsorbents. The authors reported high desorption rates ($> 85\%$). (Aghoghovwia et al., 2022) studied the desorption rate of ammonium trapped in six biochar derived from different feedstocks. The authors reported percentage desorption between 33% to 39 % for all the six biochars. The results of this study on desorption of $NH_4^+ - N$ from lateritic soils and fungal biomass highlight the potential of using these adsorbents to recover ammonium from human urine and subsequently desorb for plant growth since plants take in nitrogen in form of ammonium.

4.4.1.2 Column Desorption Experiments of Ammonium Nitrogen from Lateritic Soils and *Agaricus Impudicus*

The column desorption results for ammonium (Figure 4.15) highlight significant differences between lateritic soils and fungal adsorbents.

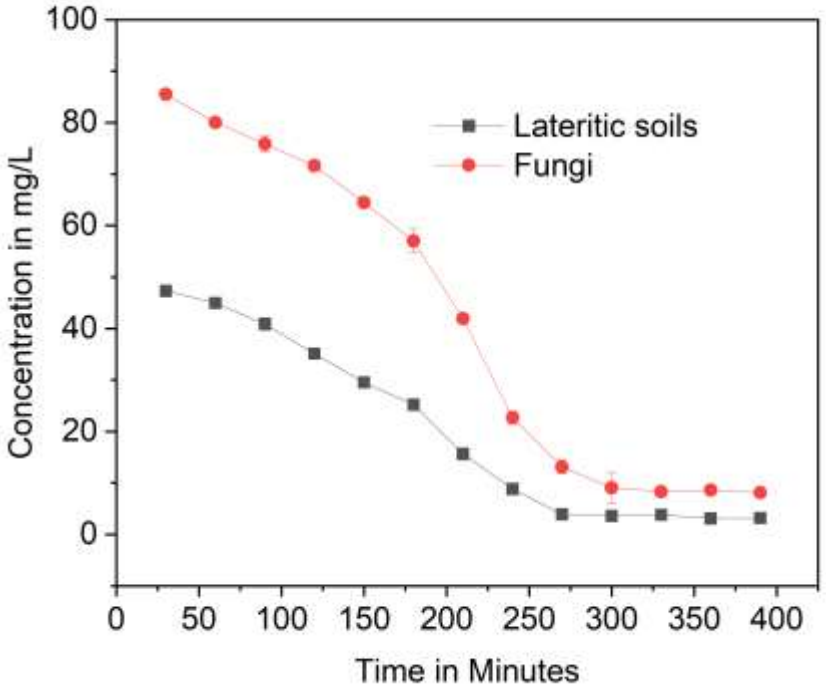

Figure 4.15: Desorption Capacities of Ammonium Nitrogen from Lateritic Soils and Fungi

At the onset of desorption, fungal columns released approximately 85.49 ± 0.68 mg/L of NH_4^+-N, while lateritic soils released 47.29 ± 0.89 mg/L. This sharp initial flush suggests that both materials contained a pool of weakly bound ammonium; however, the magnitude was greater for fungi, reflecting a higher proportion of exchangeable ammonium ions in their structure. The rapid decline in fungal desorption concentrations within the first 240 minutes further supports the dominance of weaker, reversible interactions. Beyond this point, the desorption rate declined gradually and flattened at 330 minutes with approximately 8.33 ± 0.77 mg/L indicating that most recoverable NH_4^+-N had already been released.

In contrast, lateritic soils displayed a slower desorption rate. Concentrations of NH_4^+-N desorbed dropped from 47.29 ± 0.89 mg/L to 15.66 ± 1.18 mg/L between 30 and 210 minutes. After 210 minutes, the release rate slowly declined and the graph flattened at 270 minutes with a concentration of 3.92 ± 0.52 mg/L. This gradual decline implies stronger retention mechanisms, consistent with cation exchange and

electrostatic interactions on iron and aluminum oxide surfaces abundant in lateritic matrices. The persistence of low-level ammonium release over extended time indicates partial entrapment within micro- and mesopores, which limited complete desorption.

These desorption behaviors align closely with the SEM, elemental, and FTIR characteristics of the adsorbents. SEM micrographs of lateritic soils revealed compact, crystalline structures with heterogeneous pores, providing both adsorption sites and diffusion barriers that contribute to slower ammonium release. Elemental analysis confirmed the high Fe and Al content, elements known for strong cation-exchange capacity, which explains the stronger binding and lower recovery efficiency. FTIR spectra further indicated the presence of hydroxyl and oxide groups, which form stable surface complexes with ammonium ions, thereby limiting their desorption.

For the fungal adsorbent, SEM images showed irregular, highly porous morphologies with rough surfaces that favor rapid ion exchange and surface sorption. Elemental composition revealed high carbon and oxygen content, consistent with the presence of organic functional groups. FTIR spectra confirmed abundant –OH and –COOH groups, which enable weak binding of ammonium primarily through hydrogen bonding and reversible electrostatic interactions. These structural and chemical features explain the higher initial desorption and greater recovery efficiency observed in the column studies. The findings of this study compare closely with those reported in existing literature materials. (Bulacio Fischer et al., 2025) in their study reported an initial rapid release of NH_4^+-N from zeolite adsorbent within the first 30 minutes attributing this to accessibility of surface exchange sites. (Genethliou et al., 2021) also documented zeolite desorption values of 41.86 ± 0.87 mg/L when using distilled water and 49.29 ± 2.04 mg/L when using tap water as eluents. The authors explained that the significant difference in desorption performance of the two eluents could be as a result of higher cationic exchange between the tap water and the NH_4^+ bound to the zeolites. Similarly, (Papaevangelou et al., 2023) found out that palygorskite exhibited a higher desorption capacity of 36.02 % as compared to that of zeolite (15 %) which could be linked to the structural differences of the two adsorbents.

4.4.2 Desorption Behaviour of Phosphorus from *Agaricus Impudicus* and Lateritic Soil Adsorbents

4.4.2.1 Batch Experiments for Phosphorus Desorption from Lateritic Soils and *Agaricus Impudicus*

The desorption rate of P adsorbed by lateritic soils and fungal biomass was analyzed over a period of 210 minutes. Figure 4.16 a and b illustrated the desorption efficiency (%) and desorption amounts (mg/g) of the two adsorbents.

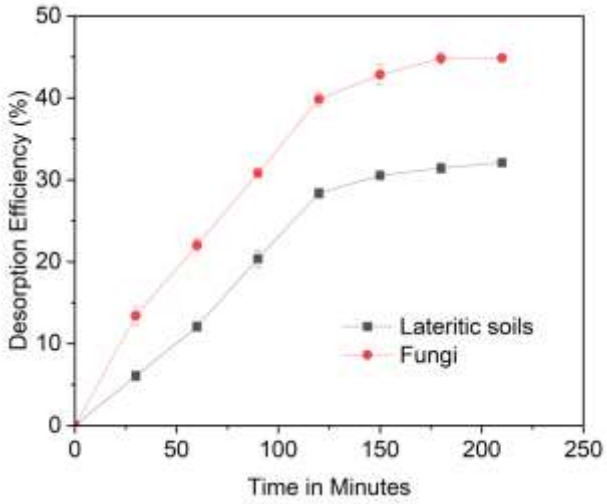

Figure 4.16: Desorption Efficiencies of Lateritic Soils and Fungi

The trend in Figure 4.16 shows that both adsorbents released P adsorbed with fungi consistently outperforming lateritic soils. Within 0 to 120 minutes, both materials exhibited a rapid release of P which could be attributed to rapid release of loosely bounded phosphates ions to the outer surface of these materials. However, the rate of release of P from fungal biomass was higher as compared to that of lateritic soils with fungi recorded a desorption efficiency of approximately 39.84 ± 0.85 % by 120 minutes whereas lateritic soils had a desorption efficiency of 28.37 ± 0.64 %. This trend imply that fungi have a weaker binding affinity for phosphate ions or more accessible binding sites as compared with lateritic soils. After 150 minutes, the desorption rate of fungi reduced and flatten at 44.83 ± 0.72 % implying that almost all readily desorbable phosphates ions have been released. Similarly, lateritic soils

exhibited a slight increase between 150 to 210 minutes with the highest desorption rate reaching approximately 32.10 ± 0.45 %. This slower release of phosphate ions between 120 and 150 minutes suggests that the remaining pores are trapped within the inner micropores of the lateritic soils matrix thus not easily released. The desorption results of this study compare closely with those recorded in existing literature. For instance, (Devesa-Rey et al., 2021) reported a desorption efficiency of 59 % in their studies on desorption of phosphates ions from synthetic clays. Similar studies by Yang et al. (Z. Yang et al., 2024) on desorption of phosphate ions from activated red mud adsorbents reported a desorption efficiency of 99. 11 % and desorption amount of 11. 29 mg/g. Additionally a desorption rate of 0.97 % to 97.08 % was reported by (Biswas et al., 2023) in their study on desorption of phosphorus from activated biochar.

The poor desorption efficiency from the lateritic soil indicates that the phosphate ions are held by stronger ionic and electrostatic bonds thus not easily released (Bhattacharjee et al., 2021). This has significant implications for reusability as it implies that the soil adsorbent is not easily regenerable with mild solvents. This highlights its potential reusability for single-use scenarios such as soil amendment or as a slow-release fertilizer (Mozaffari Majd et al., 2022). Conversely, the relatively higher desorption efficiency depicted by fungal biomass suggests a weaker, more reversible binding mechanism. The primary mechanisms are likely outer-sphere complexation, or retention within the porous fungal cell wall structure through electrostatic interactions as depicted in FTIR results. These weaker interactions allow P release, indicating that fungal biomass could be more easily regenerated for repeated adsorption–desorption cycles.

4.4.2.2 Column Desorption Experiments of Phosphorus from Lateritic Soils and *Agaricus Impudicus*

The column desorption results for phosphorus, illustrated in Figure 4.17, show clear differences in desorption behavior between lateritic soils and fungal adsorbents.

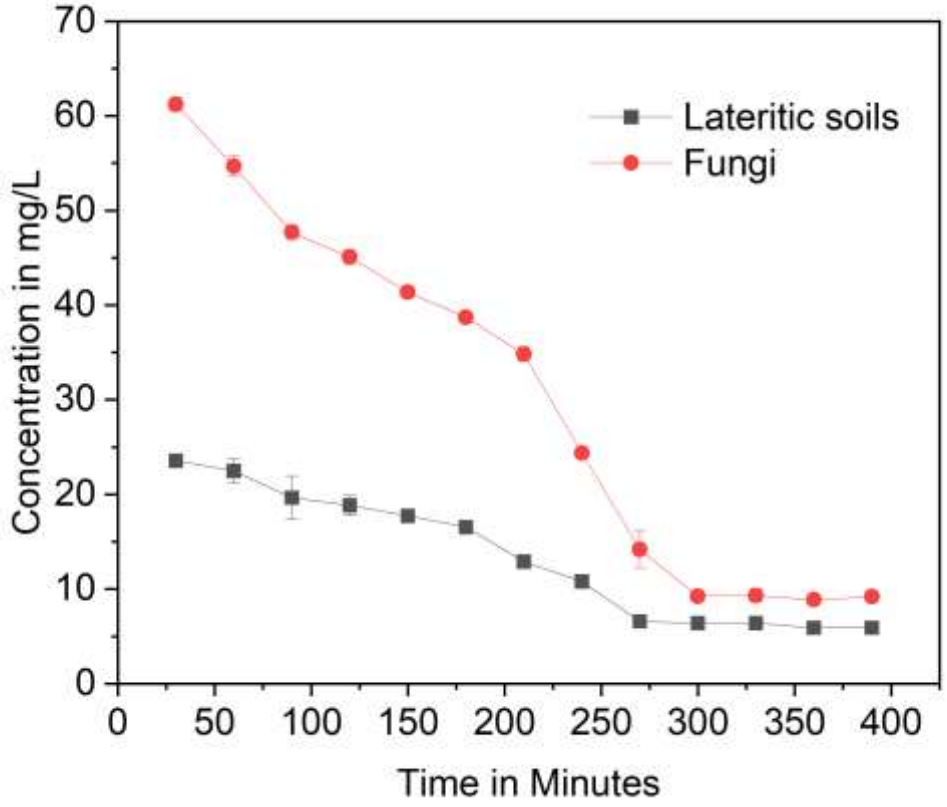

Figure 4.17: Desorption Capacities of Phosphorus from Lateritic Soils and Fungi

At the beginning of desorption experiments, P concentrations in the eluent were highest for the fungal adsorbent, reaching approximately 61.228 ± 0.71 mg/L, whereas lateritic soils released approximately 23.542 ± 0.53 mg/L. This initial sharp release indicates that both adsorbents contained a significant fraction of readily exchangeable P; however, the magnitude was considerably higher for the fungal material, suggesting that phosphorus binding in this matrix was more reversible. Similar patterns of rapid initial desorption from low-cost adsorbents have been reported in previous studies (Sellner et al., 2019), where weak surface interactions facilitated immediate release of loosely bound phosphate.

For lateritic soils, the desorption profile followed a relatively gradual pattern, with concentrations steadily declining from around 23.542 ± 0.53 mg/L to 10.786 ± 0.37

mg/L within 240 minutes. After 240 minutes, desorbed P stabilized at low concentrations 5.895 ± 0.32 mg/L, indicating that the remaining P was more strongly retained within the soil matrix. This behavior is consistent with findings from (Wu et al., 2019), who showed that Fe- and Al-rich soils exhibit low desorption due to the formation of strong inner-sphere phosphate complexes. Such mineral-bound P is known to resist desorption even under prolonged washing (Wu et al., 2019), which aligns with the limited regeneration potential observed in the present study.

In contrast, fungal adsorbents displayed a pronounced peak followed by a steep decline, with P concentrations dropping from 61.228 ± 0.71 mg/L initially to 9.254 ± 0.55 mg/L within 300 minutes. Beyond this point, the desorption curve leveled off, indicating that the majority of desorbable P had already been eluded. The high initial desorption and rapid stabilization reflect weaker binding interactions, possibly dominated by ion exchange and surface sorption, which make phosphorus more recoverable from fungal adsorbents compared to soils. This characteristic is advantageous for nutrient recycling, as it allows for greater recovery of phosphorus for potential reuse in agriculture.

CHAPTER FIVE

CONCLUSION AND RECOMMENDATIONS

5.1 Conclusions

In this study, Fungus (Agaricus Impudicus) and lateritic soils were used in recovering ammonium nitrogen and phosphorus from human urine. After adsorption, the used adsorbents were subjected to desorption experiments to evaluate the rate of release of the trapped nutrients. The following conclusions can be drawn from this study:

i. The physicochemical characterization of lateritic soil and *Agaricus impudicus* fungal biomass revealed distinct surface and structural properties that influence their adsorption performance. FTIR and XRF analysis confirmed the presence of functional groups such as hydroxyl, carboxyl, and amine groups, iron and aluminium oxides which are crucial for adsorption of ammonium nitrogen and phosphorus. SEM analysis revealed the presence of micropores which are crucial in adsorption processes. Lastly, human urine contains plant-essential metals, including calcium, copper, iron, and zinc whose concentrations were within the recommended limits by World Health Organization.

ii. Both lateritic soil and fungal biomass demonstrated effective adsorption of ammonium nitrogen (NH_4^+–N) and phosphorus (P) from human urine. Lateritic soil exhibited higher adsorption capacities (16.314 mg/g for NH_4^+–N and 24.558 mg/g for P) than fungal biomass, attributed to the ligand exchange and inner-sphere complexation facilitated by aluminium and iron oxides. Both adsorbents also showed that adsorption of ammonium nitrogen and phosphorus was majorly governed by physisorption. The varying adsorption capacities of the two adsorbents highlights their complementary potential use as engineered adsorbents within urine-diverting dry toilets. The adsorption mechanisms of these adsorbents show their suitability in recovery of ammonium nitrogen and phosphorus in support of circular nutrient economy frameworks.

iii. Fungal biomass exhibited higher desorption efficiencies (43.93% for NH_4^+–N and 44.83% for P) due to weaker electrostatic interactions, while lateritic soil showed lower desorption rates, indicating stronger ion binding. The

adsorbents' ability to release the adsorbed nutrients highlights the potential of reusing the used adsorbents as slow-release fertilizers in agriculture, thus reducing the use of synthetic fertilizers.

5.2 Recommendations

i) Organizations providing sanitation services should prioritize incorporation of low-cost and locally-sourced adsorbents in their decentralized sanitation technology like Urine Diversion and Dehydrating Toilets (UDDTs). The use of lateritic soils and the biomass of *Agaricus impudicus* as the adsorbent liners in this technology will enable these companies to perform nutrient recovery in situ. Through this, they will be able to convert human urine into a valuable resource, promoting a circular economy and while reducing nutrient pollution in freshwater bodies.

ii) Further studies should prioritize activation of Agaricus impudicus using chemical activation to improve its adsorption efficiency. Additionally, field-scale trials to evaluate the potential of lateritic soils and *Agaricus impudicus* in releasing the trapped nutrients for crop use.

REFERENCES

Afridi, H. I., Kazi, T. G., Kazi, N. G., Jamali, M. K., Arain, M. B., Sirajuddin, Baig, J. A., Kandhro, G. A., Wadhwa, S. K., & Shah, A. Q. (2010). Evaluation of cadmium, lead, nickel and zinc status in biological samples of smokers and nonsmokers hypertensive patients. *Journal of Human Hypertension*, *24*(1), 34–43. https://doi.org/10.1038/jhh.2009.39

Aghoghovwia, M. P., Hardie, A. G., & Rozanov, A. B. (2022). Characterisation, adsorption and desorption of ammonium and nitrate of biochar derived from different feedstocks. *Environmental Technology (United Kingdom)*, *43*(5), 774–787. https://doi.org/10.1080/09593330.2020.1804466

Ajmal, Z., Muhmood, A., Dong, R., & Wu, S. (2020). Probing the efficiency of magnetically modified biomass-derived biochar for effective phosphate removal. *Journal of Environmental Management*, *253*(September 2019), 109730. https://doi.org/10.1016/j.jenvman.2019.109730

Akafu, T., Chimdi, A., & Gomoro, K. (2019). Removal of fluoride from drinking water by sorption using diatomite modified with aluminum hydroxide. *Journal of Analytical Methods in Chemistry*, *2019*(1), 4831926.

Akcay, C., Ceylan, F., & Arslan, R. (2023). Production of oyster mushroom (Pleurotus ostreatus) from some waste lignocellulosic materials and FTIR characterization of structural changes. *Scientific Reports*, *13*(1), 1–13. https://doi.org/10.1038/s41598-023-40200-x

Akpan-Idiok, A. U., Udo, I. A., & Braide, E. I. (2012). The use of human urine as an organic fertilizer in the production of okra (Abelmoschus esculentus) in South Eastern Nigeria. *Resources, Conservation and Recycling*, *62*, 14–20. https://doi.org/10.1016/j.resconrec.2012.02.003

Alam, M. Z., & Anwar, A. H. M. F. (2020). Nutrients adsorption onto biochar and alum sludge for treating stormwater. *Journal of Water and Environment Technology*, *18*(2), 132–146. https://doi.org/10.2965/JWET.19-077

Alcalde-Garcia, F., Prasher, S., Kaliaguine, S., Tavares, J. R., & Dumont, M.-J. (2023). Desorption strategies and reusability of biopolymeric adsorbents and semisynthetic derivatives in hydrogel and hydrogel composites used in adsorption processes. *ACS Engineering Au*, *3*(6), 443–460.

Alemayehu, Y. A., Asfaw, S. L., & Terfie, T. A. (2020). Nutrient recovery options from human urine: A choice for large scale application. *Sustainable Production and Consumption*, *24*, 219–231. https://doi.org/10.1016/j.spc.2020.06.016

Alprol, A. E., Bakr, A., Al-Saeedi, S. I., El-Shafei, A. A., Alotaibi, F., El-Haron, E., Alharthi, M. N., & Ashour, M. (2025). Applications of marine red seaweed Pterocladia capillacea biomass in removal of hexavalent chromium and crystal violet dye from several wastewaters. *Scientific Reports*, *15*(1), 32428.

Alrefaee, S. H., Aljohani, M., Alkhamis, K., Shaaban, F., El-Desouky, M. G., El-Bindary, A. A., & El-Bindary, M. A. (2023). Adsorption and effective removal of organophosphorus pesticides from aqueous solution via novel metal-organic framework: Adsorption isotherms, kinetics, and optimization via Box-Behnken design. *Journal of Molecular Liquids*, *384*(April), 122206. https://doi.org/10.1016/j.molliq.2023.122206

Alshameri, A., He, H., Zhu, J., Xi, Y., Zhu, R., Ma, L., & Tao, Q. (2018). Adsorption of ammonium by different natural clay minerals: Characterization, kinetics and adsorption isotherms. *Applied Clay Science*, *159*(August 2017), 83–93. https://doi.org/10.1016/j.clay.2017.11.007

Amaral, L. F., Oliveira, I. R., Salomão, R., Frollini, E., & Pandolfelli, V. C. (2010). Temperature and common-ion effect on magnesium oxide (MgO) hydration. *Ceramics International*, *36*(3), 1047–1054.

An, C., Huang, G., Yao, Y., & Zhao, S. (2017). Emerging usage of electrocoagulation technology for oil removal from wastewater: A review. *Science of the Total Environment*, *579*, 537–556. https://doi.org/10.1016/j.scitotenv.2016.11.062

Aslani, C. K., & Amik, O. (2021). Active Carbon/PAN composite adsorbent for uranium removal: Modeling adsorption isotherm data, thermodynamic and kinetic studies. *Applied Radiation and Isotopes*, *168*(October), 109474. https://doi.org/10.1016/j.apradiso.2020.109474

Atanasova, N., Castellar, J. A. C., Pineda-Martos, R., Nika, C. E., Katsou, E., Istenič, D., Pucher, B., Andreucci, M. B., & Langergraber, G. (2021). Nature-based solutions and circularity in cities. *Circular Economy and Sustainability*, *1*(1), 319–332.

Avena Maia, M., Kranse, O. P., den Akker, S., & Torrente-Murciano, L. (2023). Phosphate recovery from urine-equivalent solutions for fertilizer production for plant growth. *ACS Sustainable Chemistry \& Engineering*, *11*(45), 16074–16086.

Ayawei, N., Ebelegi, A. N., & Wankasi, D. (2017). Modelling and Interpretation of Adsorption IsothermsAyawei, N., Ebelegi, A. N., & Wankasi, D. (2017). Modelling and Interpretation of Adsorption Isotherms. Journal of Chemistry, 2017, 1–11. https://doi.org/10.1155/2017/3039817. *Journal of Chemistry*, *2017*, 1–11.

Ayele, A., Haile, S., Alemu, D., & Kamaraj, M. (2021). Comparative Utilization of Dead and Live Fungal Biomass for the Removal of Heavy Metal: A Concise Review. *Scientific World Journal*, *2021*. https://doi.org/10.1155/2021/5588111

Aziz, H. A., Noor, A. F. M., Keat, Y. W., Alazaiza, M. Y. D., & Hamid, A. A. (2020). Heat Activated Zeolite for the Reduction of Ammoniacal Nitrogen, Colour, and COD in Landfill Leachate. *International Journal of Environmental Research*, *14*(4), 463–478. https://doi.org/10.1007/s41742-020-00270-5

Bahrami, M., Amiri, M. J., & Bagheri, F. (2019). Journal of Environmental Chemical Engineering Optimization of the lead removal from aqueous solution using two starch based adsorbents : Design of experiments using response surface methodology (RSM). *Journal of Environmental Chemical Engineering*, *7*(1), 102793. https://doi.org/10.1016/j.jece.2018.11.038

Balan, V., Zhu, W., Krishnamoorthy, H., Benhaddou, D., Mowrer, J., & Husain, H. (2022). Challenges and opportunities in producing high - quality edible mushrooms from lignocellulosic biomass in a small scale. *Applied Microbiology and Biotechnology*, 1355–1374. https://doi.org/10.1007/s00253-021-11749-2

Barquilha, C. E. R., & Braga, M. C. B. (2021). Adsorption of organic and inorganic pollutants onto biochars: Challenges, operating conditions, and mechanisms. *Bioresource Technology Reports*, *15*(June), 100728. https://doi.org/10.1016/j.biteb.2021.100728

Baykal, B. B. (2019). Recycling / reusing grey water and yellow water (human urine) motivations , perspectives and reflections into the future. *Desalination and*

Water Treatment, *172*(October 2018), 212–223. https://doi.org/10.5004/dwt.2019.24667

Behera, B., Patra, S., & Balasubramanian, P. (2020). Biological nutrient recovery from human urine by enriching mixed microalgal consortium for biodiesel production. *Journal of Environmental Management*, *260*(January), 110111. https://doi.org/10.1016/j.jenvman.2020.110111

Beig, S., Shah, S. A., Beig, S., & Shah, S. A. (2023). Biosorption of Cr (VI) by acid-modified based- waste fungal biomass from Calocybe indica fruiting bodies production Biosorption of Cr (VI) by acid-modified based-waste fungal biomass from. *International Journal of Phytoremediation*, *25*(10), 1269–1288. https://doi.org/10.1080/15226514.2022.2147145

Belaye, M., Taddesse, A. M., Teju, E., Sanchez-Sanchez, M., & Yassin, J. M. (2023). Preparation and Adsorption Behavior of Ce(III)-MOF for Phosphate and Fluoride Ion Removal from Aqueous Solutions. *ACS Omega*, *8*(26), 23860–23869. https://doi.org/10.1021/acsomega.3c02290

Bellahsen, N., Varga, G., Halyag, N., Kertész, S., Tombácz, E., & Hodúr, C. (2021). Pomegranate peel as a new low-cost adsorbent for ammonium removal. *International Journal of Environmental Science and Technology*, *18*(3), 711–722. https://doi.org/10.1007/s13762-020-02863-1

Benredouane, S., Berrama, T., & Doufene, N. (2016). Chemometrics and Intelligent Laboratory Systems Strategy of screening and optimization of process parameters using experimental design : application to amoxicillin elimination by adsorption on activated carbon. *Chemometrics and Intelligent Laboratory Systems*, *155*, 128–137. https://doi.org/10.1016/j.chemolab.2016.04.010

Bhattacharjee, A., Jana, B. B., Mandal, S. K., Lahiri, S., & Bhakta, J. N. (2021). Assessing phosphorus removal potential of laterite soil for water treatment and eco-technological application. *Ecological Engineering*, *166*(January), 106245. https://doi.org/10.1016/j.ecoleng.2021.106245

Bian, H., Wang, M., Huang, J., Liang, R., & Du, J. (2024). Journal of Water Process Engineering Large particle size boosting the engineering application potential of functional biochar in ammonia nitrogen and phosphorus removal from biogas

slurry. *Journal of Water Process Engineering*, *57*(November 2023), 104640. https://doi.org/10.1016/j.jwpe.2023.104640

Biliani, I., Tsavatopoulou, V., & Zacharias, I. (2024). Comparative Study of Ammonium and Orthophosphate Removal Efficiency with Natural and Modified Clay-Based Materials, for Sustainable Management of Eutrophic Water Bodies. *Sustainability*, *16*(23), 10214.

Bischak, E., Fusi, S. C., Jeliazovski, J., Beheshtian, K., & Ryals, R. (2024). Urine-enriched biochar: Coupling sustainability in sanitation and agriculture. *Elementa*, *12*(1), 1–14. https://doi.org/10.1525/elementa.2022.00118

Biswas, B., Rahman, T., Sakhakarmy, M., Jahromi, H., Eisa, M., Baltrusaitis, J., Lamba, J., Torbert, A., & Adhikari, S. (2023). Phosphorus adsorption using chemical and metal chloride activated biochars: Isotherms, kinetics and mechanism study. *Heliyon*, *9*(9), e19830. https://doi.org/10.1016/j.heliyon.2023.e19830

Bulacio Fischer, P. T., Di Trapani, D., Laudicina, V. A., Mineo, A., Muscarella, S. M., & Mannina, G. (2025). Adsorption and desorption of ammonium from treated wastewater by zeolite filled columns: An experimental study at the water resource recovery facility of Palermo University – Italy. *Journal of Environmental Management*, *375*(December 2024), 124241. https://doi.org/10.1016/j.jenvman.2025.124241

Camacho-delaCruz, A. A., Mendoza-Cano, O., Trujillo, X., Huerta, M., Ríos-Silva, M., Gonzalez-Curiel, I. E., Lugo-Radillo, A., Romo-García, M. F., Cuevas-Arellano, H. B., Hilerio-López, Á. G., Solano-Barajas, R., Bricio-Barrios, J. A., Uribe-Ramos, J. M., Ventura-Ramírez, J. F., Solano-Mendoza, A. A., Sánchez-Cárdenas, F., Benites-Godínez, V., Ríos-Bracamontes, E. F., Venegas-Ramírez, J., & Murillo-Zamora, E. (2025). The Screening and Correlation of Trace Elements in the Blood and Urine of School-Aged Children (5–12 Years): A Pilot Biomonitoring Study. *Toxics*, *13*(6), 1–10. https://doi.org/10.3390/toxics13060431

Carleton, G., & Cutright, T. J. (2020). Evaluation of alum-based water treatment residuals used to adsorb reactive phosphorus. *Water Science and Engineering*, *13*(3), 181–192. https://doi.org/10.1016/j.wse.2020.09.008

Caspersen, S., & Ganrot, Z. (2018). Closing the loop on human urine: Plant availability of zeolite-recovered nutrients in a peat-based substrate. *Journal of Environmental Management*, *211*, 177–190.

Chakraborty, R., K, V., Pradhan, M., & Nayak, A. K. (2022). Recent advancement of biomass-derived porous carbon based materials for energy and environmental remediation applications. *Journal of Materials Chemistry A*, *10*(13), 6965–7005.

Chen, X., Gao, Y., Hou, D., Ma, H., Lu, L., Sun, D., Zhang, X., Liang, P., Huang, X., & Ren, Z. J. (2017). The microbial electrochemical current accelerates urea hydrolysis for recovery of nutrients from source-separated urine. *Environmental Science & Technology Letters*, *4*(7), 305–310.

Chipako, T. L., & Randall, D. G. (2020). Urine treatment technologies and the importance of pH. *Journal of Environmental Chemical Engineering*, *8*(1), 103622. https://doi.org/10.1016/j.jece.2019.103622

Chotpantarat, S., Ong, S. K., Sutthirat, C., & Osathaphan, K. (2011). Effect of pH on transport of Pb2+, Mn2+, Zn2+ and Ni2+ through lateritic soil: Column experiments and transport modeling. *Journal of Environmental Sciences*, *23*(4), 640–648. https://doi.org/10.1016/S1001-0742(10)60417-2

Chowdhury, S., & Saha, P. (2011). Adsorption Kinetic Modeling of Safranin onto Rice Husk Biomatrix Using Pseudo-first- and Pseudo-second-order Kinetic Models: Comparison of Linear and Non-linear Methods. *Clean - Soil, Air, Water*, *39*(3), 274–282. https://doi.org/10.1002/clen.201000170

Das, S. K., Ghosh, P., Ghosh, I., & Guha, A. K. (2008). Adsorption of rhodamine B on Rhizopus oryzae: Role of functional groups and cell wall components. *Colloids and Surfaces B: Biointerfaces*, *65*(1), 30–34. https://doi.org/10.1016/j.colsurfb.2008.02.020

de Luna, M. D. G., Futalan, C. M., Jurado, C. A., Colades, J. I., & Wan, M. W. (2018). Removal of ammonium-nitrogen from aqueous solution using chitosan-coated bentonite: Mechanism and effect of operating parameters. *Journal of Applied Polymer Science*, *135*(9), 1–11. https://doi.org/10.1002/app.45924

Demirbas, A. (2004). Combustion characteristics of different biomass fuels. *Progress in Energy and Combustion Science*, *30*(2), 219–230.

Devesa-Rey, R., Del Val, J., Feijoo, J., González-Coma, J., Castiñeira, G., & González-Gil, L. (2021). Preparation of synthetic clays to remove phosphates and ibuprofen in water. *Water (Switzerland)*, *13*(17). https://doi.org/10.3390/w13172394

Devlin, M., & Brodie, J. (2023). Nutrients and eutrophication. In *Marine pollution–monitoring, management and mitigation* (pp. 75–100). Springer.

Dey, S., Basha, S. R., Babu, G. V., & Nagendra, T. (2021). Characteristic and biosorption capacities of orange peels biosorbents for removal of ammonia and nitrate from contaminated water. *Cleaner Materials*, *1*(June), 100001. https://doi.org/10.1016/j.clema.2021.100001

Divband, L., Hooshmand, A., Ali, A., Soltani, A., Abbasi, F., & Bhatnagar, A. (2016). Removal of nitrate from aqueous solution by modified sugarcane bagasse biochar. *Ecological Engineering*, *95*, 101–111. https://doi.org/10.1016/j.ecoleng.2016.06.035

Djekoune, L., Maaliou, A., Salem, Z., Ziani, D., Kamel, R., Ouakouak, A., Baigenzhenov, O., Bokov, D. O., Ivanets, A., & Hosseini-Bandegharaei, A. (2024). Phosphate adsorption on dried alum sludge: Modeling and application to treatment of dairy effluents. *Environmental Research*, *252*(P3), 118976. https://doi.org/10.1016/j.envres.2024.118976

Dodds, W. K., & Smith, V. H. (2016). Nitrogen, phosphorus, and eutrophication in streams. *Inland Waters*, *6*(2), 155–164.

Dong, X. Q., Yang, J. S., Zhu, N., Wang, E. T., & Yuan, H. L. (2013). Sugarcane bagasse degradation and characterization of three white-rot fungi. *Bioresource Technology*, *131*, 443–451. https://doi.org/10.1016/j.biortech.2012.12.182

Eisazadeh, A., Kassim, K. A., & Nur, H. (2012). Solid-state NMR and FTIR studies of lime stabilized montmorillonitic and lateritic clays. *Applied Clay Science*, *67–68*, 5–10. https://doi.org/10.1016/j.clay.2012.05.006

Ertul, \cSeref, Bayrakc\i, M., & Yilmaz, M. (2010). Removal of chromate and phosphate anion from aqueous solutions using calix [4] aren receptors containing proton switchable units. *Journal of Hazardous Materials*, *181*(1–3), 1059–1065.

Fan, R., Chen, C., Lin, J., Tzeng, J., Huang, C., & Dong, C. (2019). Bioresource Technology Adsorption characteristics of ammonium ion onto hydrous biochars in dilute aqueous solutions. *Bioresource Technology*, *272*(September 2018), 465–472. https://doi.org/10.1016/j.biortech.2018.10.064

FAO, F., & others. (2017). The future of food and agriculture--Trends and challenges. *Annual Report*, *296*, 1–180.

Feng, M., Li, M., Zhang, L., Luo, Y., Zhao, D., Yuan, M., Zhang, K., & Wang, F. (2022). Oyster Shell Modified Tobacco Straw Biochar: Efficient Phosphate Adsorption at Wide Range of pH Values. *International Journal of Environmental Research and Public Health*, *19*(12). https://doi.org/10.3390/ijerph19127227

Fetene, Y., & Addis, T. (2020). Adsorptive Removal of Phosphate From Wastewater Using Ethiopian Rift Pumice: Batch Experiment. *Air, Soil and Water Research*, *13*. https://doi.org/10.1177/1178622120969658

Foo, K. Y., & Hameed, B. H. (2010). Insights into the modeling of adsorption isotherm systems. *Chemical Engineering Journal*, *156*(1), 2–10.

Freguia, S., Logrieco, M. E., Monetti, J., Ledezma, P., Virdis, B., & Tsujimura, S. (2019). Self-powered bioelectrochemical nutrient recovery for fertilizer generation from human urine. *Sustainability*, *11*(19), 5490.

Frutos, I., García-Delgado, C., Gárate, A., & Eymar, E. (2016). Biosorption of heavy metals by organic carbon from spent mushroom substrates and their raw materials. *International Journal of Environmental Science and Technology*, *13*(11), 2713–2720. https://doi.org/10.1007/s13762-016-1100-6

Ganesapillai, M., Simha, P., Gupta, K., & Jayan, M. (2016). Nutrient Recovery and Recycling from Human Urine : A Circular Perspective on Sanitation and Food Security. *Procedia Engineering*, *148*, 346–353. https://doi.org/10.1016/j.proeng.2016.06.461

Gao, J., Gong, J., Yang, J., Wang, Z., Fu, Y., Tang, S., & Ma, S. (2023). Spatial distribution and ecological risk assessment of soil heavy metals in a typical volcanic area: Influence of parent materials. *Heliyon*, *9*(1).

Gao, Y., Li, J., Zhang, Y., Sun, X., & Yang, L. (2021). Mechanical and Microscopic Properties of Graphite/Laterite Nanocomposites. *Advances in Materials Science and Engineering*, *2021*. https://doi.org/10.1155/2021/1175621

Geissler, B., Mew, M. C., Weber, O., & Steiner, G. (2015). Resources, Conservation and Recycling Efficiency performance of the world's leading corporations in phosphate rock mining. *"Resources, Conservation & Recycling," 105*, 246–258. https://doi.org/10.1016/j.resconrec.2015.10.008

Gelaw, Y. B., Dagne, H., Adane, B., Yirdaw, G., Moges, M., Aneley, Z., Kumlachew, L., Aschale, A., Deml, Y. A., Tegegne, E., & Birhan, T. A. (2024). Adsorptive removal of cadmium (II) from wastewater using activated carbon synthesized from stem of Khat (Catha edulis). *Heliyon*, *10*(22), e40389. https://doi.org/10.1016/j.heliyon.2024.e40389

Genethliou, C., Triantaphyllidou, I. E., Giannakis, D., Papayianni, M., & Sygellou, L. (2021). Simultaneous removal of ammonium nitrogen , dissolved chemical oxygen demand and color from sanitary landfill leachate using natural zeolite. *Journal of Hazardous Materials*, *406*(September 2020), 124679. https://doi.org/10.1016/j.jhazmat.2020.124679

Genetie Abetu, A., & Befekadu Kebede, A. (2021). Crushed Concrete As Adsorptive Material for Removal of Phosphate Ions From Aqueous Solutions. *Water Conservation & Management*, *5*(2), 71–77. https://doi.org/10.26480/wcm.02.2021.71.77

Geng, Y., Wang, Y., Li, H., Li, R., Ge, S., Wang, H., Wu, S., & Liu, H. (2024). Optimization of manure-based substrate preparation to reduce nutrients losses and improve quality for growth of Agaricus bisporus. *Agriculture*, *14*(10), 1833.

Gilman, J., Walls, L., Bandiera, L., & Menolascina, F. (2021). Statistical Design of Experiments for Synthetic Biology. *ACS Synthetic Biology*, *10*(1), 1–18. https://doi.org/10.1021/acssynbio.0c00385

Grenon, G., Singh, B., de Sena, A., Madramootoo, C. A., von Sperber, C., Goyal, M. K., & Zhang, T. (2021). Phosphorus fate, transport and management on subsurface drained agricultural organic soils: A review. *Environmental Research Letters*, *16*(1). https://doi.org/10.1088/1748-9326/abce81

Guida, S., Potter, C., Jefferson, B., & Soares, A. (2020). Preparation and evaluation of zeolites for ammonium removal from municipal wastewater through ion exchange process. *Scientific Reports*, 1–11. https://doi.org/10.1038/s41598-020-69348-6

Gunarathne, V., Ashiq, A., Ramanayaka, S., Wijekoon, P., & Vithanage, M. (2019). Biochar from municipal solid waste for resource recovery and pollution remediation. *Environmental Chemistry Letters*, *17*(3), 1225–1235. https://doi.org/10.1007/s10311-019-00866-0

Guo, X., & Wang, J. (2019). A general kinetic model for adsorption : Theoretical analysis and modeling. *Journal of Molecular Liquids*, *288*, 111100. https://doi.org/10.1016/j.molliq.2019.111100

Halajnia, A., Oustan, S., Najafi, N., Khataee, A. R., & Lakzian, A. (2013). Adsorption--desorption characteristics of nitrate, phosphate and sulfate on Mg--Al layered double hydroxide. *Applied Clay Science*, *80*, 305–312.

Halder, P., Marzbali, M. H., Patel, S., Short, G., Surapaneni, A., Gupta, R., & Shah, K. (2023). Ammonium nitrogen (NH4+-N) recovery from synthetic wastewater using biosolids-derived biochar. *Bioresource Technology Reports*, *23*(August), 101592. https://doi.org/10.1016/j.biteb.2023.101592

Hellal, M. S., Rashad, A. M., Kadimpati, K. K., Attia, S. K., & Fawzy, M. E. (2023). Adsorption characteristics of nickel (II) from aqueous solutions by Zeolite Scony Mobile - 5 (ZSM - 5) incorporated in sodium alginate beads. *Scientific Reports*, *5*(Ii), 1–16. https://doi.org/10.1038/s41598-023-45901-x

Hou, Y., & Wu, W. (2026). Adsorptive removal of phosphate from water using corn straw derived biochar. *Environmental Progress \& Sustainable Energy*, *45*(3), e70125.

Huang, X., Sheng, X., Guo, Y., Sun, Y., Fatehi, P., & Shi, H. (2022). Rice straw derived adsorbent for fast and efficient phosphate elimination from aqueous solution. *Industrial Crops and Products*, *184*(February), 115105. https://doi.org/10.1016/j.indcrop.2022.115105

Huong, L., & Phuoc, N. Van. (2024). Sugarcane bagasse - derived biochar modified by alkali for enriching surface functional groups to effectively treat

ammonium - contaminated water. *Environmental Geochemistry and Health*, *46*(11), 1–19. https://doi.org/10.1007/s10653-024-02248-0

Husien, S., Labena, A., El-belely, E. F., Mahmoud, H. M., & Hamouda, A. S. (2019). Journal of Environmental Chemical Engineering Adsorption studies of hexavalent chromium [Cr (VI)] on micro-scale biomass of Sargassum dentifolium , Sea weed. *Journal of Environmental Chemical Engineering*, *7*(6), 103444. https://doi.org/10.1016/j.jece.2019.103444

Ilyas, H., & Masih, I. (2017). Intensification of constructed wetlands for land area reduction: a review. *Environmental Science and Pollution Research*, *24*(13), 12081–12091.

Imessaoudene, A., Cheikh, S., Hadadi, A., Hamri, N., Bollinger, J. C., Amrane, A., Tahraoui, H., Manseri, A., & Mouni, L. (2023). Adsorption Performance of Zeolite for the Removal of Congo Red Dye: Factorial Design Experiments, Kinetic, and Equilibrium Studies. *Separations*, *10*(1). https://doi.org/10.3390/separations10010057

Indah, S., Helard, D., Primasari, B., Edwin, T., & Hexa Putra, R. (2019). Modification of natural pumice by physical and chemical treatments for removal of zinc ions from aqueous solution. *MATEC Web of Conferences*, *276*, 06009. https://doi.org/10.1051/matecconf/201927606009

International Energy Agency. (2021). *Ammonia technology roadmap: towards more sustainable nitrogen fertiliser production*. OECD Publishing.Paris

Iriel, A., Bruneel, S. P., Schenone, N., & Cirelli, A. F. (2018). The removal of fluoride from aqueous solution by a lateritic soil adsorption: Kinetic and equilibrium studies. *Ecotoxicology and Environmental Safety*, *149*(November 2017), 166–172. https://doi.org/10.1016/j.ecoenv.2017.11.016

Isik, Z., Saleh, M., & Dizge, N. (2021). Adsorption studies of ammonia and phosphate ions onto calcium alginate beads. *Surfaces and Interfaces*, *26*(May), 101330. https://doi.org/10.1016/j.surfin.2021.101330

islam, I. ul, Ahmad, M., Shah, B., Ahmad, H. M., Janiad, S., Shah, N., & Yabalak, E. (2025a). Parthenium hysterophorus-derived iron-coated biochar: a sustainable solution for nitrate and phosphate removal from water. *Biomass Conversion and Biorefinery*, *15*(7), 10773–10790.

islam, I. ul, Ahmad, M., Shah, B., Ahmad, H. M., Janiad, S., Shah, N., & Yabalak, E. (2025b). Parthenium hysterophorus-derived iron-coated biochar: a sustainable solution for nitrate and phosphate removal from water. *Biomass Conversion and Biorefinery*, *15*(7), 10773–10790. https://doi.org/10.1007/s13399-024-05821-w

Kabdaşlı, I., & Tünay, O. (2018). Nutrient recovery by struvite precipitation, ion exchange and adsorption from source-separated human urine–a review. *Environmental Technology Reviews*, *7*(1), 106–138. https://doi.org/10.1080/21622515.2018.1473504

Kabuba, J., & Lephallo, J. (2023). Removal of ammonia nitrogen from wastewater using activated carbon prepared from waste tyres. *Water Practice and Technology*, *18*(6), 1479–1499. https://doi.org/10.2166/wpt.2023.086

Kalam, S., Abu-Khamsin, S. A., Kamal, M. S., & Patil, S. (2021). Surfactant adsorption isotherms: A review. *ACS Omega*, *6*(48), 32342–32348.

Kalaruban, M., Loganathan, P., Shim, W. G., Kandasamy, J., Ngo, H. H., & Vigneswaran, S. (2016). Enhanced removal of nitrate from water using amine-grafted agricultural wastes. *Science of the Total Environment*, *565*, 503–510.

Karak, T., & Bhattacharyya, P. (2011). Human urine as a source of alternative natural fertilizer in agriculture: A flight of fancy or an achievable reality. *Resources, Conservation and Recycling*, *55*(4), 400–408. https://doi.org/10.1016/j.resconrec.2010.12.008

Karunanithi, R., Szogi, A., Bolan, N. S., Naidu, R., Ok, Y. S., Krishnamurthy, S., & Seshadri, B. (2016). Phosphorus Recovery From Wastes. *Environmental Materials and Waste: Resource Recovery and Pollution Prevention*, 687–705. https://doi.org/10.1016/B978-0-12-803837-6.00027-5

Khalil, A. K. A., Dweiri, F., Almanassra, I. W., Chatla, A., & Atieh, M. A. (2022). Mg-Al Layered Double Hydroxide Doped Activated Carbon Composites for Phosphate Removal from Synthetic Water: Adsorption and Thermodynamics Studies. *Sustainability (Switzerland)*, *14*(12). https://doi.org/10.3390/su14126991

Khan, M. A., ALOthman, Z. A., Naushad, M., Khan, M. R., & Luqman, M. (2015). Adsorption of methylene blue on strongly basic anion exchange resin (Zerolit

DMF): kinetic, isotherm, and thermodynamic studies. *Desalination and Water Treatment*, *53*(2), 515–523.

Kiani, D., Sheng, Y., Lu, B., Barauskas, D., Honer, K., Jiang, Z., & Baltrusaitis, J. (2018). Transient struvite formation during stoichiometric (1: 1) NH4+ and PO43–adsorption/reaction on magnesium oxide (MgO) particles. *ACS Sustainable Chemistry & Engineering*, *7*(1), 1545–1556.

Kizito, S., Wu, S., Kipkemoi Kirui, W., Lei, M., Lu, Q., Bah, H., & Dong, R. (2015). Evaluation of slow pyrolyzed wood and rice husks biochar for adsorption of ammonium nitrogen from piggery manure anaerobic digestate slurry. *Science of the Total Environment*, *505*, 102–112. https://doi.org/10.1016/j.scitotenv.2014.09.096

Konneh, M., Wandera, S. M., Murunga, S. I., & Raude, J. M. (2021). Adsorption and desorption of nutrients from abattoir wastewater: modelling and comparison of rice, coconut and coffee husk biochar. *Heliyon*, *7*(11), e08458. https://doi.org/10.1016/j.heliyon.2021.e08458

Kosre, A., Koreti, D., Mahish, P. K., & Chandrawanshi, N. K. (2021). Current perspective of sustainable utilization of agro waste and biotransformation of energy in mushroom. *Energy: Crises, Challenges and Solutions*, 274–302.

Krishna, K. C. B., Aryal, A., & Jansen, T. (2016). Comparative study of ground water treatment plants sludges to remove phosphorous from wastewater. *Journal of Environmental Management*, *180*, 17–23. https://doi.org/10.1016/j.jenvman.2016.05.006

Kujawa-Roeleveld, K., & Zeeman, G. (2006). Anaerobic treatment in decentralised and source-separation-based sanitation concepts. *Reviews in Environmental Science and Biotechnology*, *5*(1), 115–139. https://doi.org/10.1007/s11157-005-5789-9

Kumar, P., & Chauhan, M. S. (2019). Adsorption of chromium (VI) from the synthetic aqueous solution using chemically modified dried water hyacinth roots. *Journal of Environmental Chemical Engineering*, *7*(4), 103218. https://doi.org/10.1016/j.jece.2019.103218

Kushwaha, S., Soni, H., Ageetha, V., & Padmaja, P. (2013). An Insight Into the Production , Characterization , and Mechanisms of Action of Low-Cost

Adsorbents for Removal of Organics From Aqueous Solution *3389*. https://doi.org/10.1080/10643389.2011.604263

Lacerda, L., Consalter, I., Perretto, F., Carolina, R., Rizzo-domingues, P., Hermes, F., & De, K. Q. (2021). Adsorption and desorption of phosphate onto chemically and thermochemically pre-activated red ceramic waste : Characteristics , batch studies , and mechanisms. *Journal of Environmental Chemical Engineering 9*(December 2020). https://doi.org/10.1016/j.jece.2021.106695

Lala, M. A., Ntamu, T. E., Adesina, O. A., Popoola, L. T., Yusuff, A. S., & Adeyi, A. A. (2023). Adsorption of hexavalent chromium from aqueous solution using cationic modified rice husk : Parametric optimization via Taguchi design approach. *20*. https://doi.org/10.1016/j.sciaf.2023.e01633

Larsen, T. A., Riechmann, M. E., & Udert, K. M. (2021). State of the art of urine treatment technologies: A critical review. *Water Research X*, *13*, 100114. https://doi.org/10.1016/j.wroa.2021.100114

Laskar, N., & Kumar, U. (2022). Application of low-cost, eco-friendly adsorbents for the removal of dye contaminants from wastewater: Current developments and adsorption technology. *Environmental Quality Management*, *32*(1), 209–221.

Latif, W., Ciniglia, C., Iovinella, M., Shafiq, M., & Papa, S. (2023). Role of White Rot Fungi in Industrial Wastewater Treatment: A Review. *Applied Sciences (Switzerland)*, *13*(14). https://doi.org/10.3390/app13148318

Lee, J., Oh, J., Yoo, S., Hea, E., Lee, C., & Park, J. (2022). Journal of Environmental Chemical Engineering Removal of phosphorus from water using calcium-rich organic waste and its potential as a fertilizer for rice growth. *Journal of Environmental Chemical Engineering*, *10*(2), 107367. https://doi.org/10.1016/j.jece.2022.107367

Leng, L., Xu, S., Liu, R., Yu, T., Zhuo, X., Leng, S., Xiong, Q., & Huang, H. (2020). Nitrogen containing functional groups of biochar: An overview. *Bioresource Technology*, *298*, 122286. https://doi.org/10.1016/j.biortech.2019.122286

Lepohi, B., Laurent, G., Tang, W., & Chen, J. (2022). N-doped and activated porous biochar derived from cocoa shell for removing norfloxacin from aqueous

solution : Performance assessment and mechanism insight. *Environmental Research*, *214*(April), 113951. https://doi.org/10.1016/j.envres.2022.113951

Li, H., Wang, F., Li, J., Deng, S., & Zhang, S. (2021). Adsorption of three pesticides on polyethylene microplastics in aqueous solutions: Kinetics, isotherms, thermodynamics, and molecular dynamics simulation. *Chemosphere*, *264*, 128556. https://doi.org/10.1016/j.chemosphere.2020.128556

Li, M., Li, M., & Li, X. (2025). Phosphorus capturing from biogas slurry using different adsorbents: adsorption and mechanism. *Water Science and Technology : A Journal of the International Association on Water Pollution Research*, *92*(5), 770–784. https://doi.org/10.2166/wst.2025.129

Li, X., & Shi, J. (2022). Simultaneous adsorption of tetracycline, ammonium and phosphate from wastewater by iron and nitrogen modified biochar: Kinetics, isotherm, thermodynamic and mechanism. *Chemosphere*, *293*(November 2021), 133574. https://doi.org/10.1016/j.chemosphere.2022.133574

Liu, C., Wang, Y., Li, X., Li, J., Dong, S., Hao, H., Tong, Y., & Zhou, Y. (2022). Highly efficient P uptake by Fe3O4 loaded amorphous Zr-La (carbonate) oxides: Electrostatic attraction, inner-sphere complexation and oxygen vacancies acceleration effect. *Journal of Environmental Sciences (China)*, *120*, 18–29. https://doi.org/10.1016/j.jes.2022.01.003

Liu, J., Zheng, M., Wang, C., Liang, C., Shen, Z., & Xu, K. (2020a). A green method for the simultaneous recovery of phosphate and potassium from hydrolyzed urine as value-added fertilizer using wood waste. *Resources, Conservation and Recycling*, *157*(October 2019), 104793. https://doi.org/10.1016/j.resconrec.2020.104793

Liu, J., Zheng, M., Wang, C., Liang, C., Shen, Z., & Xu, K. (2020b). Resources , Conservation & Recycling A green method for the simultaneous recovery of phosphate and potassium from hydrolyzed urine as value-added fertilizer using wood waste. *Resources, Conservation & Recycling*, *157*(March), 104793. https://doi.org/10.1016/j.resconrec.2020.104793

Liu, K. (2019). E ff ects of sample size , dry ashing temperature and duration on determination of ash content in algae and other biomass. *Algal Research*, *40*(April), 101486. https://doi.org/10.1016/j.algal.2019.101486

Liu, Q., Sun, J., Liu, X., Li, Y., Shen, C., Gadow, S. I., Li, H., & Zhang, Y. (2025). Journal of Environmental Chemical Engineering Low-cost municipal solid waste incineration fly ash adsorbents for phosphate recovery : A potential green treatment process. *Journal of Environmental Chemical Engineering*, *13*(5), 117998. https://doi.org/10.1016/j.jece.2025.117998

Liu, R., Zhao, Y., Doherty, L., Hu, Y., & Hao, X. (2015). A review of incorporation of constructed wetland with other treatment processes. *CHEMICAL ENGINEERING JOURNAL*, *279*, 220–230. https://doi.org/10.1016/j.cej.2015.05.023

Loganathan, P., Vigneswaran, S., Kandasamy, J., & Bolan, N. S. (2014). *Technology Removal and Recovery of Phosphate From Water Using Sorption*. *3389*. https://doi.org/10.1080/10643389.2012.741311

Low, W. P., Siow, J. M., Lee, H. P., Abdul Rahman, N., Jusli, E., & Putra Jaya, R. (2022). Mass transfer analysis of total nitrogen adsorption from river water onto tea waste (Camellia Sinensis). *Physics and Chemistry of the Earth*, *128*(September), 103249. https://doi.org/10.1016/j.pce.2022.103249

Lu, N., Hu, T., Zhai, Y., Qin, H., Aliyeva, J., & Zhang, H. (2020). Fungal cell with artificial metal container for heavy metals biosorption: Equilibrium, kinetics study and mechanisms analysis. *Environmental Research*, *182*(November 2019), 109061. https://doi.org/10.1016/j.envres.2019.109061

Luo, W., Qian, L., Liu, W., Zhang, X., Wang, Q., Jiang, H., & Cheng, B. (2021). Science of the Total Environment A potential Mg-enriched biochar fertilizer : Excellent slow-release performance and release mechanism of nutrients. *Science of the Total Environment*, *768*, 144454. https://doi.org/10.1016/j.scitotenv.2020.144454

Maged, A., Ismael, I. S., Kharbish, S., Sarkar, B., Peräniemi, S., & Bhatnagar, A. (2020). Enhanced interlayer trapping of Pb (II) ions within kaolinite layers: intercalation, characterization, and sorption studies. *Environmental Science and Pollution Research*, *27*(2), 1870–1887.

Maleki, S., & Karimi-jashni, A. (2017). Applied Clay Science Effect of ball milling process on the structure of local clay and its adsorption performance for Ni (II)

removal. *Applied Clay Science*, *137*, 213–224. https://doi.org/10.1016/j.clay.2016.12.008

Manawi, Y., Gaashani, R. Al, Simson, S., Tong, Y., Lawler, J., & Kochkodan, V. (2024). Adsorptive removal of phosphate from water with biochar from acacia tree modified with iron and magnesium oxides. *Scientific Reports*, (0123456789), 1–20. https://doi.org/10.1038/s41598-024-66965-3

Manikam, M. K., Halim, A. A., Hanafiah, M. M., & Krishnamoorthy, R. R. (2019). Removal of ammonia nitrogen, nitrate, phosphorus and cod from sewage wastewater using palm oil boiler ash composite adsorbent. *Desalination and Water Treatment*, *149*(2019), 23–30. https://doi.org/10.5004/dwt.2019.23842

Mansing R, P., & Rout, P. D. (2013). Removal of phosphorus from sewage effluent by adsorption on Laterite. *International Journal of Engineering Research & Technology*, *2*(9), 551–559.

Martin, T. M. P., Aubin, J., Gilles, E., Auberger, J., Esculier, F., Levavasseur, F., McConville, J., & Houot, S. (2023). Comparative study of environmental impacts related to wheat production with human-urine based fertilizers versus mineral fertilizers. *Journal of Cleaner Production*, *382*, 135123.

Martin, T. M. P., Esculier, F., Levavasseur, F., & Houot, S. (2022). Human urine-based fertilizers: A review. *Critical Reviews in Environmental Science and Technology*, *52*(6), 890–936. https://doi.org/10.1080/10643389.2020.1838214

Martin, T. M. P., Esculier, F., Levavasseur, F., Houot, S., Martin, T. M. P., Esculier, F., Levavasseur, F., & Houot, S. (2020). Technology Human urine-based fertilizers : A review. *Critical Reviews in Environmental Science and Technology*, *0*(0), 1–47. https://doi.org/10.1080/10643389.2020.1838214

Mazarji, M., Aminzadeh, B., Baghdadi, M., & Bhatnagar, A. (2017). Removal of nitrate from aqueous solution using modified granular activated carbon. *Journal of Molecular Liquids*, *233*, 139–148. https://doi.org/10.1016/j.molliq.2017.03.004

McDowell, R. W., & Haygarth, P. M. (2024). Reducing phosphorus losses from agricultural land to surface water. *Current Opinion in Biotechnology*, *89*, 103181. https://doi.org/10.1016/j.copbio.2024.103181

Mehta, C. M., Khunjar, W. O., Nguyen, V., Tait, S., & Batstone, D. J. (2015). Technologies to recover nutrients from waste streams: a critical review. *Critical Reviews in Environmental Science and Technology*, *45*(4), 385–427.

Mihelcic, J. R., Fry, L. M., & Shaw, R. (2011). Global potential of phosphorus recovery from human urine and feces. *Chemosphere*, *84*(6), 832–839. https://doi.org/10.1016/j.chemosphere.2011.02.046

Mitrogiannis, D., Psychogiou, M., Bourazas, K., Palles, D., Kamitsos, E. I., Mavrogonatos, C., & Baziotis, I. (2023). Interactions of Real Urine with Modified Palygorskite and Zeolite Focusing on Adsorption Mechanisms, Nutrient Bioavailability and Soil Conditioner Upgrade. *Water, Air, and Soil Pollution*, *234*(6), 1–23. https://doi.org/10.1007/s11270-023-06414-5

Mitrogiannis, D., Psychoyou, M., Baziotis, I., Inglezakis, V. J., Koukouzas, N., Tsoukalas, N., Palles, D., Kamitsos, E., Oikonomou, G., & Markou, G. (2017). Removal of phosphate from aqueous solutions by adsorption onto Ca (OH) 2 treated natural clinoptilolite. *Chemical Engineering Journal*, *320*, 510–522. https://doi.org/10.1016/j.cej.2017.03.063

Mohamed Nasser, S., Abbas, M., & Trari, M. (2024). Understanding the rate-limiting step adsorption kinetics onto biomaterials for mechanism adsorption control. *Progress in Reaction Kinetics and Mechanism*, *49*, 14686783241226858.

Montgomery, D. C. (2017). Design and Analysis of Experiments (9th ed.). John Wiley & Sons. Hoboken,NJ

Mozaffari Majd, M., Kordzadeh-Kermani, V., Ghalandari, V., Askari, A., & Sillanpää, M. (2022). Adsorption isotherm models: A comprehensive and systematic review (2010−2020). *Science of the Total Environment*, *812*. https://doi.org/10.1016/j.scitotenv.2021.151334

Mtaallah, S., Marzouk, I., & Hamrouni, B. (2018). Factorial experimental design applied to adsorption of cadmium on activated alumina. *Journal of Water Reuse and Desalination*, *8*(1), 76–85. https://doi.org/10.2166/wrd.2017.112

Musah, M., Azeh, Y., Mathew, J., Umar, M., Abdulhamid, Z., & Muhammad, A. (2022). Adsorption Kinetics and Isotherm Models: A Review. *Caliphate Journal of Science and Technology*, *4*(1), 20–26. https://doi.org/10.4314/cajost.v4i1.3

Muscarella, S. M., Laudicina, V. A., Di Trapani, D., & Mannina, G. (2024). Recovering ammonium from real treated wastewater by zeolite packed columns: The effect of flow rate and particle diameter. *Sustainable Chemistry and Pharmacy*, *41*, 101659. https://doi.org/10.1016/j.scp.2024.101659

Naghipour, D., Taghavi, K., Ashournia, M., Jaafari, J., & Arjmand Movarrekh, R. (2020). A study of Cr(VI) and NH4+adsorption using greensand (glauconite) as a low-cost adsorbent from aqueous solutions. *Water and Environment Journal*, *34*(1), 45–56. https://doi.org/10.1111/wej.12440

Najibul, M., Musheer, M., Khan, N. A., Husain, A., Ali, A., Ahmed, S., Kumar, P. S., Naushad, M., Upamali, A., Iqbal, J., Tirth, V., & Islam, S. (2021). Chemosphere Recent technologies for nutrient removal and recovery from wastewaters : A review. *Chemosphere*, *277*, 130328. https://doi.org/10.1016/j.chemosphere.2021.130328

Nandi, N., Ghosh, G. K., & Kundu, M. C. (2024). Comprehensive Study on Macronutrient Status and Physicochemical Characteristics of Lateritic Soils of Bankura District, West Bengal, India. *International Journal of Plant & Soil Science*, *36*(5), 1008–1015. https://doi.org/10.9734/ijpss/2024/v36i54597

Ng, C. W. W., Akinniyi, D. B., Zhou, C., & Chiu, C. F. (2019). Comparisons of weathered lateritic, granitic and volcanic soils: Compressibility and shear strength. *Engineering Geology*, *249*, 235–240. https://doi.org/10.1016/j.enggeo.2018.12.029

Nguyen, V. Q., Van, H. T., Le, S. H., Nguyen, T. H., Nguyen, H. T., Lan, N. T., Pham, Q. T., Nguyen, T. T., Tran, T. N. H., Nguyen, T. B. H., & Hoang, T. K. (2021). Production of hydroponic solution from human urine using adsorption–desorption method with coconut shell-derived activated carbon. *Environmental Technology and Innovation*, *23*. https://doi.org/10.1016/j.eti.2021.101708

Nie, J., Feng, H., Witherell, B. B., Alebus, M., Mahajan, M. D., Zhang, W., & Yu, L. (2018). Causes, assessment, and treatment of nutrient (N and P) pollution in rivers, estuaries, and coastal waters. *Current Pollution Reports*, *4*(2), 154–161.

Ogunlalu, O., Oyekunle, I. P., Iwuozor, K. O., Aderibigbe, A. D., & Emenike, E. C. (2021). Trends in the mitigation of heavy metal ions from aqueous solutions using unmodified and chemically-modified agricultural waste adsorbents.

Current Research in Green and Sustainable Chemistry, *4*(June), 100188. https://doi.org/10.1016/j.crgsc.2021.100188

Olawale, S. A. (2020). Biosorption of Heavy Metals from Aqueous Solutions:Insight and Review. *Archives of Industrial Engineering*, *3*(October), 1–31. https://doi.org/10.31829/2637-9252/aie2020-3(1)-113

Osmond, D. L., Shober, A. L., Sharpley, A. N., Duncan, E. W., & Hoag, D. L. K. (2019). Increasing the Effectiveness and Adoption of Agricultural Phosphorus Management Strategies to Minimize Water Quality Impairment. *Journal of Environmental Quality*, *48*(5), 1204–1217. https://doi.org/10.2134/jeq2019.03.0114

Otieno, A. O., Home, P. G., Raude, J. M., Murunga, S. I., Munala, G., Ojwang, D. O., & Tuhkanen, T. (2023a). Phosphorous removal from human urine using lateritic soil. *Cleaner Waste Systems*, *4*(January), 100081. https://doi.org/10.1016/j.clwas.2023.100081

Otieno, A. O., Home, P. G., Raude, J. M., Murunga, S. I., Munala, G., Ojwang, D. O., & Tuhkanen, T. (2023b). Phosphorous removal from human urine using lateritic soil. *Cleaner Waste Systems*, *4*(January), 100081. https://doi.org/10.1016/j.clwas.2023.100081

Otieno, A. O., Home, P. G., Raude, J. M., Murunga, S. I., Ngumba, E., Ojwang, D. O., & Tuhkanen, T. (2021). Pineapple peel biochar and lateritic soil as adsorbents for recovery of ammonium nitrogen from human urine. *Journal of Environmental Management*, *293*(May), 112794. https://doi.org/10.1016/j.jenvman.2021.112794

Ou, W., Lan, X., Guo, J., Cai, A., Liu, P., Liu, N., Liu, Y. Y., & Lei, Y. (2023). Preparation of iron/calcium-modified biochar for phosphate removal from industrial wastewater. *Journal of Cleaner Production*, *383*(November 2022), 135468. https://doi.org/10.1016/j.jclepro.2022.135468

Panić, S., Rakić, D., Guzsvány, V., Kiss, E., Boskovic, G., Kónya, Z., & Kukovecz, Á. (2015). Optimization of thiamethoxam adsorption parameters using multi-walled carbon nanotubes by means of fractional factorial design. *Chemosphere*, *141*, 87–93.

Pap, S., Gaffney, P. P. J., Bremner, B., Turk, M., Maletic, S., Gibb, S. W., & Taggart, M. A. (2022). Science of the Total Environment Enhanced phosphate removal and potential recovery from wastewater by thermo-chemically calcinated shell adsorbents. *Science of the Total Environment, 814*, 152794. https://doi.org/10.1016/j.scitotenv.2021.152794

Pap, S., Kirk, C., Bremner, B., Turk, M., Shearer, L., Gibb, S. W., & Taggart, M. A. (2020). Low-cost chitosan-calcite adsorbent development for potential phosphate removal and recovery from wastewater ef fl uent. *Water Research, 173*, 115573. https://doi.org/10.1016/j.watres.2020.115573

Papaevangelou, V., Bakalakou, K. A., Tsilinikos, J., & Akratos, C. S. (2023). Testing zeolite and palygorskite as a potential medium for ammonium recovery and brewery wastewater treatment. *Water, 15*(23), 4069.

Patel, A., Mungray, A. K., & Mungray, A. (2021). Recovery of high quality water from human urine using a novel vertical up-flow forward osmosis reactor. *Sustainable Energy Technologies and Assessments*, *45*(September 2020), 101124. https://doi.org/10.1016/j.seta.2021.101124

Pathy, A., Ray, J., & Paramasivan, B. (2021). Challenges and opportunities of nutrient recovery from human urine using biochar for fertilizer applications. *Journal of Cleaner Production, 304*, 127019. https://doi.org/10.1016/j.jclepro.2021.127019

Paul, P., Parbat, S., & Aditya, G. (2022). Phosphate ion removal from aqueous solution using snail shell dust: biosorption potential of waste shells of edible snails. *RSC Advances*, *12*(46), 30011–30023. https://doi.org/10.1039/d2ra03852h

Pecková, V., Legerská, B., Chmelová, D., Horník, M., & Ondrejovič, M. (2020). Comparison of efficiency for monoazo dye removal by different species of white-rot fungi. *International Journal of Environmental Science and Technology*, (0123456789). https://doi.org/10.1007/s13762-020-02806-w

Pepper, I. L., & Gerba, C. P. (2015). Environmental Sample Collection and Processing. In *Environmental Biology*. Elsevier Inc. https://doi.org/10.1016/B978-0-12-394626-3.00008-9

Perera, M. K., Englehardt, J. D., & Dvorak, A. C. (2019). Technologies for recovering nutrients from wastewater: a critical review. *Environmental Engineering Science*, *36*(5), 511–529.

Pham, T. D., Nguyen, H. H., Nguyen, N. V., Vu, T. T., Pham, T. N. M., Doan, T. H. Y., Nguyen, M. H., & Ngo, T. M. V. (2017). Adsorptive Removal of Copper by Using Surfactant Modified Laterite Soil. *Journal of Chemistry*, *2017*(Ii). https://doi.org/10.1155/2017/1986071

Photiou, P., Koutsokeras, L., & Constantinides, G. (2021). Phosphate removal from synthetic and real wastewater using thermally treated seagrass residues of Posidonia oceanica. *Journal of Cleaner Production*, *278*, 123294. https://doi.org/10.1016/j.jclepro.2020.123294

Pourhakkak, P., Taghizadeh, A., Taghizadeh, M., Ghaedi, M., & Haghdoust, S. (2021). Fundamentals of adsorption technology. In *Adsorption: Fundamental Processes and Applications* (1st ed., Vol. 33). Elsevier Ltd. https://doi.org/10.1016/B978-0-12-818805-7.00001-1

Pradhan, S. K., Nerg, A. M., Sjöblom, A., Holopainen, J. K., & Heinonen-Tanski, H. (2007). Use of human urine fertilizer in cultivation of cabbage (Brassica oleracea) - Impacts on chemical, microbial, and flavor quality. *Journal of Agricultural and Food Chemistry*, *55*(21), 8657–8663. https://doi.org/10.1021/jf0717891

Qian, J., Zhou, X., Cai, Q., Zhao, J., & Huang, X. (2023). The Study of Optimal Adsorption Conditions of Phosphate on Fe-Modified Biochar by Response Surface Methodology. *Molecules*, *28*(5). https://doi.org/10.3390/molecules28052323

Rakshit, A., Abhilash, P. C., Singh, H. B., & Ghosh, S. (2017). Adaptive soil management: From theory to practices. *Adaptive Soil Management: From Theory to Practices*, 1–571. https://doi.org/10.1007/978-981-10-3638-5

Rathi, T. A., Gomase, V., Sadanand, D. S., & Jugade, R. (2025). Mathematical Modelling for Fixed - Bed Column and Batch Adsorption Studies of Antibiotic and CO 2 Capture Using Soybean Stover Biochar. *BioNanoScience*. https://doi.org/10.1007/s12668-024-01694-5

Rose, C., Parker, A., Jefferson, B., Cartmell, E., Parker, A., Jefferson, B., & Characterization, E. C. T. (2015). *The Characterization of Feces and Urine : A Review of the Literature to Inform Advanced Treatment Technology The Characterization of Feces and Urine : A*. *3389*(May). https://doi.org/10.1080/10643389.2014.1000761

Rout, P. R., Dash, R. R., & Bhunia, P. (2016). Nutrient removal from binary aqueous phase by dolochar : Highlighting optimization , single and binary adsorption isotherms and nutrient release. *Process Safety and Environmental Protection*, *100*, 91–107. https://doi.org/10.1016/j.psep.2016.01.001

Rudakiya, D. M., & Gupte, A. (2019). Assessment of white rot fungus mediated hardwood degradation by FTIR spectroscopy and multivariate analysis. *Journal of Microbiological Methods*, *157*(July 2018), 123–130. https://doi.org/10.1016/j.mimet.2019.01.007

Saliu, T. D., & Oladoja, N. A. (2021). Nutrient recovery from wastewater and reuse in agriculture: a review. *Environmental Chemistry Letters*, *19*(3), 2299–2316. https://doi.org/10.1007/s10311-020-01159-7

Santha Kumar, G., Saini, P. K., Deoliya, R., Mishra, A. K., & Negi, S. K. (2022). Characterization of laterite soil and its use in construction applications: A review. *Resources, Conservation and Recycling Advances*, *16*(November), 200120. https://doi.org/10.1016/j.rcradv.2022.200120

Santos, F. M., & Pires, J. C. M. (2018). Bioresource Technology Nutrient recovery from wastewaters by microalgae and its potential application as bio-char. *Bioresource Technology*, *267*(July), 725–731. https://doi.org/10.1016/j.biortech.2018.07.119

Saravanan, A., Senthil Kumar, P., Jeevanantham, S., Karishma, S., Tajsabreen, B., Yaashikaa, P. R., & Reshma, B. (2021). Effective water/wastewater treatment methodologies for toxic pollutants removal: Processes and applications towards sustainable development. *Chemosphere*, *280*, 130595. https://doi.org/10.1016/j.chemosphere.2021.130595

Sarker, P., Liu, X., Hata, N., Takeshita, H., Miyamura, H., & Maruo, M. (2023). Thermally modified bamboo-eggshell adsorbent for phosphate recovery and its

sustainable application as fertilizer. *Environmental Research*, *231*(P1), 115992. https://doi.org/10.1016/j.envres.2023.115992

Sarvajayakesavalu, S., Lu, Y., Withers, P. J. A., Pavinato, P. S., Pan, G., & Chareonsudjai, P. (2018). Phosphorus recovery: a need for an integrated approach. *Ecosystem Health and Sustainability*, *4*(2), 48–57. https://doi.org/10.1080/20964129.2018.1460122

Sathya, A. B., Sivashankar, R., Kanimozhi, J., Devika, R., & Balaji, R. (2021). Biosorption and Different Native Sources for Preparation of Biosorbents. *Biosorption for Wastewater Contaminants*, 23–41. https://doi.org/10.1002/9781119737629.ch2

Sellner, B. M., Hua, G., & Ahiablame, L. M. (2019). Fixed bed column evaluation of phosphate adsorption and recovery from aqueous solutions using recycled steel byproducts. *Journal of Environmental Management*, *233*(September 2018), 595–602. https://doi.org/10.1016/j.jenvman.2018.12.070

Semerci, N., Ahadi, S., & Coşgun, S. (2021). Comparison of dried sludge and sludge ash for phosphorus recovery with acidic and alkaline leaching. *Water and Environment Journal*, *35*(1), 359–370. https://doi.org/10.1111/wej.12633

Sen, T. K. (2023). Agricultural Solid Wastes Based Adsorbent Materials in the Remediation of Heavy Metal Ions from Water and Wastewater by Adsorption: A Review. *Molecules*, *28*(14). https://doi.org/10.3390/molecules28145575

Sene, M., Hijikata, N., Ushijima, K., & Funamizu, N. (2018). Application of human urine in agriculture. In *Resource-Oriented Agro-sanitation Systems: Concept, Business Model, and Technology* (pp. 213–242). Springer.

Sengupta, S., Nawaz, T., & Beaudry, J. (2015a). Nitrogen and phosphorus recovery from wastewater. *Current Pollution Reports*, *1*(3), 155–166.

Sengupta, S., Nawaz, T., & Beaudry, J. (2015b). *Nitrogen and Phosphorus Recovery from Wastewater*. 155–166. https://doi.org/10.1007/s40726-015-0013-1

Serban, G. V., Iancu, V. I., Dinu, C., Tenea, A., Vasilache, N., Cristea, I., Niculescu, M., Ionescu, I., & Chiriac, F. L. (2023). *Removal Efficiency and Adsorption Kinetics of Methyl Orange from Wastewater by Commercial Activated Carbon*.

Sereenonchai, K., Inla, C., & Buajarern, S. (2022). Thread-Based Analytical Device for Determination of Phosphorus Content in Fertilizers. *Trends in Sciences*, *19*(16), 1–11. https://doi.org/10.48048/tis.2022.5616

Sharma, K. R., Giri, R., & Sharma, R. K. (2020). Lead, cadmium and nickel removal efficiency of white-rot fungus Phlebia brevispora. *Letters in Applied Microbiology*, *71*(6), 637–644. https://doi.org/10.1111/lam.13372

Shumiye, E., Nadew, T. T., Tedla, T. S., Getiye, B., Mengie, D. A., & Ayalew, A. G. (2024). Preparation of an activated adsorbent from water treatment plant sludge for phosphate removal from wastewater: optimization, characterization, isotherm, and kinetics studies. *Journal of Water Sanitation and Hygiene for Development*, *14*(2), 122–143. https://doi.org/10.2166/washdev.2024.278

Simha, P., Barton, M. A., Perez-Mercado, L. F., McConville, J. R., Lalander, C., Magri, M. E., Dutta, S., Kabir, H., Selvakumar, A., Zhou, X., Martin, T., Kizos, T., Kataki, R., Gerchman, Y., Herscu-Kluska, R., Alrousan, D., Goh, E. G., Elenciuc, D., Głowacka, A., … Vinnerås, B. (2021). Willingness among food consumers to recycle human urine as crop fertiliser: Evidence from a multinational survey. *Science of The Total Environment*, *765*, 144438. https://doi.org/https://doi.org/10.1016/j.scitotenv.2020.144438

Simha, P., Zabaniotou, A., & Ganesapillai, M. (2018). Continuous urea--nitrogen recycling from human urine: A step towards creating a human excreta based bio--economy. *Journal of Cleaner Production*, *172*, 4152–4161.

Singh, B., & Craswell, E. (2021). Fertilizers and nitrate pollution of surface and ground water : an increasingly pervasive global problem. *SN Applied Sciences*, *3*(4), 1–24. https://doi.org/10.1007/s42452-021-04521-8

Sohn, W., Jiang, J., Phuntsho, S., Choden, Y., Tran, V. H., & Shon, H. K. (2023). Nutrients in a circular economy: Role of urine separation and treatment. *Desalination*, *560*(April), 116663. https://doi.org/10.1016/j.desal.2023.116663

Stoops, G., & Marcelino, V. (2018). Lateritic and bauxitic materials. In *Interpretation of micromorphological features of soils and regoliths* (pp. 691–720). Elsevier.

Sun, C., Huang, C., Wang, P., Yin, J., Tian, H., Liu, Z., Xu, H., Zhu, J., Hu, X., & Liu, Z. (2024). Low-cost eggshell-fly ash adsorbent for phosphate recovery: A

potential slow-release phosphate fertilizer. *Water Research*, *255*(November 2023), 121483. https://doi.org/10.1016/j.watres.2024.121483

Suvokhiaw, S., Deeleepojananan, C., Konraeng, K., Laohhasurayotin, K., & Suwanchawalit, C. (2025). Fabrication of ZnAl layered double hydroxide films on recycled aluminum sheets and phosphate removal. *Results in Surfaces and Interfaces*, *20*(April). https://doi.org/10.1016/j.rsurfi.2025.100606

Tan, I. A. W., Ahmad, A. La, & Hameed, B. H. (2008). Adsorption of basic dye on high-surface-area activated carbon prepared from coconut husk: Equilibrium, kinetic and thermodynamic studies. *Journal of Hazardous Materials*, *154*(1–3), 337–346.

Tang, R., Qiu, S., Wu, C., & Tan, J. (2025). Biochar: from agricultural waste byproducts to novel adsorbents for ammonia and micro/nanoplastics (MNPs). *Biochar*, *7*(1), 122.

Tang, Z., Chi, Z., Jiang, F., Zhao, M., Fu, S., Wei, L., Feng, Q., Wu, Y., & Xu, N. (2025). Mechanisms and implications of phosphate retention in soils: insights from batch adsorption experiments and geochemical modeling. *Water*, *17*(7), 998.

Tefera, N., Mulualem, Y., & Fito, J. (2020). Adsorption of Fluoride from Aqueous Solution and Groundwater onto Activated Carbon of Avocado Seeds. *Water Conservation Science and Engineering*, *5*(3–4), 187–197. https://doi.org/10.1007/s41101-020-00093-7

Thorat, D. S., Ushir, Y. V, & Singh, S. (2025). Value-added-peanut shell as potential source for biofilters: an eco-friendly way to clean water and manage nutrients. *Biotechnology for Sustainable Materials*, *2*(1), 12.

Thorslund, J., Jarsjo, J., Jaramillo, F., Jawitz, J. W., Manzoni, S., Basu, N. B., Chalov, S. R., Cohen, M. J., Creed, I. F., Goldenberg, R., Hylin, A., Kalantari, Z., Koussis, A. D., Lyon, S. W., Mazi, K., Mard, J., Persson, K., Pietro, J., Prieto, C., … Destouni, G. (2017). Wetlands as large-scale nature-based solutions: Status and challenges for research, engineering and management. *Ecological Engineering*, *108*, 489–497. https://doi.org/https://doi.org/10.1016/j.ecoleng.2017.07.012

Tibebu, S., Kassahun, E., Worku, A., Kebede, S., & Sime, T. (2025). Cr (VI) removal from aqueous solutions using Cordia Africana -based activated carbon / red clay / magnetite nanocomposite : optimization via one factor at a time and response surface methodology. *Biomass Conversion and Biorefinery*, *15*(14), 21133–21159. https://doi.org/10.1007/s13399-025-06684-5

Toptas, A., Demierege, S., Mavioglu Ayan, E., & Yanik, J. (2014). Spent mushroom compost as biosorbent for dye biosorption. *Clean - Soil, Air, Water*, *42*(12), 1721–1728. https://doi.org/10.1002/clen.201300657

Tosun, I. (2012). Ammonium Removal from Aqueous Solutions by Clinoptilolite: Determination of Isotherm and Thermodynamic Parameters and Comparison of Kinetics by the Double Exponential Model and Conventional Kinetic Models. *International Journal of Environmental Research and Public Health 2012, Vol. 9, Pages 970-984*, *9*(3), 970–984. https://doi.org/10.3390/IJERPH9030970

Trinh, V. T., Nguyen, T. M. P., Van, H. T., Hoang, L. P., Nguyen, T. V., Ha, L. T., Vu, X. H., Pham, T. T., Nguyen, T. N., Quang, N. V., & Nguyen, X. C. (2020). Phosphate Adsorption by Silver Nanoparticles-Loaded Activated Carbon derived from Tea Residue. *Scientific Reports*, *10*(1), 1–13. https://doi.org/10.1038/s41598-020-60542-0

Udert, K. M., Larsen, T. A., & Gujer, W. (2006). Fate of major compounds in source-separated urine. *Water Science and Technology*, *54*(11–12), 413–420.

Udert, K. M., & Wächter, M. (2012). Complete nutrient recovery from source-separated urine by nitrification and distillation. *Water Research*, *46*(2), 453–464.

United Nations. (2019). *World Population Prospects 2019: Highlights*. United Nations, Department of Economic and Social Affairs, Population Division.

Unuabonah, E. I., Olu-Owolabi, B. I., Oladoja, A. N., Ofomaja, A. E., & Yang, Z. L. (2010). Pb/Ca ion exchange on kaolinite clay modified with phosphates. *Journal of Soils and Sediments*, *10*(6), 1103–1114.

U.S. Geological Survey. (2022). *Mineral Commodity Summaries 2022*. https://doi.org/10.3133/mcs2022

Usman, M. O., Aturagaba, G., Ntale, M., & Nyakairu, G. W. (2022). A review of adsorption techniques for removal of phosphates from wastewater. *Water Science \& Technology*, *86*(12), 3113–3132.

Viskari, E.-L., Grobler, G., Karimäki, K., Gorbatova, A., Vilpas, R., & Lehtoranta, S. (2018). Nitrogen recovery with source separation of human urine—preliminary results of its fertiliser potential and use in agriculture. *Frontiers in Sustainable Food Systems*, *2*, 32.

Wahab, M. A., Jellali, S., & Jedidi, N. (2010). Ammonium biosorption onto sawdust: FTIR analysis, kinetics and adsorption isotherms modeling. *Bioresource Technology*, *101*(14), 5070–5075. https://doi.org/10.1016/j.biortech.2010.01.121

Wang, R., Yu, J., Chen, Y., Li, X., Zhang, Z., & Xiao, C. (2025). The adsorption mechanism of NH + 4 on clay mineral surfaces : Experimental and theoretical studies. *Separation and Purification Technology*, *354*(P1), 128521. https://doi.org/10.1016/j.seppur.2024.128521

Wang, S., Zhao, H., Liu, J., Wang, X., Li, J., Shi, E., Wang, C., Yang, J., & Zhang, Z. (2023). A study on and adsorption mechanism of ammonium nitrogen by modified corn straw biochar. *Royal Society Open Science*, *10*(2), 221535. https://doi.org/10.1098/rsos.221535

Wei, S. P., Rossum, F. Van, Jan, G., Pol, V. De, & Winkler, M. H. (2018). Chemosphere Recovery of phosphorus and nitrogen from human urine by struvite precipitation , air stripping and acid scrubbing : A pilot study. *Chemosphere*, *212*, 1030–1037. https://doi.org/10.1016/j.chemosphere.2018.08.154

WHO. (2006). WHO Guidelines for the Safe Use of Wastewater, Excreta and Greywater, Volumes 1–4. *International Journal of Environmental Studies*, *65*(1), 157–176. https://doi.org/10.1080/00207230701846598

Wilsenach, J. A., Schuurbiers, C. A. H., & van Loosdrecht, M. C. M. (2007). Phosphate and potassium recovery from source separated urine through struvite precipitation. *Water Research*, *41*(2), 458–466. https://doi.org/10.1016/j.watres.2006.10.014

Wu, K., Li, Y., Liu, T., Zhang, N., Wang, M., Yang, S., Wang, W., & Jin, P. (2019). Evaluation of the adsorption of ammonium-nitrogen and phosphate on a granular composite adsorbent derived from zeolite. *Environmental Science and Pollution Research*, *26*(17), 17632–17643. https://doi.org/10.1007/s11356-019-05069-2

Wurtsbaugh, W. A., Paerl, H. W., & Dodds, W. K. (2019). Nutrients, eutrophication and harmful algal blooms along the freshwater to marine continuum. *Wiley Interdisciplinary Reviews: Water*, *6*(5), 1–27. https://doi.org/10.1002/WAT2.1373

Wystalska, K., & Kwarciak-kozłowska, A. (2021). The effects of using biochar to remove ammonium nitrogen generated during the processing of biodegradable waste. *Desalination and Water Treatment*, *225*, 203–213. https://doi.org/10.5004/dwt.2021.27226

Xia, S., Liang, S., Qin, Y., Chen, W., Xue, B., Zhang, B., & Xu, G. (2023). Significant Improvement of Adsorption for Phosphate Removal by Lanthanum-Loaded Biochar. *ACS Omega*, *8*(28), 24853–24864. https://doi.org/10.1021/acsomega.3c00788

Xiang, W., Zhang, X., Chen, J., Zou, W., He, F., Hu, X., Tsang, D. C. W., Ok, Y. S., & Gao, B. (2020). Biochar technology in wastewater treatment: A critical review. *Chemosphere*, *252*, 126539. https://doi.org/10.1016/j.chemosphere.2020.126539

Xu, C., Feng, Y., Li, H., Yang, Y., Jiang, S., Wu, R., Ma, R., & Xue, Z. (2023). Adsorption of phosphorus from eutrophic seawater using microbial modified attapulgite - cleaner production, remove behavior, mechanism and cost-benefit analysis. *Chemical Engineering Journal*, *458*(November 2022), 141404. https://doi.org/10.1016/j.cej.2023.141404

Yadav, A. N., Singh, S., Mishra, S., & Gupta, A. (2019). *Recent advancement in white biotechnology through fungi: volume 3: perspective for sustainable environments*. Springer.

Yadav, S., Sharma, N., Dalal, A., Panghal, P., Sharma, A. K., & Kumar, S. (2025). Cutting-edge regeneration technologies for saturated adsorbents: a systematic review on pathways to circular wastewater treatment system. In *Environmental*

Monitoring and Assessment (Vol. 197, Number 2). Springer International Publishing. https://doi.org/10.1007/s10661-025-13657-8

Yang, D., Chen, Q., Liu, R., Song, L., Zhang, Y., & Dai, X. (2022). Bioresource Technology Ammonia recovery from anaerobic digestate : State of the art , challenges and prospects. *Bioresource Technology*, *363*(September), 127957. https://doi.org/10.1016/j.biortech.2022.127957

Yang, S., Ding, D., Zhao, Y., Huang, W., Zhang, Z., Lei, Z., & Yang, Y. (2013). Journal of Environmental Chemical Engineering Investigation of phosphate adsorption from aqueous solution using Kanuma mud : Behaviors and mechanisms. *Biochemical Pharmacology*, *1*(3), 355–362. https://doi.org/10.1016/j.jece.2013.05.016

Yang, Z., Li, L., & Wang, Y. (2024). Mechanism of Phosphate Desorption from Activated Red Mud Particle Adsorbents. *Molecules*, *29*(5). https://doi.org/10.3390/molecules29050974

Ye, Y., Ngo, H. H., Guo, W., Liu, Y., Li, J., Liu, Y., Zhang, X., & Jia, H. (2017). Insight into chemical phosphate recovery from municipal wastewater. *Science of the Total Environment*, *576*, 159–171.

Yu, H., Reynolds, J. K., Koskue, V., Marchuk, S., Antille, D. L., McCabe, B. K., Beal, C. D., Freguia, S., Yadav, N., & Powell, J. R. (2026). Recovering nutrients from urine--A golden opportunity for sustainable fertiliser production. *Plants, People, Planet*, *8*(3), 747–753.

Yu, Y. hui, Du, C. ming, & Yang, X. (2023). Recovery of phosphorus from steelmaking slag and phosphate tailings by a collaborative processing method. *Separation and Purification Technology*, *313*(3), 123499. https://doi.org/10.1016/j.seppur.2023.123499

Zamparas, M., Kyriakopoulos, G. L., Drosos, M., & Kapsalis, V. C. (2021). Phosphate and ammonium removal from wastewaters using natural-based innovative bentonites impacting on resource recovery and circular economy. *Molecules*, *26*(21). https://doi.org/10.3390/molecules26216684

Zhang, H., Chen, L., Lu, M., Li, J., & Han, L. (2016). Biotechnology for Biofuels A novel film – pore – surface diffusion model to explain the enhanced enzyme

adsorption of corn stover pretreated by ultrafine grinding. *Biotechnology for Biofuels*, 1–12. https://doi.org/10.1186/s13068-016-0602-2

Zhang, L., Liu, Y., Wang, Y., Li, X., & Wang, Y. (2021). Investigation of phosphate removal mechanisms by a lanthanum hydroxide adsorbent using p-XRD, FTIR and XPS. *Applied Surface Science*, *557*(April), 149838. https://doi.org/10.1016/j.apsusc.2021.149838

Zhang, L., Tang, S., & Guan, Y. (2020). Excellent Adsorption-Desorption of Ammonium by a Poly(acrylic acid)-Grafted Chitosan and Biochar Composite for Sustainable Agricultural Development. *ACS Sustainable Chemistry and Engineering*, *8*(44), 16451–16462. https://doi.org/10.1021/acssuschemeng.0c05070

Zhang, W., Li, G., Yin, H., Zhao, K., Zhao, H., & An, T. (2022). Adsorption and desorption mechanism of aromatic VOCs onto porous carbon adsorbents for emission control and resource recovery: recent progress and challenges. *Environmental Science: Nano*, *9*(1), 81–104.

Zhang, X., Fu, W., Yin, Y., Chen, Z., Qiu, R., Simonnot, M., & Wang, X. (2018). Bioresource Technology Adsorption-reduction removal of Cr (VI) by tobacco petiole pyrolytic biochar : Batch experiment , kinetic and mechanism studies. *Bioresource Technology*, *268*(June), 149–157. https://doi.org/10.1016/j.biortech.2018.07.125

Zhou, L., & Boyd, C. E. (2016). Comparison of Nessler, phenate, salicylate and ion selective electrode procedures for determination of total ammonia nitrogen in aquaculture. *Aquaculture*, *450*, 187–193. https://doi.org/10.1016/j.aquaculture.2015.07.022

Zou, T., Zhang, X., & Davidson, E. A. (2022). Global trends of cropland phosphorus use and sustainability challenges. *Nature*, *611*(7934), 81–87.

APPENDICES

Appendix I: Fungi (*Agaricus Impudicus*) before oven-drying

Appendix II: Preparation of the Fungi Samples for drying

Appendix III: Calibration Solutions for Ammonium Nitrogen

Appendix IV: Calibration Solutions for Phosphorus

Appendix V: Calibrating the UV-Vis Spectrophotometer

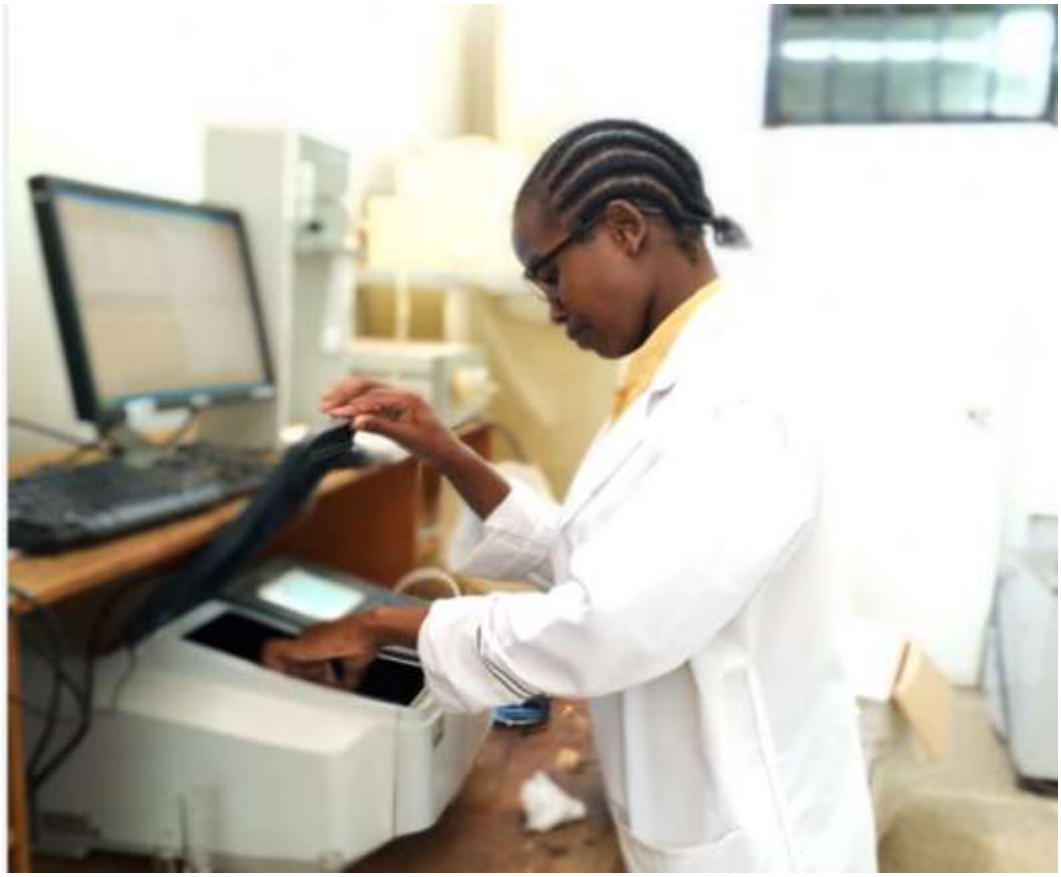

Appendix VI: Calibration Curves for NH_4^+-N Adsorption

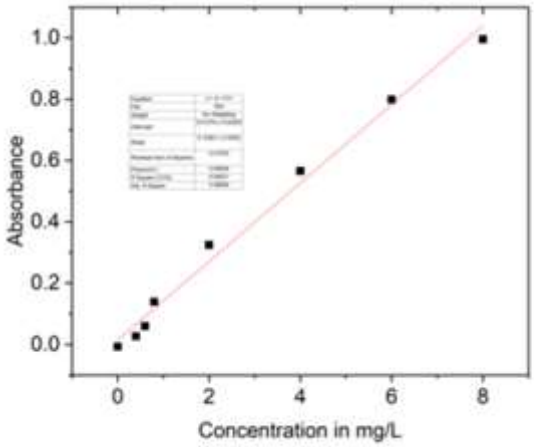

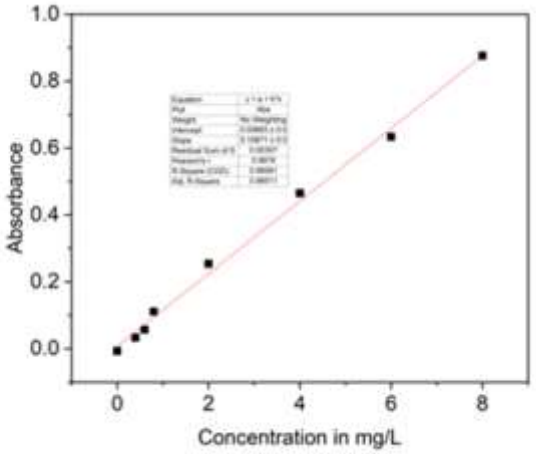

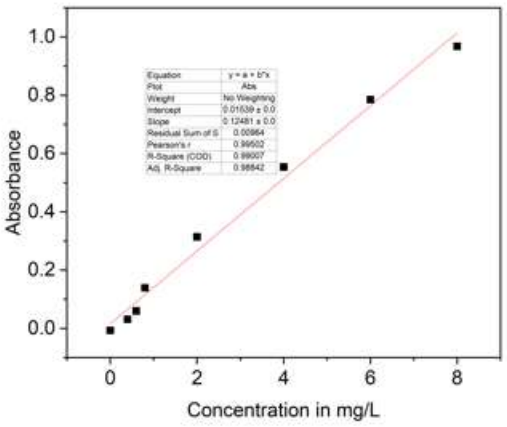

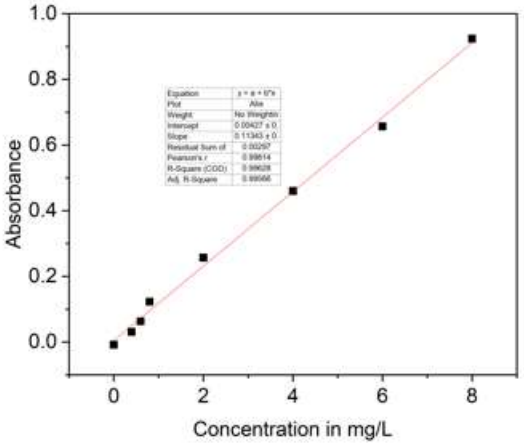

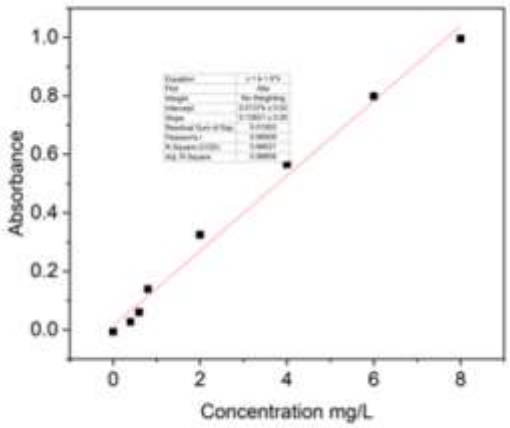

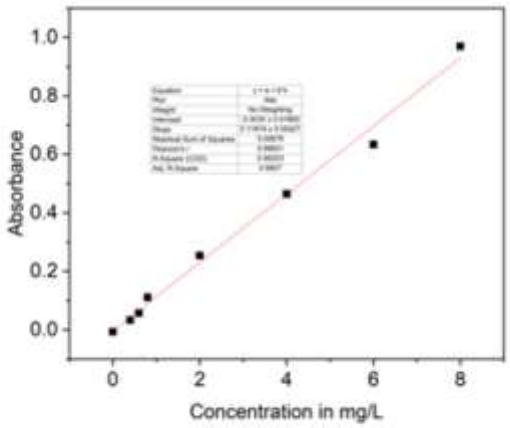

Appendix VII: Calibration Curves for P Adsorption

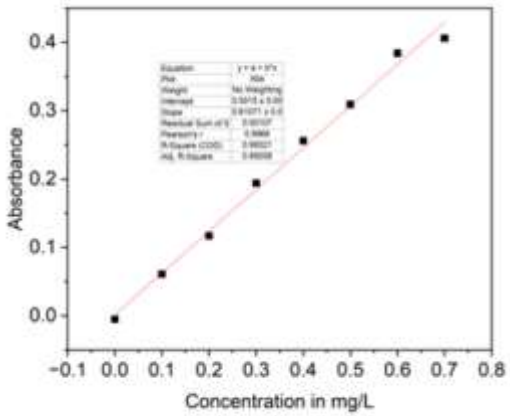

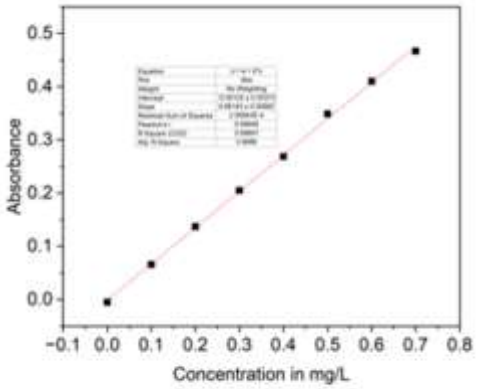

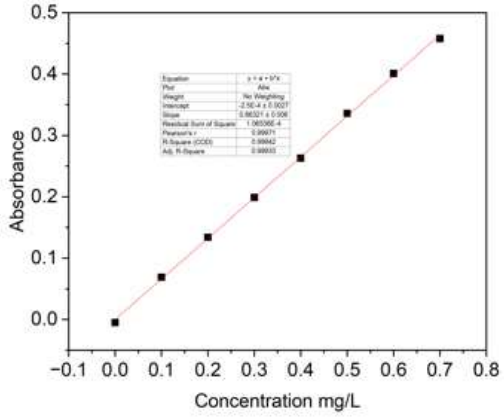
Absorbance
Concentration mg/L

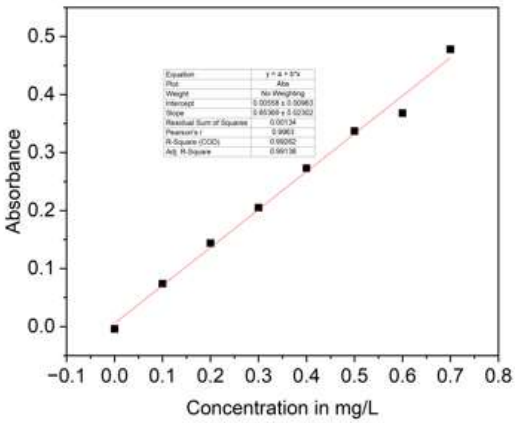
Absorbance
Concentration in mg/L

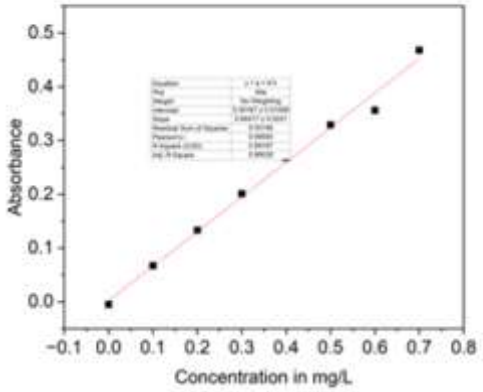
Absorbance
Concentration in mg/L

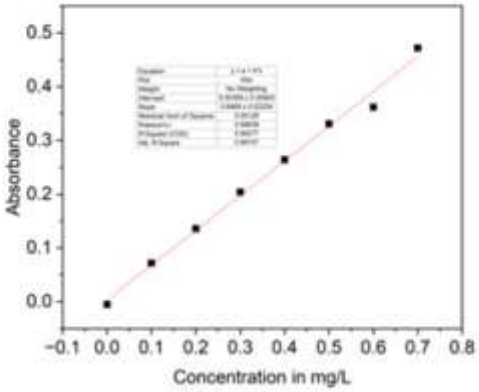
Absorbance
Concentration in mg/L